

# The application of resistivity and IP-measurements as investigation tools at contaminated sites

A case study from Kv. Renen 13,  
Varberg, SW Sweden

***Sofia Åkesson***

Dissertations in Geology at Lund University,  
Master's thesis, no 442  
(45 hp/ECTS credits)



Department of Geology  
Lund University  
2015



# **The application of resistivity and IP-measurements as investigation tools at contaminated sites**

**A case study from Kv. Renen 13,  
Varberg, SW Sweden**

Master's thesis  
Sofia Åkesson

Department of Geology  
Lund University  
2015

# Contents

<b>1 Introduction</b> .....	<b>7</b>
1.1 TRUST 2.1 .....	7
1.2 Aim .....	7
<b>2 Background</b> .....	<b>7</b>
2.1 Field site: Kv. Renen 13 .....	7
2.1.1 Earlier reports from the Kv. Renen 13 .....	10
2.2 Geology .....	10
2.3 Hydrogeology .....	13
2.4 Contamination .....	15
2.4.1 Contamination situation .....	17
2.4.2 Dechlorination .....	17
2.4.3 Pilot study of stimulated reductive dechlorination .....	18
2.5 Additional geophysical investigations .....	21
<b>3 Theory</b> .....	<b>22</b>
3.1 Resistivity .....	23
3.1.1 Field setup .....	24
3.2 Induced Polarization .....	25
3.3 Inversion modelling .....	26
<b>4 Methods</b> .....	<b>26</b>
4.1 Geological profiles .....	27
4.2 Fieldwork .....	27
4.2.1 DCIP measurements .....	27
4.2.2 Groundwater sampling .....	27
4.3 Data processing .....	27
<b>5 Results</b> .....	<b>29</b>
5.1 Geological profiles .....	29
5.2 DCIP-data .....	32
5.2.1 Resistivity .....	32
5.2.2 Induced Polarization .....	36
5.2.3 Time-lapse calculation .....	38
5.3 Groundwater chemistry .....	41
<b>6 Interpretation</b> .....	<b>42</b>
6.1 Resistivity .....	42
6.2 Induced Polarization .....	43
6.3 Time-lapse .....	43
6.4 Groundwater chemistry .....	43
6.5 Conceptual model .....	44
<b>7 Discussion</b> .....	<b>44</b>
<b>8 Conclusions</b> .....	<b>46</b>
<b>9 Acknowledgements</b> .....	<b>47</b>
<b>10 References</b> .....	<b>47</b>
<b>11 Appendix</b> .....	<b>49</b>

**Cover Picture:** DCIP equipment during field work at Kv. Renen 13

# The application of resistivity and IP-measurements as investigation tools at contaminated sites

SOFIA ÅKESSON

Åkesson, S., 2015: The application of resistivity and IP-measurements as investigation tools at contaminated sites. *Dissertations in Geology at Lund University*, No. 442, 82 pp. 45 hp (45 ECTS credits).

**Abstract:** An old industry estate, Kv. Renen 13, is located in central Varberg, southwest Sweden, and is known from previous investigations as highly polluted. Pollution started in the late 19<sup>th</sup> century with textile manufacturing, and in the 1960's changed into a precision mechanics industry using chlorinated solvents, primary trichloroethene (TCE) and 1,1,1-trichloroethane (TCA), as well as cyanide and metals. Wastewater was taken out through an escape valve to a sedimentation basin, which most likely leaked. With good subsurface conditions for dispersal, both in the sediments and in the highly fractured bedrock, a large area of the subsurface is polluted from contaminants due to the situation at Kv. Renen 13.

This thesis investigates the subsurface conditions by using resistivity and induced polarization measurements, geophysical methods based on different materials' physical responses to an electrical current. Resistivity ( $\Omega\text{m}$ ) is a physical property of the ability to isolate against electrical current. Induced polarization (IP) measures the chargeability of a material, i.e. how electrical charges polarize and depolarize when subjected to an electrical current that is turned off after an interval of time. The aim with these geophysical surveys was to create a 3D model of the subsurface ground conditions. The measurements were made at three occasions, to be able to investigate if it is possible to measure variation through time, and use the method for monitoring of *in situ* remediation.

As a result of the survey, a fracture zone with a southwest-northeast direction crossing the industrial estate, could be identified. This fracture zone was not identified at the estate before and within the zone, there is a possibility of spreading the contamination. Variations in underground conditions through time in the subsurface were measurable using the geophysical methods, and the method shows good potential to be used for in situ monitoring of pollutant remediation.

The work is part of the research project TRansparent Underground STructure, TRUST.

**Keywords:** geophysics, resistivity, induced polarization, contaminated site, hydrogeology, trichloroethene, TCE

**Supervisors:** Charlotte Sparrenbom, Torleif Dahlin

**Subject:** Quaternary geology, applied geology

*Sofia Åkesson, Department of Geology, Lund University, Sölvegatan 12, SE-223 62 Lund, Sweden.  
E-mail: sofia.akesson@gmail.com*

# Tillämpningen av resistivitet och IP-mätningar som undersökningsverktyg av förorenade områden

SOFIA ÅKESSON

Åkesson, S., 2015: The application of resistivity and IP-measurements as investigation tools at contaminated sites. *Examensarbeten i geologi vid Lunds universitet*, Nr. 442, 82 sid. 45 hp.

**Sammanfattning:** Kv. Renen 13 i centrala Varberg är sedan tidigare känt som kraftigt förorenat. På fastigheten har det från slutet av 1800-talet fram till 2003 funnits verksamheter i form av textilindustri som avlösts av finmekanisk verkstadsindustri. Det är framförallt den sistnämnda verksamheten som har orsakat rådande situation med höga halter klorerade lösningsmedel, trikloreten (TCE) och 1,1,1-trikloletan (TCA), som i verksamheten använts som fettlösande medel. Dessutom har det använts en del metaller och cyanid. Processvatten har letts ut via ett internt avloppssystem till en sedimentationsbassäng i trädgården och indikationer finns på att bassängen har läckt. Stora delar av centrala Varberg är förorenat med klorerade lösningsmedel och metaller p.g.a. de tidigare verksamheterna på Kv. Renen 13. Detta till följd av att spridningsförutsättningarna är goda, både i de lösa avlagringar och i den sprickrika berggrunden.

I det här examensarbetet har markförhållandena undersökts med geofysikiska mätningar i form av resistivitetsegenskaper och inducerad polarisation. Resistivitet är en materialegenskap som mäter ett materials resistans mot en elektrisk ström. Inducerad polarisation (IP) undersöker markens uppladdningsförmåga. Geofysik kan vara svårt att använda i urbana miljöer då det finns mycket som stör och ger upphov till brus i mätdata. Målet med undersökningen har varit att skapa en 3D-modell av markförhållandena. Mätningarna har gjorts vid flera tillfällen för att undersöka möjligheten att se förändringar med tiden och på sikt använda metoden för övervakning av *in situ*-saneringar. Som kalibrering för de geofysiska mätdata, har grundvattnet provtagits och analyserats.

Resultatet av undersökningarna visar en trolig sydvästlig-nordostlig sprickzon som korsar fastigheten och ger goda spridningsförutsättningarna av föroreningen. Förändringar med tiden var mätbara i marken och metoden visar god potential för att användas för övervakning av förändringar.

Arbetet ingår i forskningsprojektet TRansparent Underground STructore, TRUST.

**Nyckelord:** geofysik, resistivitet, inducerad polarisation, förorenad mark, hydrogeologi, trikloreten, TCE

**Handledare:** Charlotte Sparrenbom, Torleif Dahlin

**Ämne:** Kvärtärgeologi, tillämpad geologi

*Sofia Åkesson, Geologiska institutionen, Lunds Universitet, Sölvegatan 12, 223 62 Lund, Sverige.*

*E-post: sofia.akesson@gmail.com*

# 1 Introduction

In Sweden, ongoing and large environmental risk assessments of contaminated sites have identified, and more than 80,000 of these sites are regarded as potentially contaminated. They are investigated in a model called “MIFO” – Methods of Inventories of Contaminated Sites, described by the Swedish Environmental Protection Agency (Naturvårdsverket 2002). The surveys are mostly made by the respective municipalities and counties (län), where each of the counties administrative boards makes a priority list of most critical sites. In the county of Halland, the highest priority site is Kv. Renen 13, Varberg. Pollution of this site started in the late 19<sup>th</sup> century with textile manufacturing, and from the 1960’s changed into a precision mechanics industry using chlorinated solvents, primary trichloroethene (TCE) and 1,1,1-trichloroethane (TCA), as well as cyanide and metals. The products were handled in a basement and wastewater was taken out through an effluent pipe to a sedimentation basin. During transit, leaking of industrial wastewater caused the estate to become highly contaminated. Part of the pollution has moved away from the property, primarily towards the harbour, causing a contamination in central Varberg. The site’s geology consists mainly of highly fractured bedrock, which makes the direction of dispersal of the contaminants complex. In the contamination source area, the bedrock is buried beneath 5-7 meters of sediments, consisting of postglacial coarse sediments, mainly gravel and fill. Downstream towards the harbour, a layer of clay is found above the bedrock, and it divides the unconfined aquifer into two. One open part of the aquifer, and another confined to semi confined. The estate was chosen for this work because of the severe pollution situation, and it is a high priority object to remediate. Earlier investigations however, have not included geo-electrical methods. In this thesis we have measured Direct Current resistivity and time-domain Induced Polarization tomography (DCIP) and to verify the results, sampling and analyses of groundwater chemistry have been performed.

The aim is to map and create a 2D based 3D-model of Kv. Renen’s geology and contamination. The vision is to show the possibility of a better resolution of the model with a holistic view of the subsurface by using DCIP as an investigation method at contaminated sites. DCIP provide a tool to make more cost effective investigations that are less intrusive, which is especially interesting in complex urban environments containing pollutants. The thesis is part of the TRansparent Underground Structure research project (TRUST).

## 1.1 TRUST 2.1

This thesis is part of the TRansparent Underground Structure, or TRUST research project ([www.trust-geoinfra.se](http://www.trust-geoinfra.se)). The project’s vision is to develop sustainable urban underground infrastructure design, and improve methods and tools for better investigation, plan-

ning, design and finally construction and monitoring of urban underground structures. The specific aim of TRUST is to improve the geophysical measurement methods to interpret the ground conditions in regards to geology, groundwater quality, geological and urban structures and pollution therein, and at some point in the future implement the methods to reach a more cost effective planning, design and construction for underground facility projects.

The project is divided into subprojects where this thesis is included in TRUST 2.1, aimed at developing geoelectrical imaging for site investigation in urban underground infrastructural projects. It is accepted that modern geophysical methods have the capability of mapping underground in 2, 3 and 4 dimensions in an efficient way. Geophysical investigation methods obtain a broad overview of the subsurface with a better basis for further survey plans. Future drilling can be done in the locations where the geophysical methods have pinpointed problems such as contaminants or variations in geology, underground structures and/or changes within a contamination situation.

## 1.2 Aim

This study aims to investigate and map the contamination distribution in a 2D based 3D model at and around Kv. Renen 13 by using Direct Current resistivity and time-domain Induced Polarization tomography (DCIP) methods. Groundwater chemical samples from existing monitoring wells were used to verify the DCIP-data interpretation. Another part of the study was to measure the exact same profile at different times, to be able to see temporal changes within the groundwater and the contaminant conditions.

This thesis will answer:

- Is it possible to detect contamination plumes, and make a three dimensional model over the geology, and the contaminants in the urban environment around Kv. Renen with DCIP methodology?
- Is it possible to say how and/or why we get the signals in DCIP?
- Is it possible to study variations of the contamination during *in situ* remediation through time?

# 2 Background

## 2.1 Field Site: Kv. Renen 13, Varberg, SW Sweden

Kv. Renen 13 is an old industrial estate, located in an urban environment from the central part of Varberg, southwest Sweden (Fig. 1). The property is 15,000m<sup>2</sup> with buildings on 70% of the estate (Sernrot 2013). There are three buildings of which the largest is s where the handling of chemical products had been done, and the two others are the administrative build-

ing, today used for activities, like publishing, photography and a few unions, and then the old vacant director's residence. In front of the administration building, there is a garden with fruit trees. Office buildings, two day-care centres and housing estates dominate the surrounding area. No other industries are known or have existed in the area. In the flow direction of the contaminants, southwest wards towards the harbour and Kattegatt, one of the nursery schools (age 1-5 years old) is located in an area where chlorinated aliphatic compounds has been detected in the air. With ventila-

tion of the foundation, the risks are low enough to be able to continue with the children presence within the building (Sällsten & Barregård 2004). A closer view of the area with the contaminant sources presented is shown in Fig. 2. In Fig. 3 a-e some overhead photographs are shown from fieldwork at the estate.

The pollution of the area started in the late 19<sup>th</sup> century through a textile manufacturer. The business used metals such as chromium, zinc and cadmium for dyeing of fabrics (Tornberg *et al.* 2008). After 1960, the business turned gradually into a precision mechan-



Fig. 1. Location map of Sweden with Varberg highlighted. A narrow orthophoto photograph of central Varberg with Kv Renen 13 marked with a red outline. Westward of the estate is the railway, and further westwards the recipient of contamination, Varberg Harbour connected to Kattegatt (© Lantmäteriet I2014/00579).



Fig. 2. Overview of Kv Renen 13, with the source areas for the described pollutants and the day care center marked in yellow. a) Day care center, b) sedimentation basin, c) director residence, d) administration building, e) industry building with the cellar marked as contamination sources (© Lantmäteriet I2014/00579).



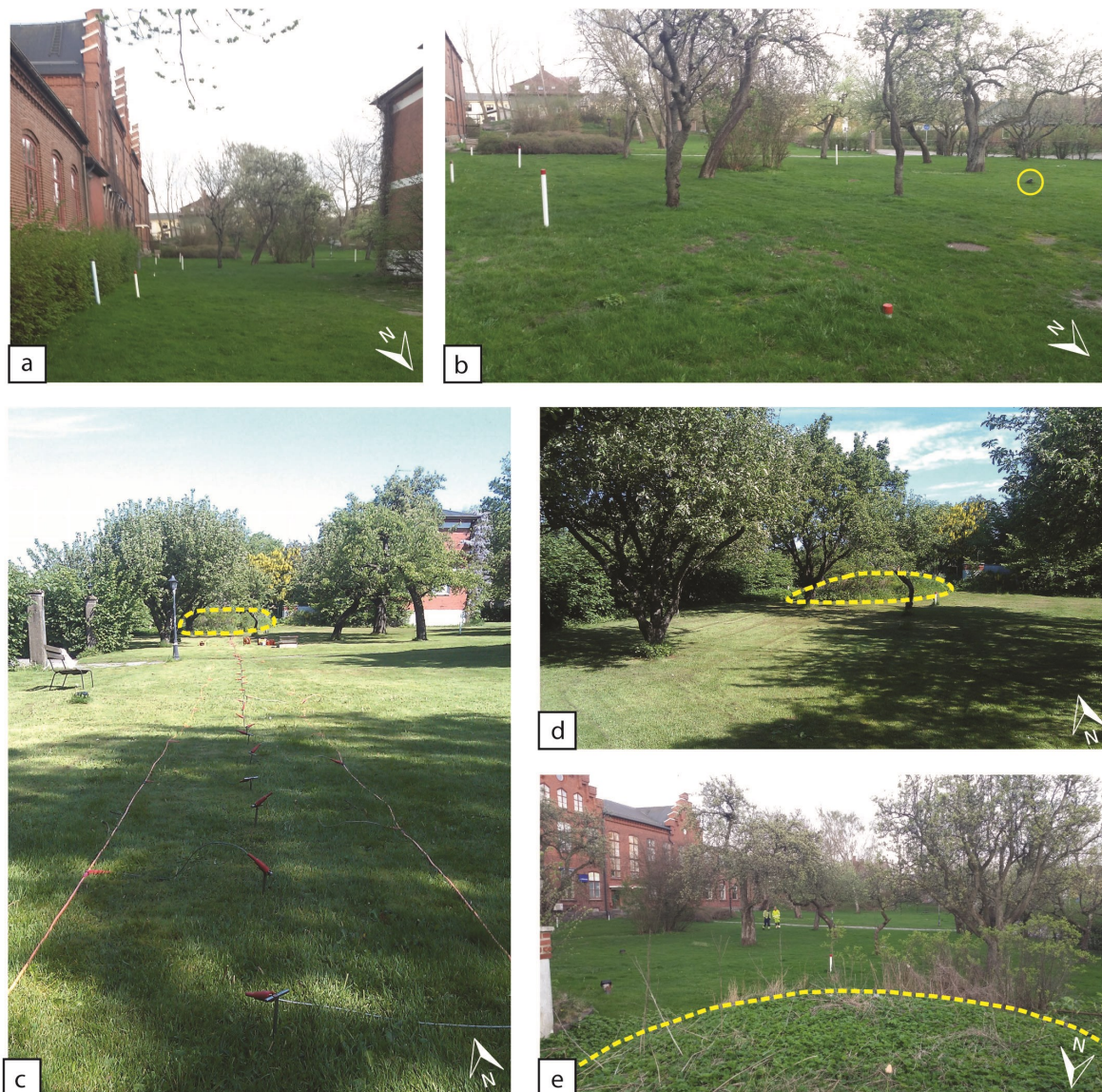


Fig. 3. Overview photos from Kv. Renen 13 taken during fieldwork on the estate; the arrow for orientation. a) The photograph is taken between the administration building and the director's residence. b) The garden area in front of the administration building. The yellow circle marks one of the deep-drilled wells according to Rahm *et al.* (2013). Both photograph a and b provides an impression of the amount of monitoring wells at Kv. Renen 13. c) The photograph is taken during the measurement of line 3; the marked area is the location of the sedimentation basin. d) A closer view of the area around the sedimentation basin. e) The photograph is taken from the sedimentation basin facing the garden in front of the administration building. The yellow line shows the edge of the sedimentation basin.

ics industry with surface finishing of metals. The activity consisted of plating with zinc and chromium, tempering with cyanide, preceded by treatment with chlorinated solvents, mainly trichloroethene (TCE) and 1,1,1-trichloroethane (TCA). The two latter have caused the main contamination situation at Kv. Renen 13 and in the surrounding central part of Varberg (Tornberg *et al.* 2008). The industrial history of the estate is shown in Table 1, together with the typical associated pollutants of that industry sector and detected pollutants causing the current situation (Naturvårdsverket 2002).

The industrial building is divided into larger and smaller sections and has a cellar. Different activities have been occurring in different parts of the building. Highest levels of chlorinated solvents have been detected in the cellar, where it is known from former employees that the handling of chemicals has been done (Tornberg *et al.* 2008). Wastewater was taken out through an escape valve that consist of earthenware, with joints of flax and tar, down to a sedimentation basin of "stone blocks", most likely concrete. The size of the basin is 5 m in width, 12 m in length and likely 5-6 m in depth (Larsson & Hübinette 2003). Investiga-

Table 1. History of industry at Kv Renen 13, with associated and detected pollutants (Naturvårdsverket 2002; Tornberg *et al.* 2008).

Period	Industrial branches	Associated pollutants	Detected pollutants
1896-1962	Textile manufacture	Heavy metals, aromatic hydrocarbons, chlorinated and non-chlorinated solvents, phenols, cyanides, PAH and oil	cadmium, chromium, zinc
1962-2003	Surface finishing of metals	Metals, fluorides, cyanides, aromatic hydrocarbons, chlorinated solvents, phenols, PAH, PCB and oils	chromium, zinc cyanide chlorinated solvents; <i>trichloroethene</i> <i>1,1,1-trichloroethane</i>

tion of the escape valve by filming inside shows potentially leaking joints (Tornberg *et al.* 2008). The sedimentation basin was in use until 1972 without any processing of wastewater before sedimentation, and thereafter transported into the municipal sewers. During 1972-1976 the wastewater was processed before transport to the basin. After 1976 the processed wastewater was taken straight to the municipal sewers without sedimentation, or collected in tubs for destruction. The municipality ordered the sedimentation basin emptied in 2003, and this was carried out in 2005. The sedimentation basin was filled up with macadam and covered with concrete, with about 1 meter of soil overburden. It was due to the municipal order that the knowledge of the contaminant situation through several investigations be carried out, resulting in many reports presented and listed in chapter 2.1.1. The cellar and the sedimentation basin are the primary contamination sources of Kv. Renen 13 (Tornberg *et al.* 2008).

The future planning for the area around Kv. Renen is primarily to expand the capacity of the railway by building a tunnel underneath the city. Secondly, there are plans to move the harbour, and use the area to build apartments. During the construction of the train tunnel it will be necessary to lower the water table with an associated increase of the hydraulic gradient that will cause increased transport of contaminants.

Kv. Renen 13 is suitable and interesting for further field investigation as:

- There is extensive background data available
- Presence of chlorinated solvents – the same pollutant type as previously investigated by the TRUST 2.1
- Good potential for water sampling with many existing monitoring wells
- Ongoing pre-investigations of the area due to the expanding of railway line, construction of a train tunnel and other planned infrastructural renovation.
- Cleaning of the site is of high priority as it is the worst polluted site in the county of Halland, and thereby it is possible to follow the remedia-

tion in the foreseeable future and develop the investigation techniques with further time-lapse studies

### 2.1.1 Earlier reports from the Kv. Renen 13

Since the decision to empty the sedimentation basin in 2003 and the plan to remediate the estate, many reports have been produced, giving extensive background material. Most of them have been written by external consultants appointed by Varberg Municipality and are presented in Table 2.

## 2.2 Geology

The regional geology of SW Sweden is part of the Precambrian Baltic Shield and has undergone poly-phase metamorphism in different periods. The most important metamorphic event was the Sveconorwegian Orogenesis during the Mesoproterozoic (1800-900 Ma). It is divided into several segments, with Varberg located in the south easternmost Eastern Segment, Fig. 4 (Lundqvist & Kero 2008).

Three types of bedrock dominate the central area of Varberg; granodiorite, gneissic granite and charnockite, a rare rock type in Sweden. The granodiorite is located in the northeast and is interbedded with gneissic granite. The bedrock in the southwest part consists of a dark charnockite. The frequency and property of the fractures vary depending on the bedrock type, as well as heterogeneities within the bedrock due to distribution of the brittle deformation in the area (SGU 2006).

The Geological Survey of Sweden (SGU) made a detailed investigation of the fracture systems in the area by using recorded alignments in the nature in conjunction with VLF-data aerial surveys. From the lineament interpretation, five dominant orientations were found, 1) northwest, 2) northnorthwest, 3) north-south, 4) northeast and 5) east-west (fairly visible in Fig. 8). A lineament is not a proof of weakness zones and fractures; however they can be good indicators (SGU 2006). The veined gneiss in the northeast has fractures parallel to the foliation and they are rather frequent. The fractures in the charnockite are more regular fissuring, and are fewer in numbers but longer. The

Table 2. A summary of existing reports concerning Kv Renen from 2003-2013. Continues on next page.

Year	Company	Authors	Title	Pages
2003	Golder	Larsson J. & Hübinette P.	Översiktlig miljöteknisk undersökning av föroreningssituationen i och kring slambassäng, Kv Renen	40
2003	Golder	Hübinette P.	PM Kompletterande grundvattenprovtagning kring slambassängen	10
2004	VMC	Sällsten G. & Barregård L.	Miljömedicinsk riskbedömning avseende klorerade kolväten i inomhusmiljön i Bullerbyns förskola, Varberg	9
2004	Tyréns	Magnusson J. & Samuelsson S.	Kompletterande undersökning av förorening runt slambassäng, Kv Renen 13	61
2004	Tyréns	Samuelsson S.	Resultatredovisning av fältarbete, Kv Renen	23
2004	Golder	Hübinette P. & Bank A.	Markföroreningar inom Kv Renen, Varbergs kommun, Miljö- och hälsorisker med klorerade alifatiska kolväten och förslag på inriktning på fortsatta utredningar,	17
2004	Golder	Bank A. & Hübinette P.	Klorerade alifater i inomhusluft i byggnader inom och invid Kv Renen	8
2006	SGU	No named author	Berggrund och grundvatten vid fastigheten Renen, Varberg	7
2006	Aqualog	Lindblad T.	Späckhuggaren 9, Varbergs kommun. Provtagning av berggrundvatten, Redovisning av resultat	19
2006	Golder	Bank A. & Hübinette P.	Samband mellan klorerade alifater i grundvatten och inomhusluft vid Bullerbyns förskola, Kv Renen 17 i Varberg	17
2008	Envipro	Bank A. & Engdahl D.	Riktvärden för klorerade alifater i berggrundvatten inom Varbergs tätort	18
2008	Niras	Tornberg, K., Andersson, J. & Falkenberg, J. A.	Markundersökning och fördjupad riskbedömning på Renen 13, Varberg	275
2008	Aqualog	No named author	Anläggning av bergvärmebrunnar. Resultat från kompletterande undersökning samt förslag till restriktionsområden avseende klorerade alifater	44
2009	Niras	No named author	VA-ledningar i närheten av Renen 13, Varbergs kommun.	5

Table 2. Continues from previous page.

Year	Company	Authors	Title	Pages
2010	Structor	Bank A. & Engelke F.	Vägledning för ny- och ombyggnation av bostäder och lokaler på områden med förorenat berggrundsvatten, Varbergs kommun	29
2011	Structor	Hübinette P. & Bank A.	Kompletterande miljöteknisk undersökning samt miljö- och hälsoriskbedömning och åtgärdsalternativ med avseende på klorerade lösningsmedel i mark, Kv Renen.	201
2012	Structor	No named author	Riskvärdering Kv Renen	20
2013	Structor	Engelke, F., Hübinette, P. & Bank, A.	Fördjupad analys av åtgärdsalternativ inför ansökan om statsbidrag för sanering av klorerade lösningsmedel i mark	212
2013	RGS90	Hinrichsen, H., Nord, H., & Davidsson, L.	Fördjupad åtgärdsutredning	140
2013	WSP	Davidsson, L.	Slutredovisning av utförda undersökningar och tester Renen 13 i Varberg	92
2013	Geosigma	Rahm, N., Nordkvist, R., Hjerne, C. & Mell, S	Fördjupade utredning om föroreningar i berg samt hydrogeologiska förhållanden vid Kv Renen	107

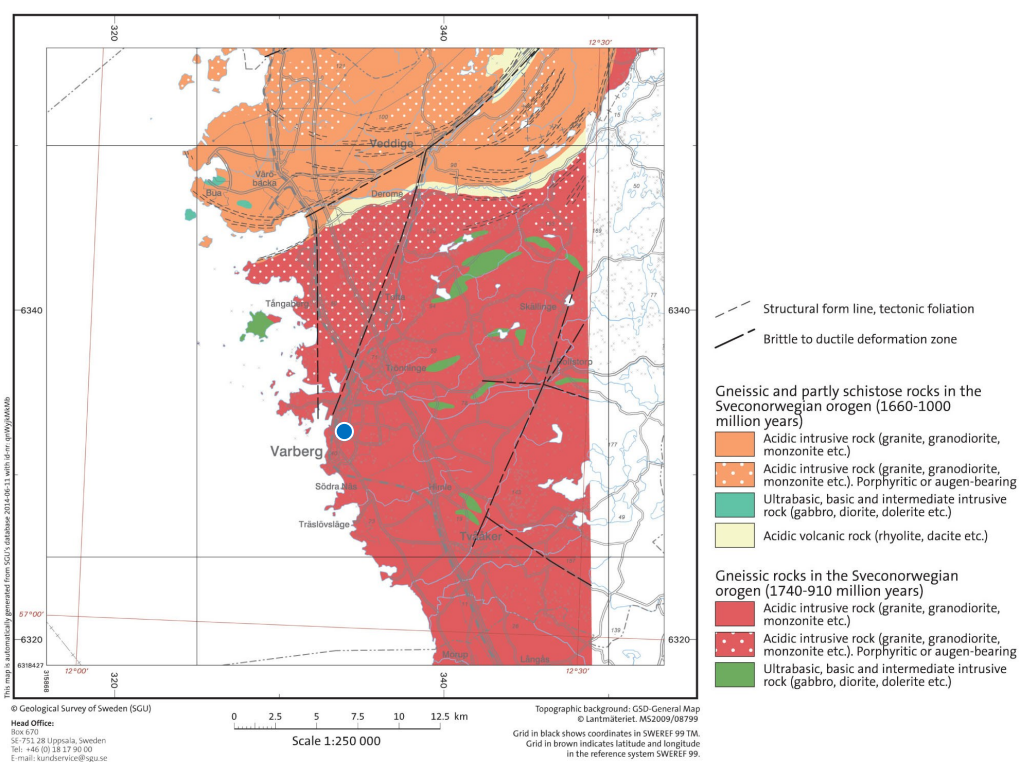


Fig. 4. Regional bedrock map in scale 1:250 000, mapped by SGU. (©Geological Survey of Sweden (SGU)). Kv Renen is marked by the blue dot.

patches of red granite are comparatively rich in fractures (SGU 2006).

The bedrock surface is rather shallow, 2.7-5.3 m below surface, according to an impact sounding investigation by Tyréns AB (Magnusson & Samuelsson 2004). Outcrops at two sides of the industrial estate also indicate the shallow bedrock surface. One in the southern part of the estate and one bigger outcrop approximately 20 m north of the estate. Niras AB made an investigation of bedrock depth by drilling and then interpolation between the points. The resultant interpretation of the bedrock surface is shown in Fig. 5 (Tornberg *et al.* 2008). It indicates that the bedrock surface is dipping in a westward direction and has a low point in the central part of the estate.

Varberg is located below the highest shoreline, with postglacial sand deposits and wave-washed gravel (see Fig. 6). These sediments dominant the lands lower than 15 m above sea level (asl) in the environs of the investigated area (Pässe 1990). At Kv. Renen 13, the sediment is overlain by fill, which consists of a combination of soil, brick and concrete fragments. The thickness of the sediment cover increases westwards in the direction towards the harbour, from 3 m at the estate to 17 m near the harbour. Downstream from Kv. Renen 13, a clay layer also exists within the gravelly sediment, and divides it into two parts (Hübinette & Bank 2011).

## 2.3 Hydrogeology

The sediments overlaying the highly fractured bedrock form together an unconfined aquifer. The highly permeable sediments and the bedrock fracture system provide a fast transport pathway. The groundwater flows west- and south-westward to the harbour in Varberg and the Kattegat Sea (SGU 2006). The silt-clay layer, which appears towards the harbour, divides the shallow aquifer into one open and unconfined part and a lower semi-confined part (Hübinette & Bank 2011). A groundwater flow in a zigzag pattern between fractures in the bedrock might be possible downwards in the aquifer. To be able to create a flowchart for the fissure flow regime, good knowledge about the fractures is required (SGU 2006). No known wells in the area are used for drinking water purposes. Niras AB made a flowchart of the groundwater direction that shows the westward direction of at least the upper part of the unconfined aquifer (see Fig. 7, Tornberg *et al.* 2008).

The hydraulic conductivity has been investigated by slug tests in 14 wells from the 6<sup>th</sup> of November 2013, and calculated both with Hvorslev and Bouwer & Rice methods. Most wells gave results in the interval of  $3.5 \cdot 10^{-5} - 1.5 \cdot 10^{-6}$  m/s, corresponding to sediment fractions of gravelly silt to medium sand (Davidsson 2013).



Fig. 5. Investigation of the bedrock location by drilling, and interpolation between the points. The points are given in meters above sea level. The map indicates a dip of the bedrock surface in a westward direction and a lower location in the middle of the estate. Used with permission from Tornberg *et al.* (2008).

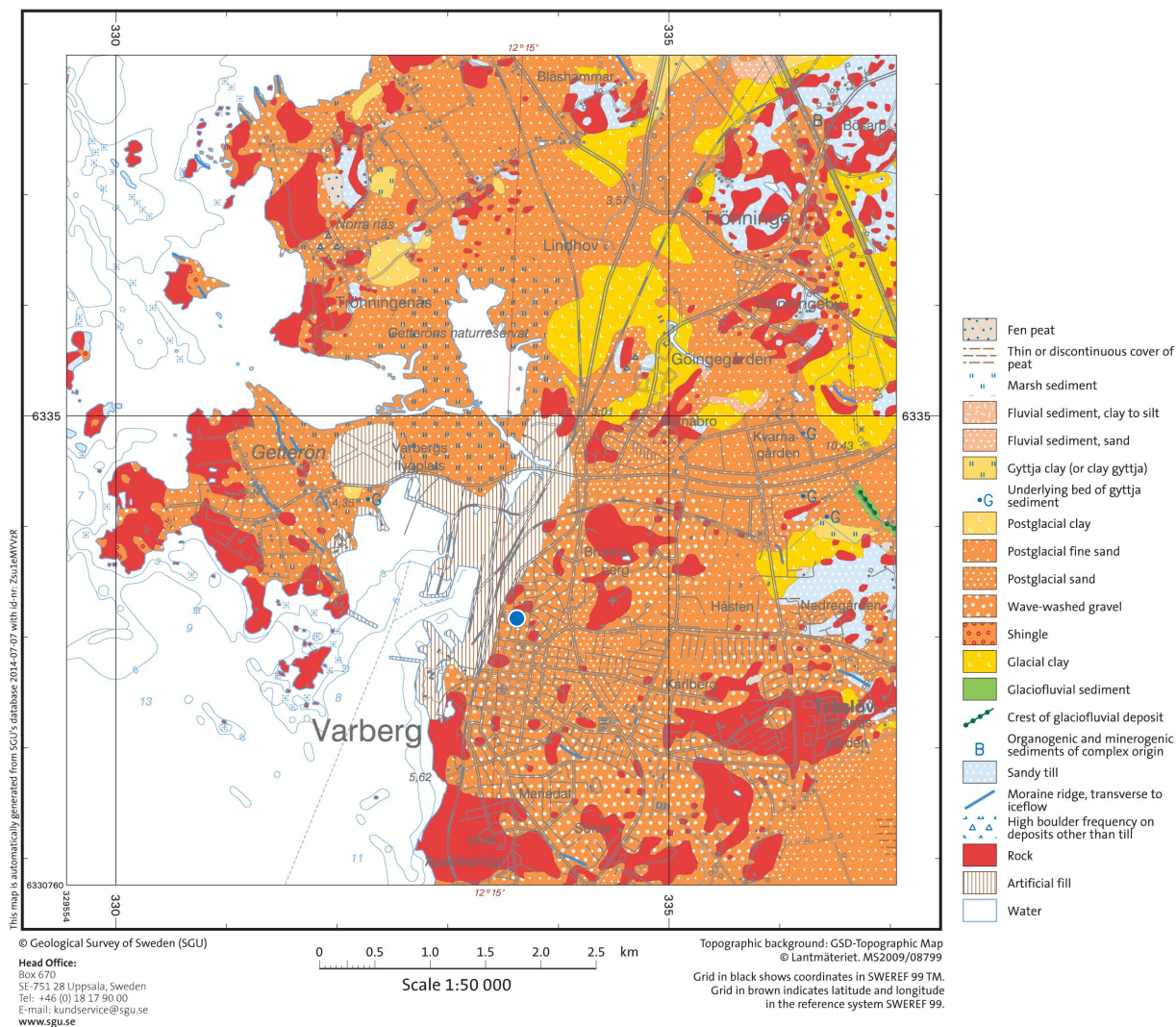


Fig. 6. Local quaternary deposit map at 1: 50 000 scale, mapped by SGU, showing the surface and near surface distribution of different soil types (© Geological Survey of Sweden (SGU)). Kv Renen is marked out by the blue dot.

The precipitation in Varberg has been measured in two series, the first obtained 1931-1960 and the second since 1961. The first series shows an approximate annual precipitation of 800 mm/year, where the second gives an average precipitation of 870 mm/year (SMHI 2013). The actual evapotranspiration in the area is >550 mm/year (Karlqvist *et al.* 1985). The run-off is calculated to be 300 mm/year and the annual mean temperature of the topmost layer of the ground is 7.5° C (Karlqvist *et al.* 1985).

The topography is slightly sloping towards the harbour in the west. Large parts of the area are paved, which decreases the infiltration and favours run-off. Due to the urban environment dispersal along pipes, a reasonable assumption is that a higher yearly level of the pollutant reaching the recipient can be assumed (Tornberg *et al.* 2008).

By combining the knowledge about the area's geology and hydrogeology a primary and a secondary risk area have been established by SGU (2006), see Fig. 8. The primary risk is established based on the

westward to southwestward groundwater flow into the bedrock. The secondary risk is established as a possible case, but relies on if the fractures hydraulically connect. Both the primary and the secondary risk areas extend east of Kv. Renen 13, as shown as a black cross in Fig. 8. This is against the groundwater's main flow direction, and this is due to the possibility of pollutants dispersing within the bedrock fracture system (SGU 2006).

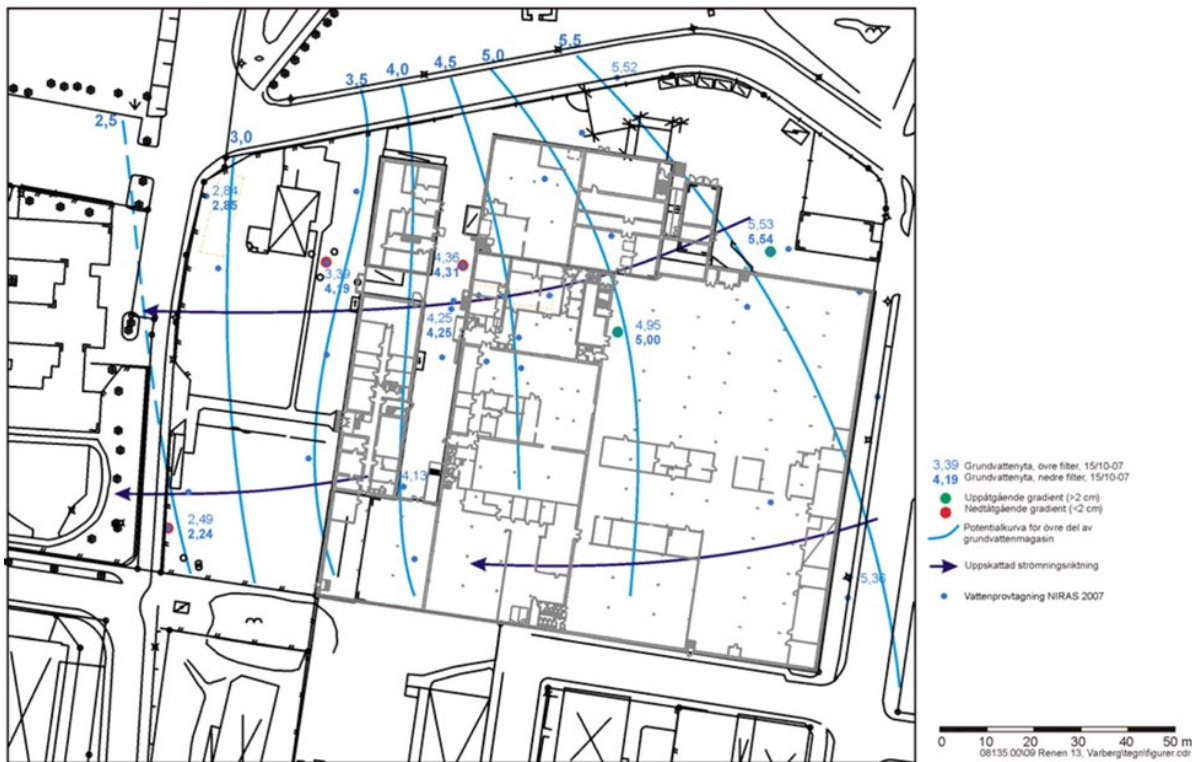


Fig. 7. Groundwater flowchart for the shallow groundwater at the industrial estate, made by Niras AB. Values in meters above sea level (used with permission, Tornberg *et al.* 2008).

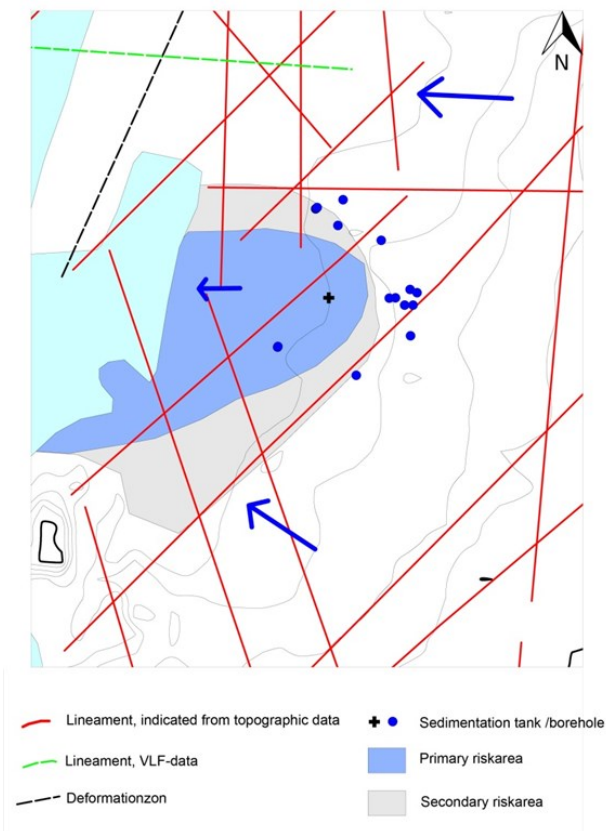


Fig. 8. A primary and secondary risk area is established and marked out on the map. It is established from the groundwater flow direction and interpreted fractures. Modified from SGU 2006.

## 2.4 Contamination

From previous investigations, knowledge about the contamination situation at Kv. Renen 13 is well understood. It is heavily contaminated with a cocktail of chlorinated solvents (trichloroethene and 1,1,1-trichloroethane), metals (cadmium, chromium, zinc) and cyanide (Tornberg *et al.* 2008). The chlorinated solvents are the main pollutants within the area, and will be the focus of this study.

Chlorinated solvents are open hydrocarbon chains, aliphatic, with substituted chloride instead of one or several hydrogens, called chlorinated aliphatic hydrocarbons (CAHs). They do not dissolve well in water; instead they are a non-aqueous phase liquid, NAPL. Chlorinated aliphatics densities are 1.2-1.7 g/cm<sup>3</sup>, which makes them denser than water, and hereby called dense NAPLs – DNAPLs (Pankow & Cherry 1996). As they do not dissolve in water and are denser, they penetrate the groundwater table and sink until they reach an aquiclude or solid surface, e.g. non-permeable bedrock. If the bedrocks surface has a swale, the DNAPLs may form a pool where it can stand for a long time, a residual of contamination. The DNAPLs will, if the bedrock is fractured, penetrate even deeper down. How deep depends on several factors, but from knowledge of other documented sites, they can reach to depths of several hundred meters and more. Maximum depth in some cases is likely greater than 1000 m (Pankow & Cherry 1996). The pattern of dispersal for DNAPL is illustrated in Fig. 9 with the pool, plume, and pathway within the bedrock fractures.

The hazard and risk of chlorinated aliphatics, especially TCE, is that it also vaporizes, as it is a volatile organic chemical (VOC). In the unsaturated zone and from shallow contaminated groundwater they can vaporize and result in vapour upwelling into buildings (Little *et al.* 1992). Chlorinated solvents are generally not noticed by typical taste or odour in levels for ground water contamination (Pankow & Cherry 1996). As it is difficult to notice chlorinated solvents, it makes them even more hazardous as contaminants. Known from Kv. Renen 13 is that the nursery school downstream has been closed due to high indoor levels of volatiles chlorinated aliphatics (Sällsten & Barregård 2004). The primary pollutant is trichloroethene (TCE) (Tornberg *et al.* 2008). It was used as a solvent during the precision mechanics period to remove organic material, e.g. fat, on metal surfaces before surface finishing. The contaminant is most often associated with dry-cleaning facilities, where it has been used as dry-cleaning fluid during the early 20<sup>th</sup> century, and is also a degradation product from tetrachloroethylene (PCE) which as well has been used as a dry-clean fluid (Englöv *et al.* 2007). TCE are carcinogenic substances, and exposure to it increases the risk for cancer in: the liver, kidney, lung, testes and haematopoiesis system according to Guha *et al.* (2012). In Sweden TCE's use has been forbidden since 1995 (Englöv *et al.* 2007), and the product is regarded by the European Union as a substance of very high concern (ECHA 2010). Acceptable levels in indoor air for lifelong exposure are very low. The national guideline value in ground water for TCE and PCE together is 10 µg/l (SGU 2013a). Within the area of Kv. Renen 13, there is currently no drinking water abstraction.

The secondary pollutant is 1,1,1-trichloroethane (TCA). Like TCE it has been used as a solvent during preparation work before surface finishing in the metal industry (Tornberg *et al.* 2008). It is classified as possibly carcinogenic to humans, based on animal testing (Guha *et al.* 2012). TCA is also a forbidden substance to use in Sweden since 1995. TCA is one of the products responsible for ozone depletion, and thereby controlled by the “Montreal Protocol on Substances that Deplete the Ozone Layer” (Englöv *et al.* 2007). Degradation of CAH can occur naturally by microbial processes in the soil and groundwater. For highly chlorinated CAHs the most common degradation is by reductive dechlorination, but for CAH chlorinated to a lower degree, degradation occurs both by oxidation and reduction. Anaerobic reductive dechlorination occurs by an exchange of chloride by hydrogen, and the process occur step wise with one exchange at a time, illustrated for TCE in Fig. 10. CAH can also degrade by co-metabolism as a by process in bacterial metabolism using other carbon sources where enzymes catalyse during the dechlorination. This can take place both under aerobic and anaerobic conditions (Englöv *et al.* 2007).

TCE decomposition products are 1,1-dichloroethene (1,1-DCE) and 1,2-dichloroethene (cis- and trans-1,2-DCE). They decompose further on to vinyl chloride (VC), with the end products being ethene and chloride ions. 1,1,1-trichloroethane (TCA) is degraded to 1,1-DCE and 1,2-dichloroethane (1,1-DCA), and further to chloroethane (CA). The mobility in water increases when the numbers of chloride atoms reduce from the CAHs (Fig. 11) (Pankow & Cherry 1996).

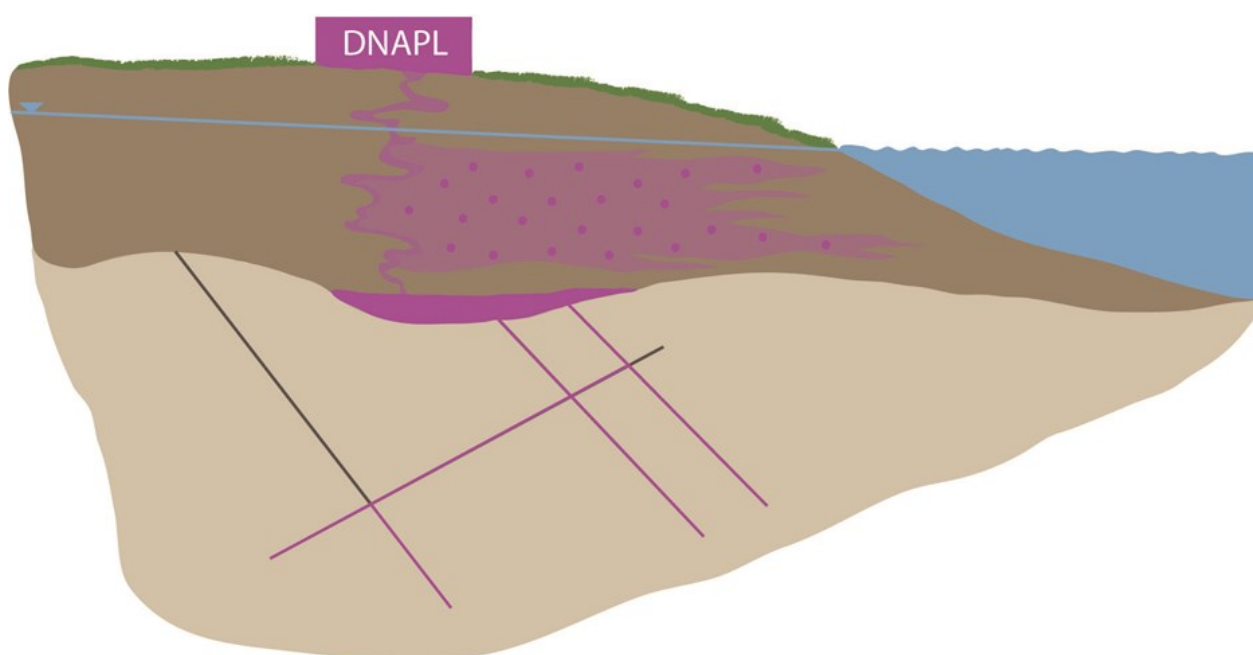


Fig. 9. Conceptual model of DNAPL subsurface dispersal.



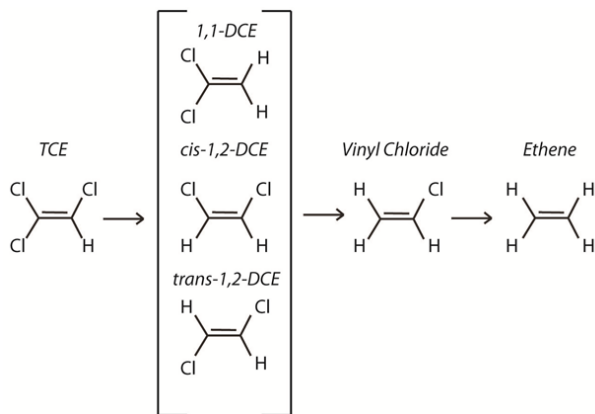


Fig. 10. Stepwise degradation of TCE

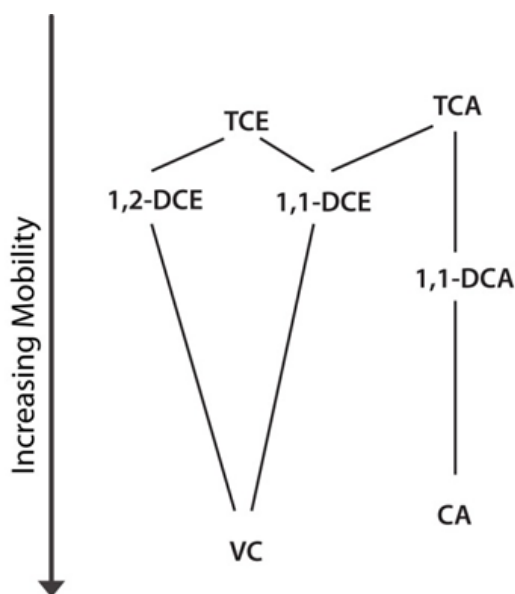


Fig. 11. Degradation of chlorinated solvents dissolved in groundwater and their relative mobility (based on Pankow & Cherry 1996).

Chlorinated solvents are the pollutants targeted within the Trust 2.1 project for investigation and for following the degradation and transport with geophysical measuring methods. As the transport of chlorinated solvents are hard to predict due to their high density and the fact that they have been used in almost every little village's dry cleaning facility, the problem in investigating and prove successful remediation, calls for a better, cheaper and non-destructive investigation method, and the resistivity and IP measurements are showing promising results in this regard.

#### 2.4.1 Contamination situation

Free-phase is assumed when the concentration in groundwater are approximately 1-5% of a substance's effective solubility in water (Swedish Geotechnical Society 2011a). The measured solubility for TCE is *c.* 1400 mg/L and for 1,1,1-TCA *c.* 1300 mg/L (Parkow & Cherry 1996). Thereby concentrations of 13,000-70,000 µg/l, or even higher, are likely in free-phase. Levels of *c.* 23,400 µg/l chlorinated solvents

have been detected in a water-bearing fracture-zone at approximately 40 m depth, on the other side of the neighbouring street (10 meters north) of Kv. Renen 13. Chlorinated solvents have also been detected towards the west in a geogeneity well located at Kv. Späckhuggaren 9 (Rahm *et al.* 2013). The level of pollutants in the lower plume is limited by degradation, as well as by dilution with fresh groundwater (HübINETTE & Bank 2011).

#### 2.4.2 Dechlorination

The body that causes contamination is in accordance to Swedish environmental law responsible for the cost of the remediation if the contamination took place after 1969 (SFS 1998:808). Länsstyrelsen in Halland (County Administrative Board in Halland) did a responsibility assessment where they found that all companies involved in processes possibly leading to the contamination situation at Kv. Renen 13 have been declared bankrupt or do no longer exist. Therefore is it not possible to consider anyone responsible for the remediation costs (Sernrot 2013). Varberg Municipality owns the estate as they received it after Givab Industriverktyg AB was declared bankrupt. As landowners, Varberg Municipality are liable to carry costs corresponding to the expected increase in property value after decontamination has been performed. The current industrial estate has no market value, and how large the increase in value will be is impossible to determine. However, the demand for a centrally located residence or commercial property provides good possibilities for exploiting the estate after decontamination (Sernrot 2013). Governmental funding can pay the rest of the cost. Varberg Municipality has applied for 91 million Swedish kronor from Naturvårdsverket (Swedish EPA) to decontaminate the estate. According to the application, the municipality will co-fund 6 million Swedish kronor. If they are granted the money, the process will start immediately and is set to be finished in 2020 (Varberg kommun 2014). The suggested decontamination includes treatment of: sediment, bedrock and groundwater (Engelke *et al.* 2013). Status for the application during the writing of this thesis is that Naturvårdsverket has requested additional information to be able to process the application (personal communication with Magnus Källström, Varberg Municipality 2014-11-26).

Structor Miljö Väst AB has on behalf of Varberg Municipality worked with alternatives to reduce the contamination and has suggested four alternatives, with varying ambition (Engelke *et al.* 2013). The municipality has, with advice from Trafikverket (Swedish Transport Administration) and Länsstyrelsen i Halland, decided to work with the most ambitious proposal. The treatment suggested within this proposal is a combination of; 1) excavating part of the soil, 2) stimulated reductive dechlorination of the source located in connection to the industrial building, 3) In Situ Thermal Desorption (ISTID) of the contamination source in the sedimentation basin and 4) stimulated

reductive dechlorination of the contaminated groundwater plume. The aim is to fulfil the overall objective as follows (Varbergs kommun 2014):

- The people in Varberg shall not be exposed for harmful concentrations of chlorinated solvents from Kv. Renen 13;
- Dispersal of chlorinated solvents from Kv. Renen 13 in sediments shall eventually be eliminated;
- Dispersal of chlorinated solvents in bedrock from Kv. Renen 13 shall be reduced significantly;
- The property Kv. Renen 13 shall be able to be used for purposes corresponding to “less sensitive land use (MKM)” without any health risks.

Stimulated reductive dechlorination is one of the suggested methods for remediation of Kv. Renen 13. Treatment *in situ* is often a good method to use, as it is comparably cheap and non-destructive. It often acts by; present existing microorganisms getting stimulated by adding organic substrate or nutrients into the

groundwater, which will stimulate the microbial growth. The result of remediation of contaminated groundwater depends on the subsurface conductions such as existing microbes and geochemical properties. It is better if the specific microbes, which are able to perform reductive dechlorination already exist, than to try adding them. It needs to be, at least locally, anaerobic conditions, and thereby an environment that has a negative redox-potential. Two other important geochemical properties that favour reductive dechlorination are the level of dissolved organic carbon (DOC) and pH. DOC is chemically important as an electron donor. It is especially important to consider the impact of other pollutants, when one chooses an *in situ* remediation method, as other pollutants may have a negative impact on the microbes performing reductive dechlorination. At Kv. Renen, there is arsenic, selenium, iron and manganese assumed to be dissolved by the low redox-potential (Swedish Geotechnical Society 2011b). Geochemical parameters limiting stimulated dechlorination are presented in Table 3 (Swedish Geotechnical Society 2011b).

Table 3. Important geochemical properties and values related to the potential of a promising stimulated dechlorination (Swedish Geotechnical Society 2011b).

Parameter	Screening value	Description
Redox potential	<-200 mV	Favourable conditions
	-200 to -100 mV	
	-100 – 200 mV	Less favourable conditions
	> 200 mV	
DOC*	>20 mg/L	Significant supply of organic electron donors
	5-20 mg/L	Possible supply of organic electron donors
	<5 mg/L	Limited supply of organic electron donors
pH	6.5- 7.5	Optimal pH
	5-6 or 8-9	Favourable conditions for microbiological increases in the aquifer (lower speed)
	<5.0 or >9.0	Unfavourable conditions for microbiological increases in the aquifer

\*Dissolved organic carbon

#### 2.4.3 Pilot study of stimulated reductive dechlorination

A pilot study of *in situ* remediation has been performed at Kv. Renen 13. The method used was the injection from a carbon source of lactic acid to stimulate the already existing bacteria in the subsurface. The injection took place on the 23<sup>rd</sup>-24<sup>th</sup> of January 2013 (Hinrichsen *et al.* 2013). The carbon source compounds injected were the 3D Microemulsion (3DMe) and HRC Primer (personal communication with Hele-

na Nord, RGS90, 2014-10-03). They were injected together in a delivered mix. The HRC Primer is used to optimize the reductive conditions in the ground.

The molecule is designed to have a microemulsion molecular structure, and thereby is both hydrophilic and hydrophobic. It consists of three parts; free lactic acid, controlled-release lactic acid (polylactate) and a fatty acid component, which is esterified to glycerin. The parts are released stepwise, which gives a long-lasting impact of the remediation; calculated to

be active 3-5 years after the injection, see Fig. 12. The lactate will immediately release with a short impact time. After a certain time period, the polylactate-based portion will be released in a more controlled way due to its metabolization. Lastly, with the longest lasting impact, the free fatty acids and fatty acid esters will be released (http://regenesi.com/products/3-d-microemulsion/).

The mixed-liquid was injected by direct-push injection in 8 locations in a small area down into the ground, see Fig. 13. The injection started at *c.* 3 m below the ground surface, where 105-315 L of the carbon source was injected, repeating each half meter

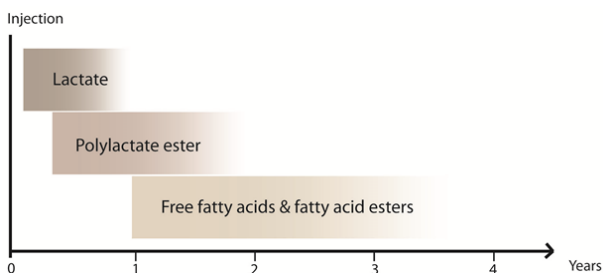


Fig. 12. 3DME has three components that stepwise will be released with an impact in the injected area lasting 3-5 years.

to a maximum depth of *c.* 5 meter (likely the bedrock basement), Tab 4 (Hinrichsen *et al.* 2013).

Monitoring of the remediation impact was performed by analyses of groundwater samples, which took place at three different times. The results from the groundwater analyses are presented in Table 5. Well GV105-2 is the only well with results both before and after the injection. The samples taken the second time, after the injection, have for all sampled parameters a higher value than before. In the other cases results show a decreased level of the high CAH, and increased levels of lower CAH and ethenes.

BioTraps were installed in wells in the vicinity of the injection area, for measurement of possible increases in the bacteria *Dehalobacter* and *Dehalococcoides* in the subsurface. Two BioTraps were installed in November 2012, before the injection and three in March 2013, after the injection. The traps showed a bacterial increase of 100-400 times during 3-4.5 months (Davidsson 2013). A supplementing microbiological analysis of functional genes was performed from the BioTrap in GV105-2, where BAV1 was found. This functional gene indicates the existence of bacteria with the capacity to fully degradate TCE into ethane, and the analyses verified their presence (Davidsson 2013). The test indicates all together, a

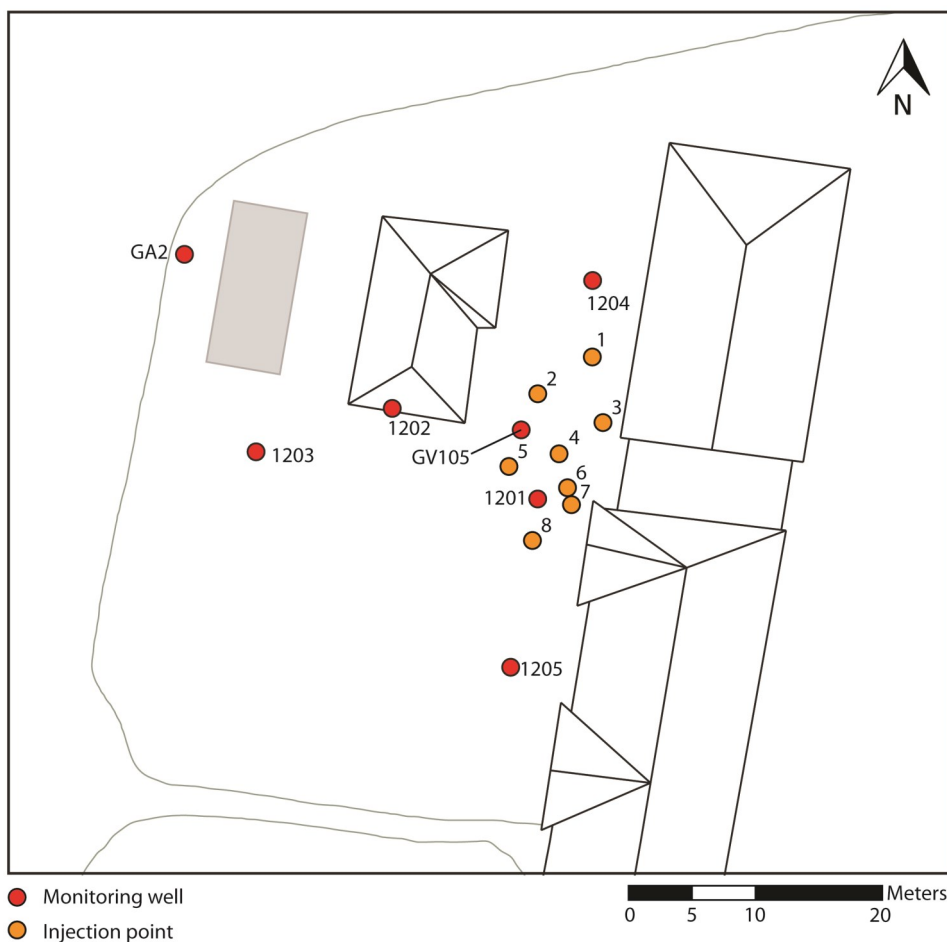


Fig. 13. Location of the direct-push injection points of 3D Microemulsion and HRC Primer, and the used monitoring wells in the area.

*Table 4.* The protocol from the injection of a pre-mixed substance of 3D Microemulsion and HRC Primer into the eight injection points shown in Fig. 13. The total volume of injection was 4410 L (Davidsson 2013). In two points, only small volumes were possible to inject in the bottom part.

<b>Injection point</b>		<b>1</b>	<b>2</b>	<b>3</b>	<b>4</b>	<b>5</b>	<b>6</b>	<b>7</b>	<b>8</b>
Meter below surface	3	105	105	105	105	105	105	105	105
	3.5	105	105	105	105	105	105	105	105
	4	105	105	105	105	105	105	105	105
	4.1						small volume	small volume	315
	4.5	105	105	105	315	315			
	4.8			210					
	5	210	105						
	5.2		105						
Total volume (L)		630	630	630	630	630	315	315	630
Maximum depth (m)		5	5.2	4.8	4.5	4.5	4.1	4.1	4.1

*Table 5.* Levels of substances in the groundwater samples from the remediation zone. Samples were taken before the injection (November 2012), shortly after (March 2013) and c. 5 months after (June 2013) (Davidsson 2013).

<b>Well</b>	<b>Date</b>	<b>TCE (µg/l)</b>	<b>cis-DCE (µg/l)</b>	<b>VC (µg/l)</b>	<b>1,1,1-TCA (µg/l)</b>	<b>1,1-DCA (µg/l)</b>	<b>Ethene (µg/l)</b>
GV105-2	Nov. 2012	1 300	4 620	67	1000	680	<2.0
	March 2013	73 800	33 067	428	6310	2010	34
	June 2013	5 300	25 250	870	3400	1600	84
1201	March 2013	13 300	53 644	107	4100	2570	15
	June 2013	5 700	32 330	240	4100	1700	10
1202	March 2013	2 170	18 610	205	174	1320	12
	June 2013	200	28 250	300	160	1400	-
1203	March 2013	211	11 0898	938	326	2290	11
	June 2013	220	45 510	4 400	20	150	22
GA2	Nov. 2012	539	4 510	114	188	181	-

positive response of the injection (Hinrichsen *et al.* 2013). The method is claimed to give an increased degradation effect during 3-5 years (<http://regenes.com/products/3-d-microemulsion/>). However, no monitoring is currently taking place.

This pilot study was unknown to the TRUST-project before this survey began.

## 2.5 Additional geophysical investigations

During the process of this thesis, other geophysical methods have been used by the Trust 2.1 project to investigate the estate. The data and results are unpublished, but used with permission from Sara Johansson, LTH/Tyréns AB (personal communication, 2014-11-30). Used methods were time domain electromagnetic metal detector (Geonics EM61) and magnetic gradiometry (Geonics G-858 MagMapper), aiming to find and verify the existence of objects which can cause a response in DCIP, for example metal reinforcements, cables, drainage pipes and alike. The

measurements were done in three areas, one by the sedimentation basin, Survey I, one in the northern part of the estate, Survey II, and one in the southern part, Survey III.

Time-domain electromagnetic methods measure the response decay of the signal in the receiver coil (mV), which arises due to electromagnetic induction in metal objects in the ground. The maximum depth penetration of the instrument is 3-4 m (Yarie, *without year*). Interesting anomalies are marked out on the map, Fig. 14, which shows the values of the first time window (mV) measured with EM61. Anomalies A in Survey I correlate to the sedimentation basin and represent the reinforced concrete of the basin construction. Anomaly B in Survey II correlates very well with the well covers of metal. In Survey III, the anomaly C likely shows something leaking out from the house towards the west.

Magnetic gradiometers measures the magnetic field gradient (nT/m) between two sensors. With the sensors in a vertical orientation, the method is sensi-

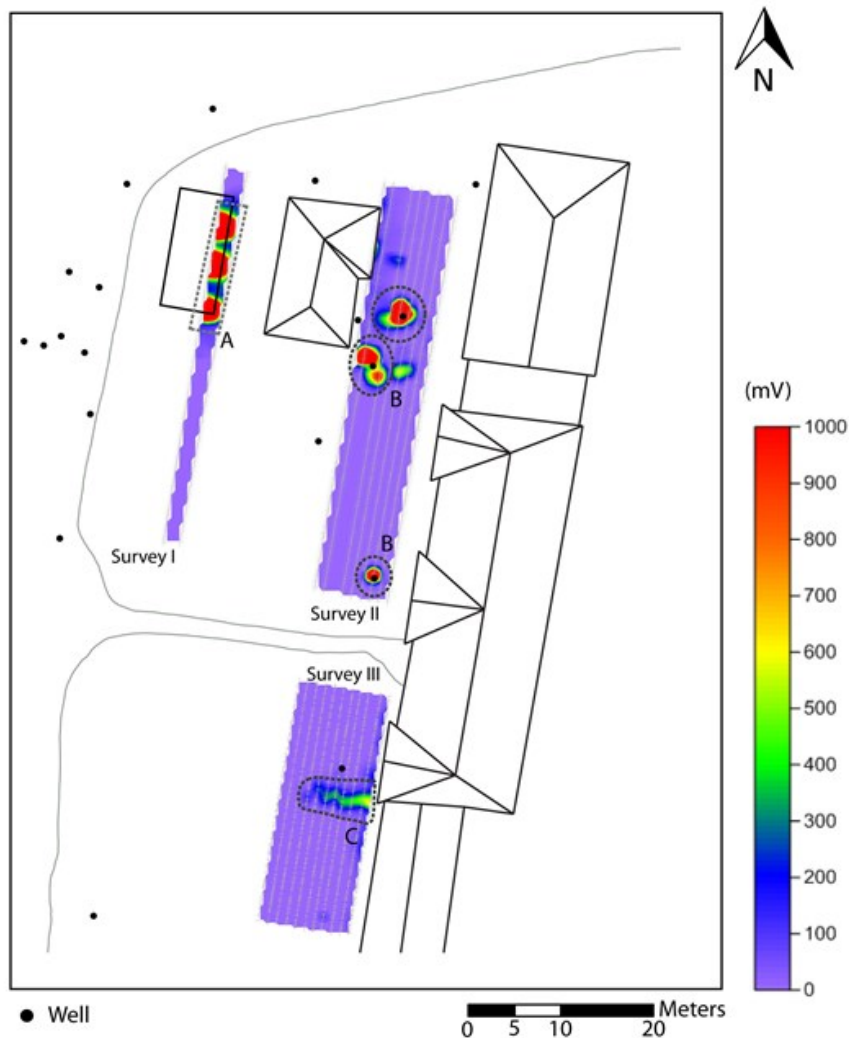


Fig. 14. Survey I show anomaly A corresponding to the concrete reinforcement of the sedimentation basin. Survey II's anomaly B, correlate to well covers of metal. In survey III, an anomaly shows something leaking out, possibly to the concrete covered well.

tive to near surface magnetic objects. Positive and negative values correlate to the same object, depending on the direction when passing the object. The results from the magnetometer measurements are presented in Fig. 15. Due to large variation in values between Survey I and Survey II-III is it necessary to use different scales. The anomalies in survey I correlate to the sedimentation basin and indicate the concrete reinforcement therein. The westernmost anomalies turns elongated and smoothers out as an effect of the data processing, as they have been interpolated with data a bit too far way. The anomalies marked B are interferences from the neighbouring buildings. In survey II area there are two anomalies marked C. They are not fully known for a certain interpretation; however is it assumed a cable for electricity has been drawn from the administration building to the director residence.

Conclusions from these two investigations are that there are some possible metal objects or other sources of noise in the uppermost meters of the subsurface, and that the sedimentation basin probably was constructed out of reinforced concrete. This gives additional and useful information for the following DCIP-data interpretation herein. Even though the DCIP data

at shallow depths should be interpreted with awareness of the electromagnetic and magnetic results, the values and amount of metallic objects are not dense enough in survey areas II and III. Metallic objects at greater depths than 3-4m cannot be detected with these methods, and there are no specific suspicions of metallic objects at these depths.

### 3 Theory

All materials have their own diagnostic physical properties, relating to what they are made up of. The Direct Current resistivity and time-domain Induced Polarization tomography (DCIP) method is based on material's different physical responses to an electrical current. The method consists of two features measured, resistivity and induced polarization (IP). They are commonly measured in the same survey, as it is possible to measure with the same equipment and array. Resistivity is a materials property to isolate a current. Resistivity has the symbol  $\rho$  and is measured in  $\Omega\text{m}$ . Induced polarization is a measure of how a material responds to a voltage, and can be measured in two ways. Here the focus will be on time-domain IP, expressed as chargeability (symbol  $s$ ), in mV/V (Sharma 1997). The varia-

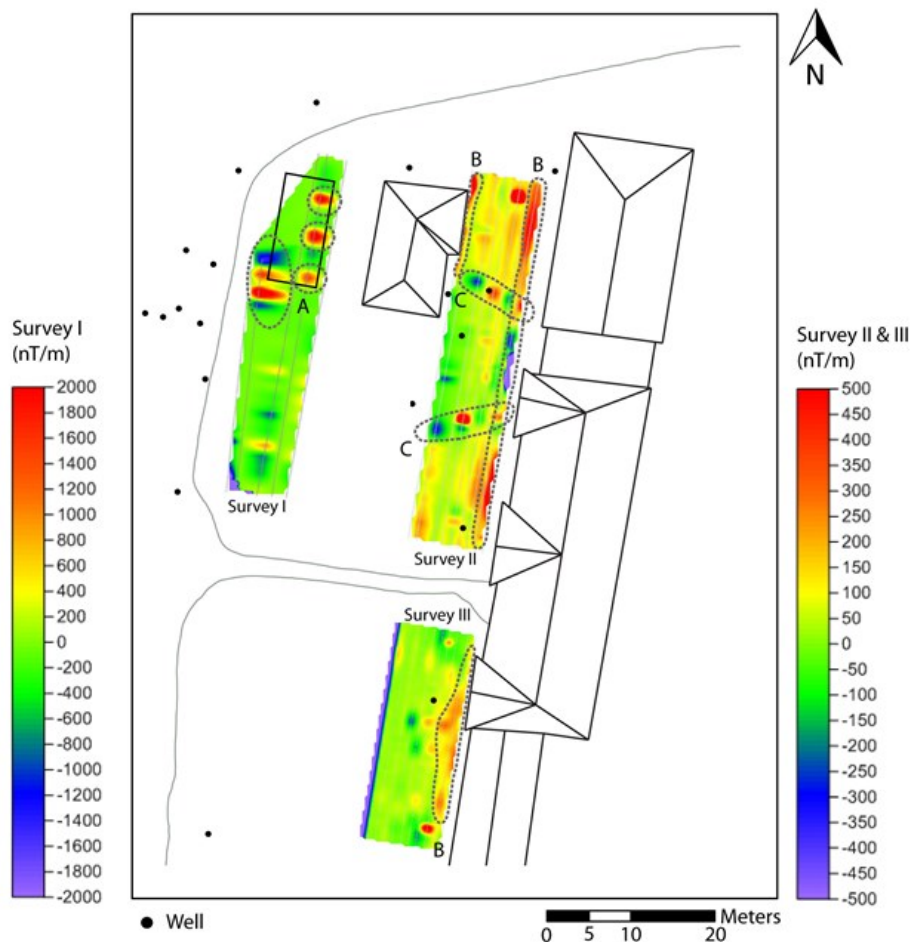


Fig. 15. The Survey I area is located over the sedimentation basin and the anomalies therein indicate a construction of reinforced concrete. The B-anomalies correspond to the neighboring buildings. The Survey II area show two anomalies marked C, which could be cables for electricity.

tion of the response is interesting for the interpretation of the components and situation of the subsurface. The resistivity method was developed in the early 20<sup>th</sup> century, but has become, with example, stronger computers from the 1970s, a more widely used method. It can be used for the investigation and evaluation of bedrock features, groundwater detection and landfill characteristics (Reynolds 1997). Induced polarization was reported by Conrad Schlumberger in 1912 and it has since the 1940s been used for metal exploration (Reynolds 1997). However, it has lately been used for a wider application, such as investigations of environmental and hydrological issues.

### 3.1 Resistivity

Resistivity,  $\rho$ , is a material dependant parameter that quantifies how strongly the given material resists the flow of an electrical current. The resistivity is measured in the unit  $\Omega\text{m}$ , given as the product of the resistance,  $R$ , ( $\Omega$ ) and the geometrical factor,  $K$ , (m) (Eq. 1). The geometrical factor is dependent on the distance between the electrodes and the electrode array, and can be described as the quotient of length,  $L$ , (m) by the cross sectional area,  $A$ , ( $\text{m}^2$ ) Eq. 2 (Reynolds 1997).

$$\rho = R \cdot K \quad \text{Eq. 1}$$

$$K = \frac{A}{L} \quad \text{Eq. 2}$$

Which gives that the resistivity can be described as;

$$\rho = R \frac{A}{L} \quad \text{Eq. 3}$$

Ohm's law describes resistance as the quotient of voltage, (V), by the amperage,  $I$ , (A);

$$R = \frac{V}{I} \quad \text{Eq. 4}$$

By combining Eq. 3 and Eq. 4 gives

$$\frac{\rho L}{A} = \frac{V}{I} \quad \text{Eq. 5}$$

The geometrical factors,  $L$  and  $A$ , can be estimated by using the definition of voltage as the product of  $E$ , the electrical field (V/m) and  $L$ , the distance (m)

$$V = E \cdot L \quad \text{Eq. 6}$$

and amperage is the product of  $J$ , current density ( $\text{A}/\text{m}^2$ ) and  $A$ , Area ( $\text{m}^2$ )

$$I = J \cdot A \quad \text{Eq. 7}$$

By combining former equations 6-7, the resistivity is given by the quotient of the electrical field by the current density;

$$\frac{\rho L}{A} = \frac{E \cdot L}{J \cdot A} \rightarrow \rho = \frac{E}{J} \quad \text{Eq. 8}$$

which show an existing relationship between the material dependent property and the electrical field and current density. When  $\rho$  is a material dependant property, then  $E$  and  $J$  will be so too (Jeppsson & Dahlin 2014).

This will just be true if the material is homogenous which is very rare within earth materials. In reality we assume that the measured volume is heterogeneous and consists of several materials with different resistivity. The measured resistivity will then be a mean value, and which is called apparent resistivity (Reynolds 1997). The data can be presented as apparent resistivity in a pseudosection, and requires processing by inverse numerical modelling to build a model of the real resistivity, see chapter 3.3.

In order to get a current to flow through a medium it is required that the material is conductive. In a geological perspective, this can take place in different ways; most geological medium are porous or have fractures where the current can flow in connected systems by fluids. The current can also flow through mineral grains or at the surface of mineral grains by absorbed ions. Resistivity can vary widely between different geological materials and within the same type, from  $<1$  to  $>10^6 \Omega\text{m}$ . Typical ranges of resistivity for geological materials are presented in Fig. 16. Additional for the data for the diagram (fig. 16); dry gravel has a higher resistivity than saturated gravel, i.e. groundwater lowers the resistivity. Topsoil has a wide spread, depending to its contents, often between 250 and 1700  $\Omega\text{m}$  (Reynolds 1997).

The interval of resistivity for one geological material is wide and often overlaps with other materials, which is important to keep in mind when interpreting the results. Different geological settings or models can give the same measured result, equivalence problems, and is a well-known issue when using geophysical measuring methods, e.g. DCIP (Reynolds 1997). Knowledge of the subsurface geology, such as layering and other existing properties are required to make a good interpretation of the data.

The voltage around an electrode is spread in a hemisphere, such as a 3D electrical conductor (Fig. 17). Anomalies in the ground close to the electrodes will have a strong impact on the 2D-data, and generate 3D-effects, which makes the interpretation difficult. When or if anomalies occur, one should try, if possible, to place the survey line so the impact of the 3D effect becomes as low as possible (Jeppsson & Dahlin 2014).

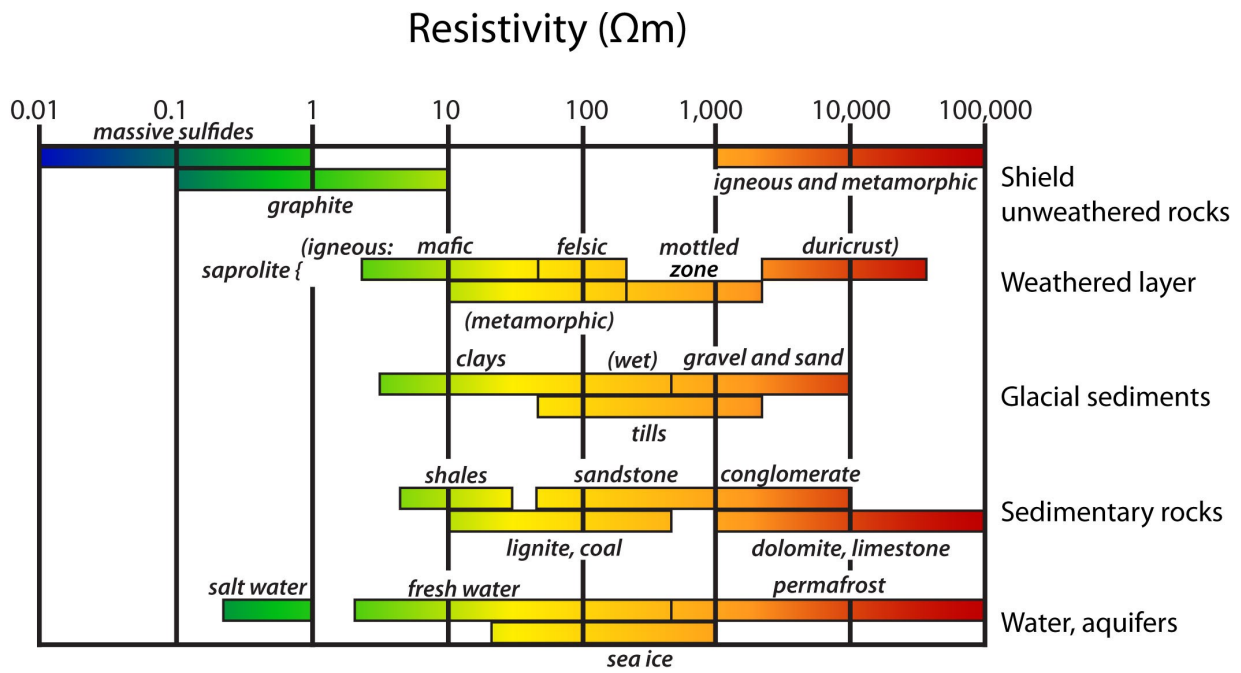


Fig. 16. Typical ranges of resistivity for geological materials, showing the overlap of value (based on Palacky 1987).

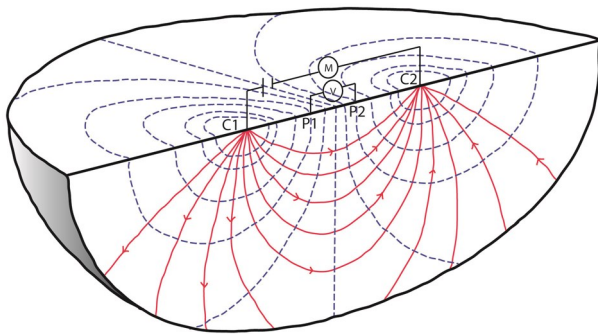


Fig. 17. A visualization of how the current flow as a hemisphere through earth. Red lines show the electric flow field, where the dashed blue lines are the equipotential lines.

### 3.1.1 Field setup

Resistivity is measured by using four electrodes, two for leading a known direct current into the ground and two for measuring the voltage. The two types of electrodes are called current and potential electrodes, and form a quadrupole. This quadrupole was set up in a specific array, and historically to be able to make a profile it was necessary to move the electrodes after each measurement was done. The depths depend on the distance between the current electrodes, the array and the subsurface layer properties. There are several classic types of electrode arrays that give different qualities of the results, e.g. penetration depth and vertical resolution (Reynolds 1997). Measurements with a multi-electrode setup are a more modern and common way to perform a survey. Several electrodes are used (e.g. 82 for full length in this survey) in a line, and a

whole profile can be done without any electrode movements in this way. An embedded relay switch in the instrument selects which electrodes should be included in a specific measurement. Multiple electrode measurements use a gradient array (a type of Schlumberger-array), where it is possible to vary which electrode are the current and the potential one (Loke 2004). By varying which electrodes are included in the quadrupole, and thereby its internal spacing, a pseudosection is built up in both horizontal and vertical directions. Fig. 18 illustrates how a profile is carried out, where the internal distance change for each quadrupole, a wider spacing gives a deeper level (n) into the section and the section is built up horizontally. Each data point is unique and correlates to a point between the two potential electrodes. The set up generates more data in the uppermost part of the profile and fewer in the bottom and along the margins; therefore the results will have the highest quality are in the upper part of the profile with a decreasing quality downwards. The instrument controls the measurements and navigates which electrodes are included by the use of a pre-programmed protocol.

Multi-electrode measurements make the survey more effective and the amount of data obtained increases. In this survey, the electrodes were connected to two cables in order to obtain data with higher quality and less noise, by using one for transmitting current and the other for measuring the potential (Dahlin & Leroux 2012). Data with good quality require good electrode contact with the ground. The instrument controlled a test before starting the measurements, and the target for the best data quality is as high amperage as possible.



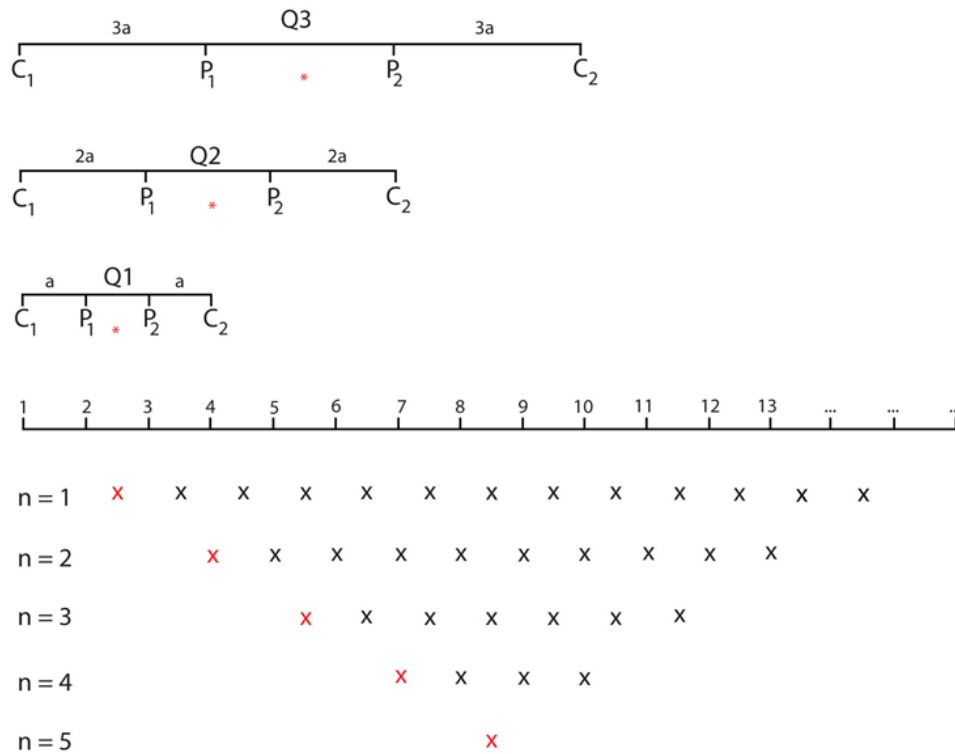


Fig. 18. An example of how the measurement sequence for building a pseudosection can be set up, showing three electrode quadrupole combinations. The greater the internal spacing in the quadrupole, the greater the depth (n) will be for which the data point can be plotted, i.e. the greater electrode distance, the deeper the measurement data point.

### 3.2 Induced Polarization

Induced Polarization, IP, describes the ground's ability to polarize as a response to voltage. To be able to use this method for investigation it is necessary that the ground can be polarized, i.e. have ions or electrons that can move, and is known as the material IP-effect. Waste, contaminants, clay minerals and ore mineral are examples of objects that can be detected by using IP-survey (Reynolds 1997).

IP-effects are complex and the phenomena are not fully investigated. However, polarization of the ground can occur in two ways; electrode polarization or membrane polarization. Electrode polarization takes place if the material consists of free charges, e.g. metal sulphide and metal oxides. Grains are often negatively charged, surrounded by positive sharing particles and thereby possible to investigate with IP, where an applied voltage disturbs the ion balance and causes a current flow, as visualized in Fig. 19 (Reynolds 1997).

Membrane polarization takes place in two ways; by the conditions inside a pore channel which is similar to the single grain and is a negative charged surface with positive charges within in the pore, often into fluid. The other way is the presence of clay particles or filaments of fibrous minerals in the subsurface. Both tend to be covered by a net of negative charge (Reynolds 1997). For all these cases in which the negative charge are attracted by the surrounding positive charge, an applied current will interrupt the normal balance distribution. When the current turns off, the

imbalance of concentration will reset to natural balance by diffusion, this produces a measurable IP responses (Reynolds 1997).

IP measurements can be based on either of two main methods, time-domain and frequency-domain (Reynolds 1997). Time-domain IP is measured with direct current and investigates the voltage decay curve. Frequency domain IP is performed with alternating current to investigate the resistivity's dependence on the two different currents used frequency (Sharma 1997). Further description will focus on IP measurements based on the time-domain method as it has been used in this survey.

The equipment and array used for IP-survey is the same as in resistivity measurements using four

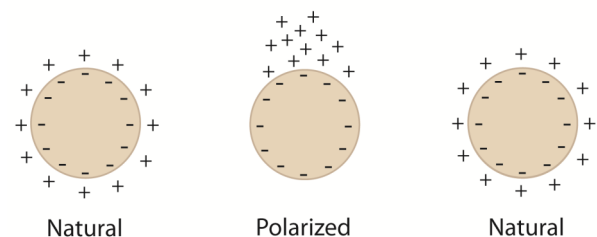


Fig. 19. A natural case with the grain negatively charged, most often, surrounded by positive charge. By turning on a current the surrounding charge will be polarized, when the current turns off the charging will stabilize to the natural conditions. The time it will take is measured during time-domain IP.

electrodes, two current electrodes and two potential electrodes. The time-domain IP method can be described as measuring the decay curve after transmitting a known current ( $I$ ) switch-off. It is measured during a definite time interval,  $t_1$ -  $t_2$  (Sharma 1997).  $t_1$  is often defined after the current has been switched off, to avoid influences of electromagnetic induction effects, see Fig. 20. The determined time of measuring, the decay curve can be divided in time intervals, called windows, where each window can afterwards be analysed separately. Time-domain IP is measured as chargeability ( $M$ ), in mV/V (Reynolds 1997).

Chargeability  $M$  can be described with an integral, where  $M$  is the area under the decay curve during the determined interval of time, (Sharma 1997):

$$M = \frac{1}{V_0} \int_{t_1}^{t_2} V(t) dt \quad \text{Eq. 9}$$

Similar to the resistivity, measured IP is an apparent value and require processing of data through inversion, described in chapter 3.3, to provide an interpretable model of the acquired data.

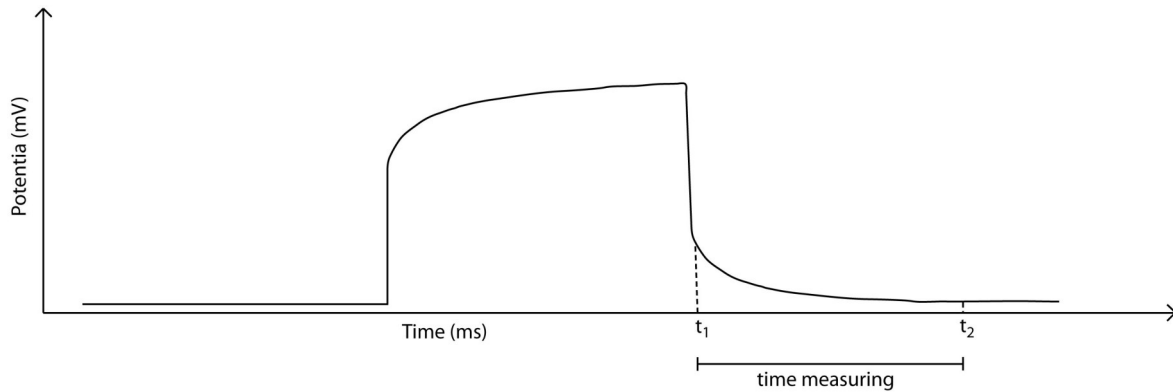


Fig. 20. A current transmitted and turned off, and the delayed decay curve measured during a defined time.

## 4 Methods

To acquire material and results to reach the aims of the thesis, to construct a 2D model based 3D model of the estate's geology and contamination distribution, a combination of methods have been used. Firstly, four geological profiles have been constructed from bore-hole data in earlier reports concerning the area. This was done with the intent to get as detailed knowledge and better understanding of the geology as possible. Secondly, fieldwork was performed at three different times, the 20<sup>th</sup>-21<sup>st</sup> of May 2014, the 25<sup>th</sup>-26<sup>th</sup> of No-

## 3.3 Inversion modelling

The acquired data are giving an apparent depth and data values in order to find an interpretable model, and for the data required to be processed. In most cases when modelling data the model parameters are known, and it is possible to set up a model to give a prediction of data. In inversion modelling it is the data acquired, and a general model used which together estimates the model parameters (Menke 1989). There are several software packages able to operate inversion modelling, e.g. Res2Dinv and Res3Dinv. These are used in this thesis, using a robust (L1-norm) inversion technique (Geotomo software 2014).

The simplest way to describe an inversion problem is to describe it with a linear relation (Eq 10). Where  $d$  is the obtained data,  $G$  is the matrix (integral equations) and  $m$  is the model parameters;

$$d = G \cdot m \quad \text{Eq. 10}$$

The DCIP data and model parameters will be used to estimate a model giving the real depth and value, according to the given data. If the calculated model and the measured values for it do not fit, the program will process the model parameters to fit the data by iterations. It will run for the set numbers of iterations or when the change between two iterations is very small. The resulting model will have a RMS-error, given in percent, a value of deviation between the measured and calculated values (Loke 2004).

vember 2014 and the 17<sup>th</sup> of February 2015. In the field DCIP was measured and the electrode positions were given using Global Navigation Satellite System (GNSS). In November, groundwater was sampled to receive data for verification of the interpretation of the DCIP-data. The DCIP-data needed to be processed to create models for interpretation, which was performed at the office after the fieldwork. All data will be the basis for an interpreted conceptual model of the conditions at Kv. Renen 13, including geology, hydrogeology and the contamination situation.

## 4.1 Geological profiles

Four geological profiles have been constructed from borehole logs in the surveyed area according to Larsson & Hübinette (2003), Magnusson & Samuelsson (2004), Tornberg *et al.* (2008), Hübinette & Bank (2011), Davidsson (2013), and data from probing to identify the bedrock surface (Tornberg *et al.* 2008). The location and orientation of the geological profiles are shown in Fig. 21. For more extensive information see Appendix I.

The first geological profile constructed corresponds to DCIP-line 1 (a-c), the second profile crosses the sedimentation basin, the third profile is situated at the miniature-golf course (corresponds to the DCIP line called MC) and the fourth is crossing the estate between the administration building and the directors residence.

There is an uncertainty in constructing profiles from descriptions in different sources, as the knowledge and type of information is varying with the author and sometimes parts are lacking. For example, in some of the borehole logs, one unit is sometimes described as sand, but in others as grey sand. Uncertainty according to the location of the bedrock exists, however, as it has to be located below the shallow monitoring wells, which are all located in the unconsolidated sediments, we know that the minimum extent of the sediments are at least the depth of the wells. For profile 3, only two wells exist. When possible, the groundwater table measured in November has been included in the profiles. In other cases, no measurements could be made during the field work in November, as some of the wells were not available or uncertainties in location were too large.

## 4.2 Field work

Data were collected in three periods; May 2014, November 2014 and February 2015. The weather in May was warm *c.* 20°C and sunny, in November *c.* 7°C and foggy, and in February it was foggy with temperatures of *c.* 5°C. In total, this survey includes 11 DCIP-lines (four in May, five in November and two in February), presented in Fig. 22-23 and in Table 6. Ground water levels were measured manually in November 2014 in nine wells (Fig. 22-23) with an analogue water level meter.

### 4.2.1 DCIP measurements

Resistivity and IP data were measured using an ABEM Terrameter LS, connected to an ES10-64 external relay switch in order to use parallel cable pairs. Electrode cables with 21 electrode take-outs and 2 meter spacing were used, arrayed midway for electrodes spaced 1 m. The total number of electrodes in the spread was 82. A sketch of the set-up is presented in Fig. 24. Stainless steel electrodes were used. If the pre-measurement contact resistance check indicated poor contact to the ground, electrodes were added where it was necessary. The survey was carried out using mul-

iple gradient array, to be able to use multi electrodes measurement. The power supply was a 12 V battery. A GPS Topcon GNSS GR3 was used in order to obtain positions for the electrodes.

Six survey lines, measured in May and February, consist of 1603 data points each. The survey lines in November consisted of 1141 data points, with the exception of the shorter diagonal survey line Diagonal, where only 553 data points could be acquired. The IP-data measured in May and February were made using IP off time 2 seconds and 10 time windows, whereas in November, 1 second was used as off time with 9 time windows. The differences in settings are fully presented into Appendix II, including the test to recalculate the data acquired in May.

### 4.2.2 Groundwater sampling

Water samples were taken the 26<sup>th</sup> of November with an Eijkelkamp peristaltic pump (12 V) from nine existing monitoring wells, 1201, 1202, 1203, 1204, 1205, GV105-1, GA2, 1012 and 1009 (Figs. 22-23). Before sampling, the wells were pumped and groundwater extracted equal to approximately three times each well's volume. This pumped water was collected, filtered through a carbon filter and let out in the municipality sewer system, with permission from Varberg Municipality. The wells then had time to recover and stabilise before taking the samples.

Samples were investigated both in field with an Aquareader flowcell AP-800 Aquaprobe® and in the AlControl AB laboratory. Parameters measured in the field were: temperature, oxidation-reduction potential, pH, electrical conductivity, total dissolved solids, salinity and turbidity. Collected samples were sent to the laboratory in Helsingborg on the 27<sup>th</sup> of November, and were kept cold in a cooler until delivered. The samples were analysed for metals, dissolved organic carbons (DOC), total organics carbons (TOC), chlorinated solvents (*1,1-dichloroethane, 1,2-dichloroethane, dichloro-methane, trans-1,2-dichloroethene, cis-1,2-dichloro-ethene, 1,1,1-trichloroethane, 1,1,2-trichloroethane, tetrachloroethene, tetrachloro-methane, trichloroethene trichloromethane, monochlorobenzene, dichlorobenzenes, 1,2-dichloropropane, 1,1-dichloroethene and vinyl chloride*), cyanide and chloride. Protection equipment was required during sampling due to expected high levels of hazardous substances. The protective suit used was the Cat. III type 5/6, gasmask with filter A and gloves as shown in Fig. 25.

## 4.3 Data processing

ABEM Terrameter LS Toolbox (version: 1.2.0.1) was used to export the data from the Terrameter LS. Eri-graph (ABEM, version: 2.20.01) was used for quality control of the data. Topographic data were added to the data files, even though the difference in topography is small; see example in Appendix III. The data were exported as DAT-files and opened with the pro-

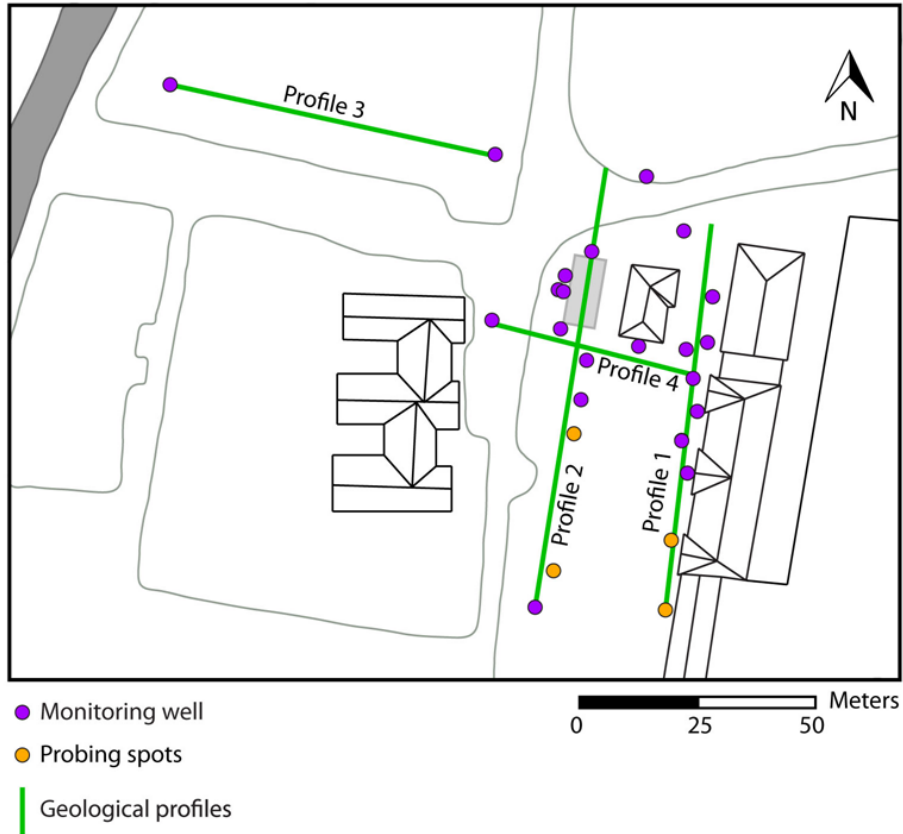


Fig. 21. The location of the geological profiles are shown in green, used monitoring wells in purple and probing in yellow. The same map is presented in appendix I with references for each data point.

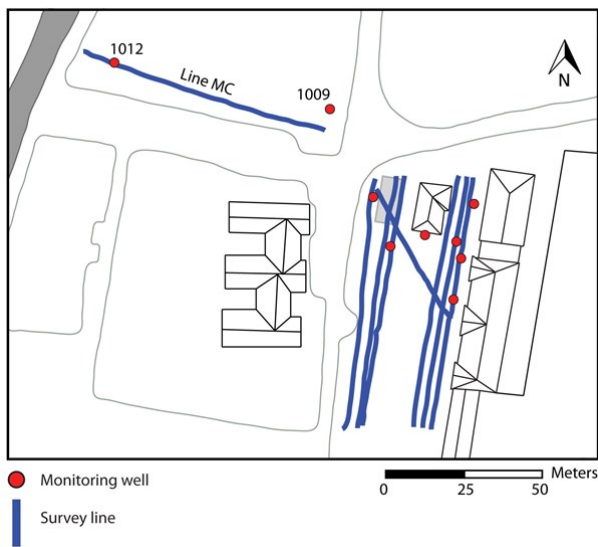


Fig. 22. Map of the DCIP-lines and monitoring wells. A closer view of the survey lines and sampled wells on the estate is given in the next figure (Fig. 23), including names. Compare the DCIP-lines with table 6.

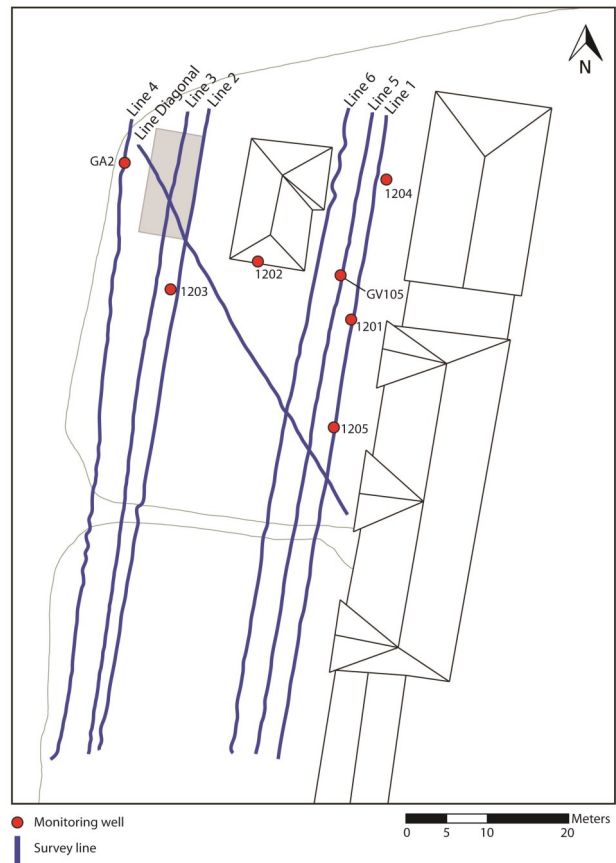


Fig. 23. (To the right) DCIP-lines of the survey, and the monitoring wells used for water sampling. See the measuring date of the DCIP-lines in table 6.

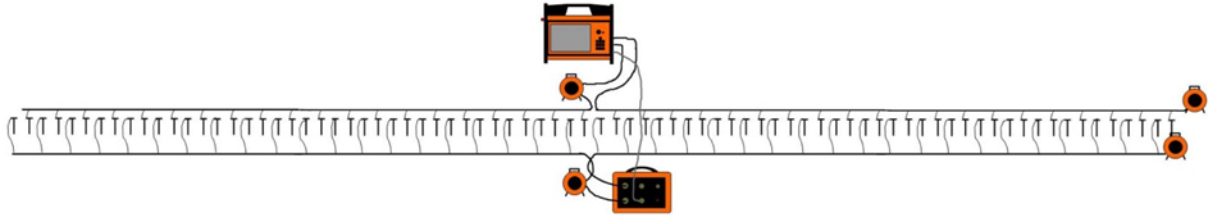


Fig. 24. Sketch of the set-up with separated cable spreads surveyed using 2x2 cables with 21 electrode take-outs each (personal communication Torleif Dahlin).

Table 6. Dates of field surveys and the order of the survey lines (see Fig. 22 and Fig. 23).

Survey Day	Date	Survey Line
1	2014-05-20	Line 1a, Line 2
2	2014-05-21	Line 3, Line 4
3	2014-11-25	Line MC, Line Diagonal
4	2014-11-26	Line 1b, Line 5, Line 6a
5	2015-02-17	Line 1c, Line 6b

gram Res2dinvx32 (Geotomo Software, version: 3.71.115.) for inversion. Instructions to inverting was followed from the manual for RES2Dinv (Geotomo Software 2015, vers: 3.71), appendix IV lists the analysis inversion settings. Outliers were removed. As inversion settings, a robust inversion (L1-norm) was selected with 20 iterations. The inversion was carried out and the inverted model was opened with EriGraph. Fence diagrams of 2D inverted data were made in EriViz. This allows fence diagrams to be turned around in their projection. A time-lapse was made for line 1a and line 1c, in Excel of the inverted model values to achieve results of the variation through time, by calculating the differences in DCIP data of the two lines inverted data.

## 5 Results

### 5.1 Geological profiles

The four geological profiles created from borehole logs are presented in Figs. 26-29. For profiles 1 and 2 drawn in a south-north direction, the ground surface is almost plain and located at 5 m.a.s.l. and for profiles 3 -4, surface level is at 5 m.a.s.l. in the east and dipping down to c. 3 m.a.s.l. in the west. The bedrock surface is for the first two profiles situated at approximately sea-level, however, undulating within the profile area, see Fig. 25 and 26. In profile 1, there is a dip in the middle of the profile, and in profile 2, the bedrock surface rises towards the north. In profile 3 and 4, the bedrock is also dipping westwards. The sediments consist of two-three layers, depending on if the sand layer should be described as one or two different layers. The sediments consist of sands and filling material in all the profiles. The sediment layers change in thickness in between less than 2 m and up to 5 m. In profile 3, the thickness increases westwards, but in profile 4 it stays roughly the same following the bedrock surface.



Fig. 25. Water sampling in progress; the expected high levels of hazardous substances in the water required the use of protective equipment.

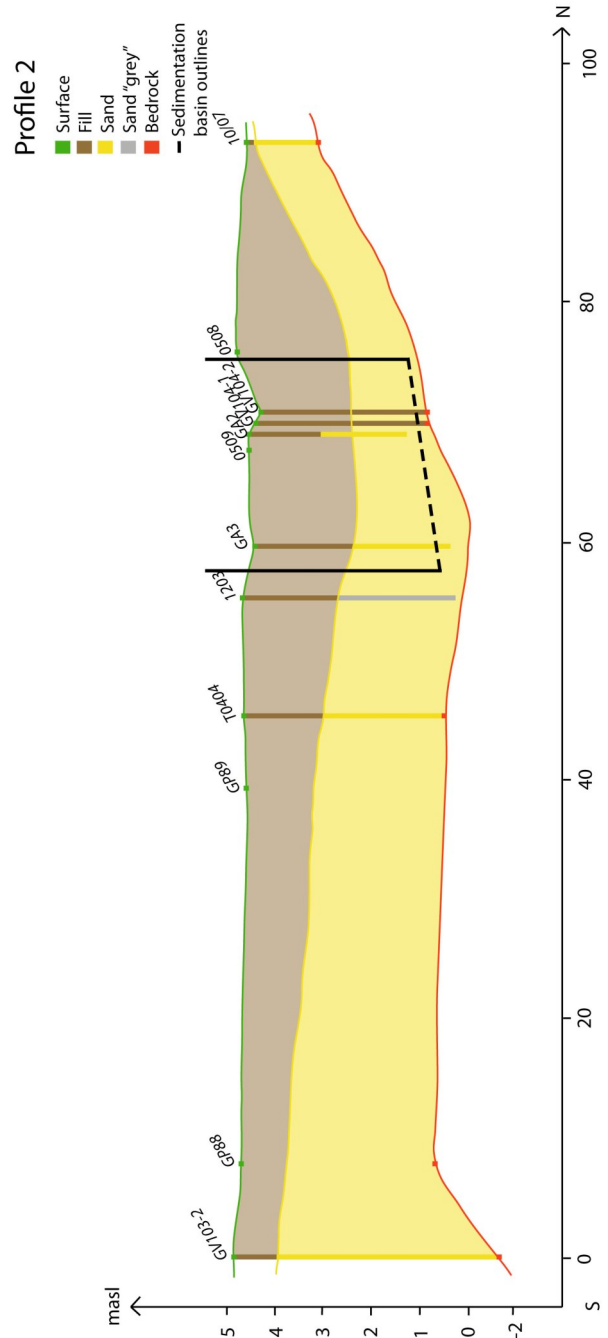
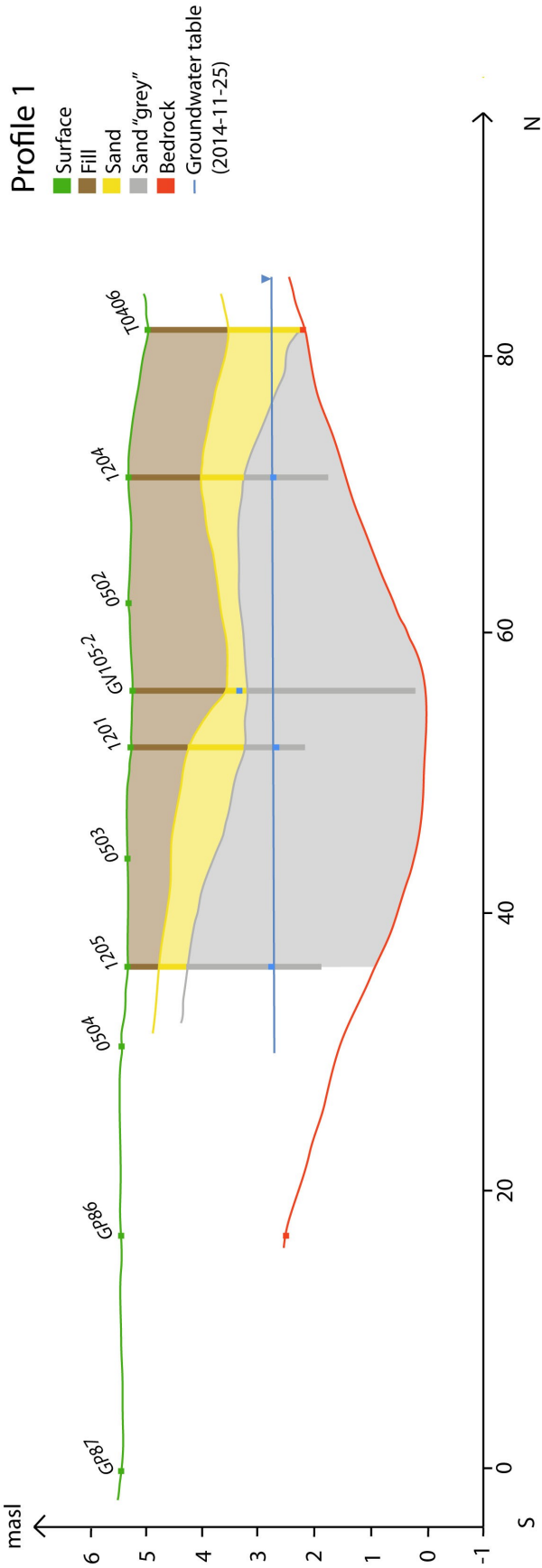


Fig. 27. Profile 2 crosses the sedimentation basin (outline marked as black lines (Larsson & Hübinette 2003)). The sedimentation basin depth is uncertain. The profile correlates to DCIP-survey line 2-4. The bedrock surface is elevated towards the north. The groundwater table is excluded in the figure due to the lack of reliable measurements.

Fig. 26. (To the left) Profile 1 is located along DCIP line 1, and close to DCIP line 5-6. The bedrock has a topographic low in the middle, which does not appear on the ground surface due to the sediment cover.

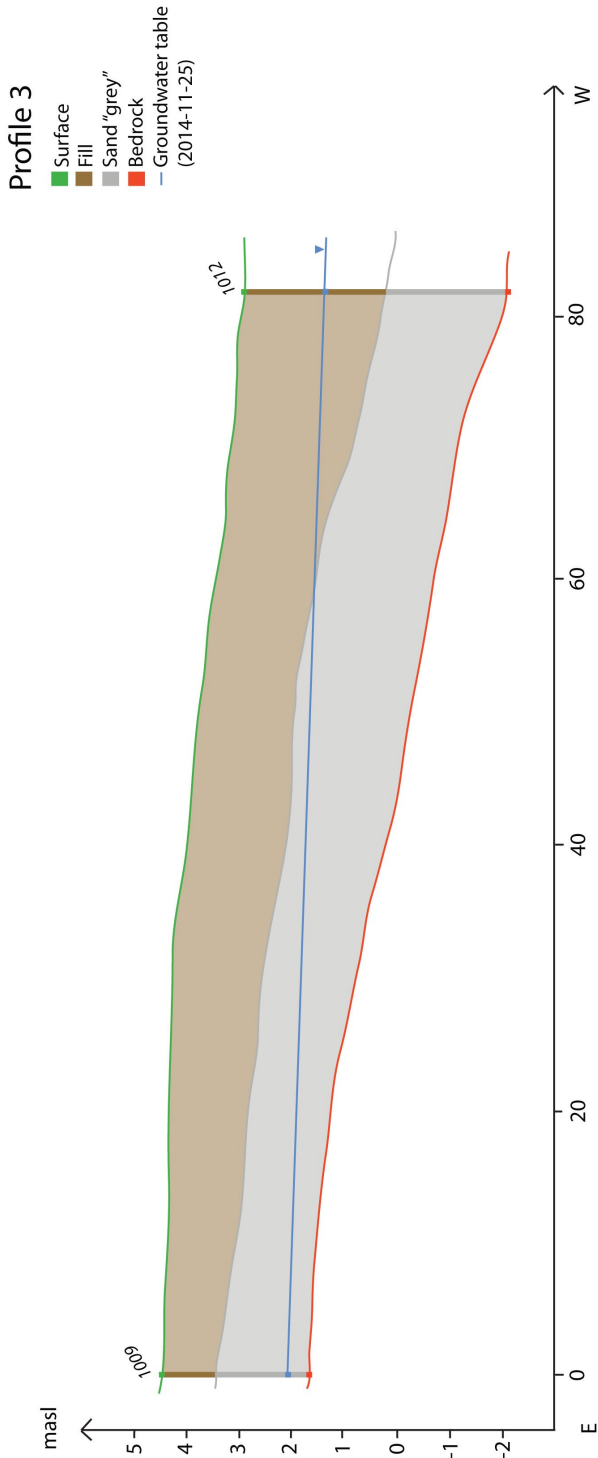


Fig. 28. Profile 3 correlates with the DCIP survey line MC by the miniature-golf course. The bedrock is dipping westward and the overlying sediments increase in thickness in the same direction. Notice the profile's direction, premeditated to correlate with the DCIP-survey line direction.

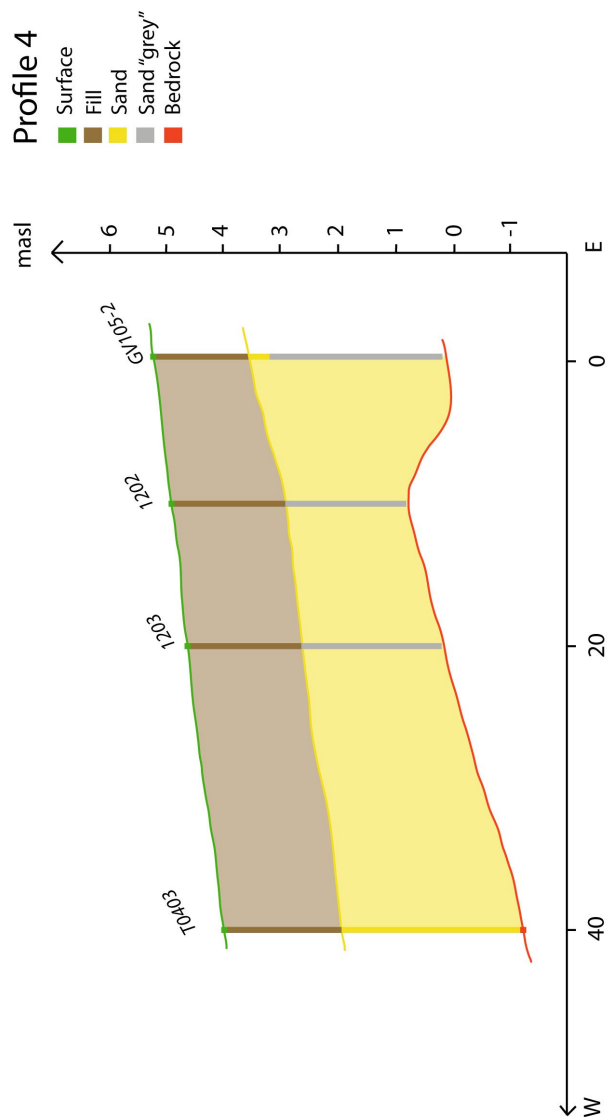


Fig. 29. Profile 4 crosses the estate south of the director's residence. The bedrock slopes westward with roughly the same thickness of sediment above. Groundwater levels were excluded due to the lack of reliable measurements. Notice the direction with east on the right hand and west to the left.

## 5.2 DCIP-data

The DCIP-data results are presented in figure 30 through 43. All the following profiles and figures, except of the DCIP-lines “Diagonal” and “MC”, are projected for the viewer standing in the east facing westwards, with south to the left in the figure and north to the right. In the few other cases not following this rule, it will be noted in the figure and the figure text. The locations of all profiles are presented in Fig. 22-23, chapter 4.2. The profiles are presented joined together in a fence diagram (Fig. 30) and thereafter, the most representative and interesting will be discussed independently. However, all profiles are presented independently in Appendix V.

### 5.2.1 Resistivity

Resistivity profiles from inside the estate, measured in May and November, are joined together in the fence diagram (Fig. 30). Interesting units are marked in the fence diagram, and shows two continuous anomalies through the area, where the northern “edge” has an uncertain limit marked with a dashed line. The diagram also shows two anomalies in the area of line 2 and line 3, circled in Fig. 30 with a black line. The most interesting details can be seen in profiles of line 1a, line 2, line 3 and line Diagonal, and these are presented in more detail hereafter (Figs. 31-34). Line MC outside the estate is too distant to be included into the fence diagram. However, this profile is presented in Fig. 35. The monitoring wells are included in each single DCIP-profile following and the groundwater level from the fieldwork in November is marked as a blue line in each well.

A common feature for the resistivity profiles are the three main horizontal layers, marked as A, B and C in Figs. 31-32 and Figs. 34-35. The middle one has a lower resistivity and appears at *c.* 3 m.a.s.l. down to *c.* 0 m.a.s.l. The deepest unit has a high resistivity and starts at about sea-level, but is not as sharp as the border between the uppermost and middle units. The northernmost continuous anomaly marked as a straight line in the fence diagram (Fig. 30), can be identified in all survey lines inside the estate. It is distinct in the DC-profile line 2 and line Diagonal as a vertical anomaly.

#### 5.2.1.1 Direct current (DC)-line 1a

The three horizontal layers A, B and C marked within Fig. 31 have been examined in more detail, and at 40 m into the profile, the B unit gets thicker and has a lower resistivity, whereas C decreases in thickness. At 50 m, the C unit increases in thickness, whereas the B unit- thins out, and at 60 m, C disappears and B increases in depth.

#### 5.2.1.2 DC-line 2

In Fig 32, line 2 is presented and as in line 1, three main horizontal layers A (high resistivity), B (lower resistivity) and C (higher resistivity) are marked with white dashed lines in the southern part of the profile. At approximately 45 m into the DC-profile, the high

resistivity unit C disappears. An area marked D appears and can be divided into three horizontal parts with an uncertain border between the lower two. In Fig. 32, a black dashed square is marked, where a zoom in for a closer view in the following figure 33. The units therein are in two; one delimited anomaly (E) with low resistivity and anomaly F with a high resistivity value.

#### 5.2.1.3 DC-line Diagonal

Line Diagonal combines the two swarms of DCIP-lines and is presented in Fig. 34. The pattern is as in line 1a and line 2, with three layers A, B and, C in the southeast part of the profile, where the C-layer ends distinct and an anomaly D, with low resistivity, appears. The D anomaly is covered by an area of higher resistivity values. In the north-west area, the units shown in line 2 (here E and G) are possible to detect as well, but also a small and deep unit F can be distinguished in the northernmost part.

#### 5.2.1.4 DC-line MC

In the DC-profile from the MC-line situated outside the estate, there are three horizontal distinct layers (Fig. 35). Unit A show resistivity values between 250 and 1500  $\Omega\text{m}$ , which is a wider interval than in e.g. line 1a. The B-unit has an interval of resistivity values between 100-330 $\Omega\text{m}$ , which is similar to corresponding parts in the other lines. The thickness of unit B is increasing westward as unit C decreases and slopes towards the west. The lowermost unit C has similar resistivity values to the C-unit in the other DC-profiles.



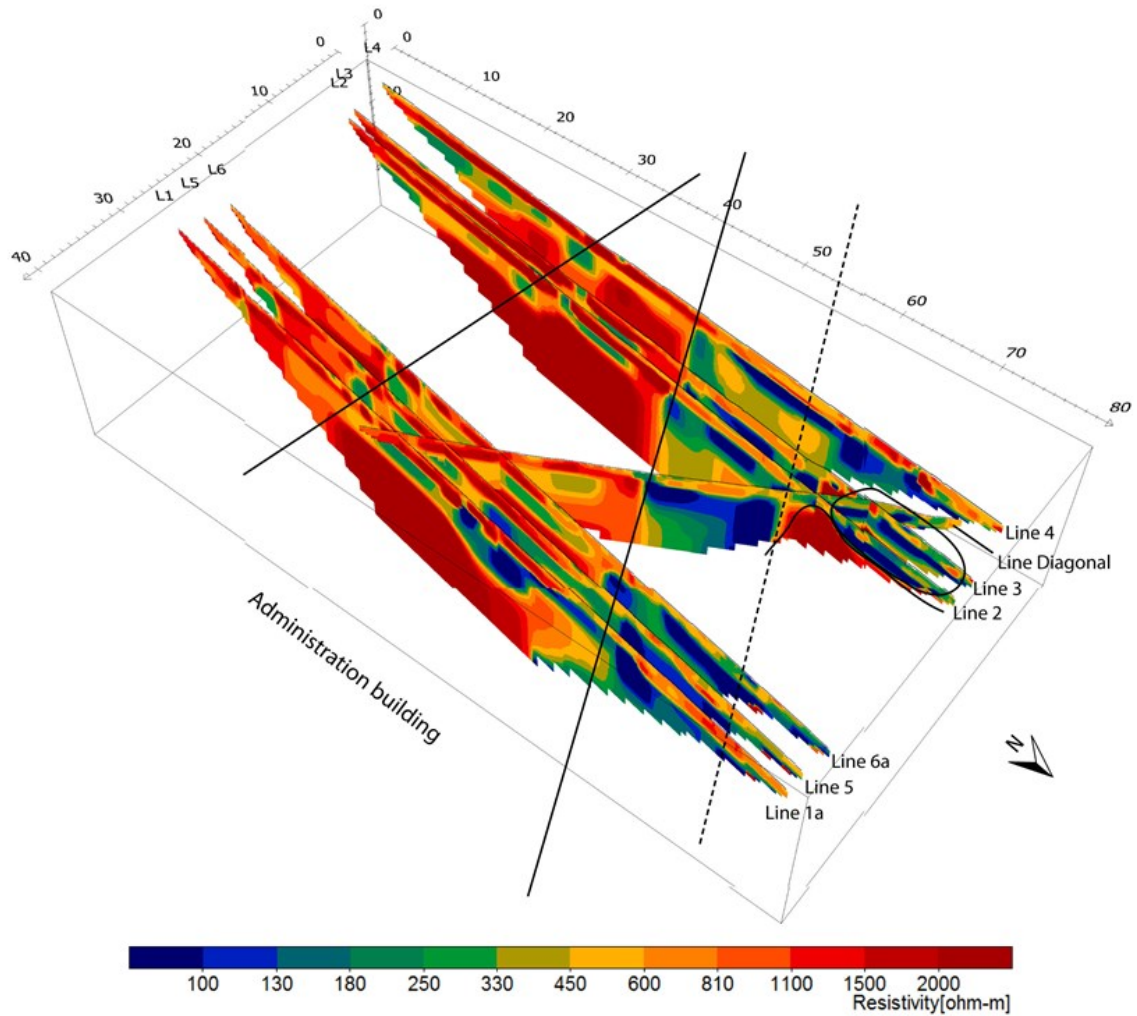


Fig. 30. Resistivity profiles from inside the estate, measured in May and November, are joined in a fence diagram. Noted units and anomalies are marked with black lines, dashed lines and circled. Note that north is towards the right hand side and downwards in the picture. It is presented this way to optimize the visualization of the most interesting features in the results.

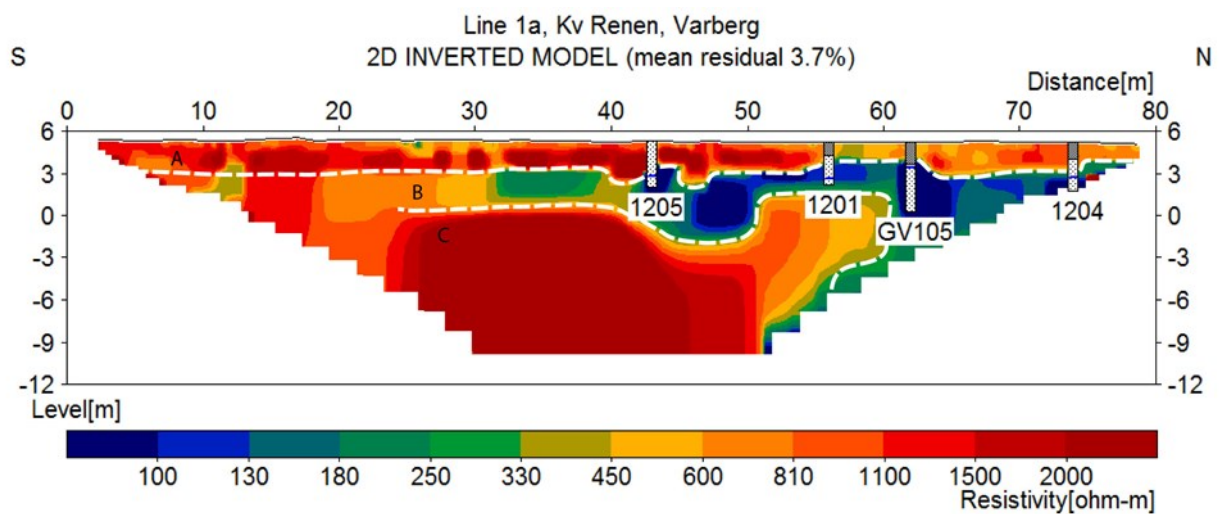


Fig. 31. Three fairly horizontal layers A, B and C are marked with white dashed lines. At 40 m into the DC-profile, the B unit gets thicker, and its resistivity decreases, while the unit C gets thinner. At 50 m, the C unit increases as the B unit thins out. At 60 m unit C disappears and B increases in depth.

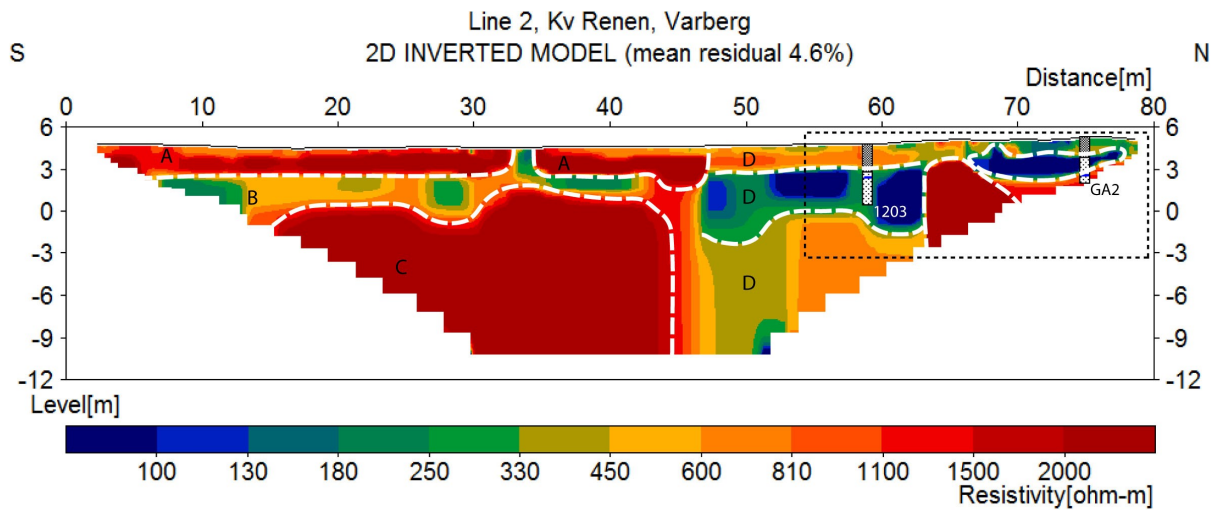


Fig. 32. Three main horizontal layers A, B and C are marked in the southern part of the profile. At approximately 45 m into the profile, unit C disappears. The area marked D is also divided into three layers with a less certain border between the lower two. The black dashed square marks the area where a closer zoom is shown in figure 33

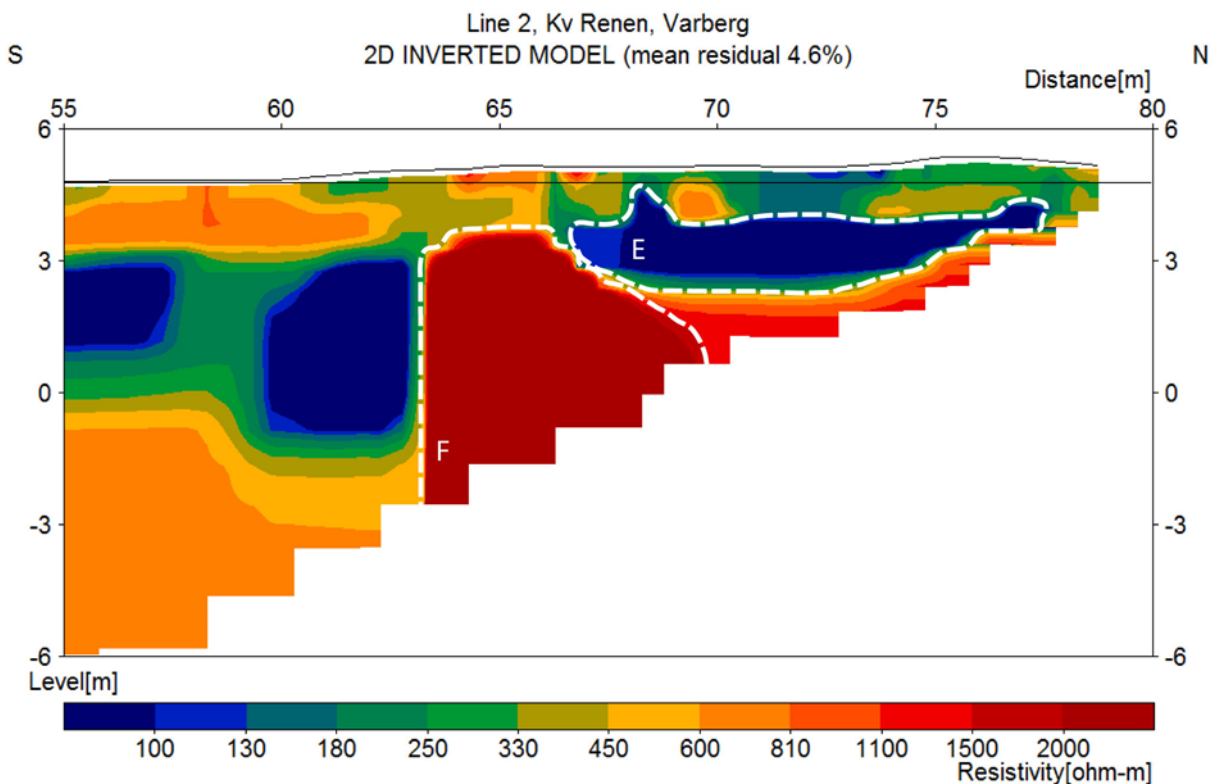


Fig. 33. A closer view of line 2, correlates to the dashed square in Fig. 32. Anomaly E is a strongly delimited structure with a low resistivity value. F has high resistivity values and is in the north not so well defined.

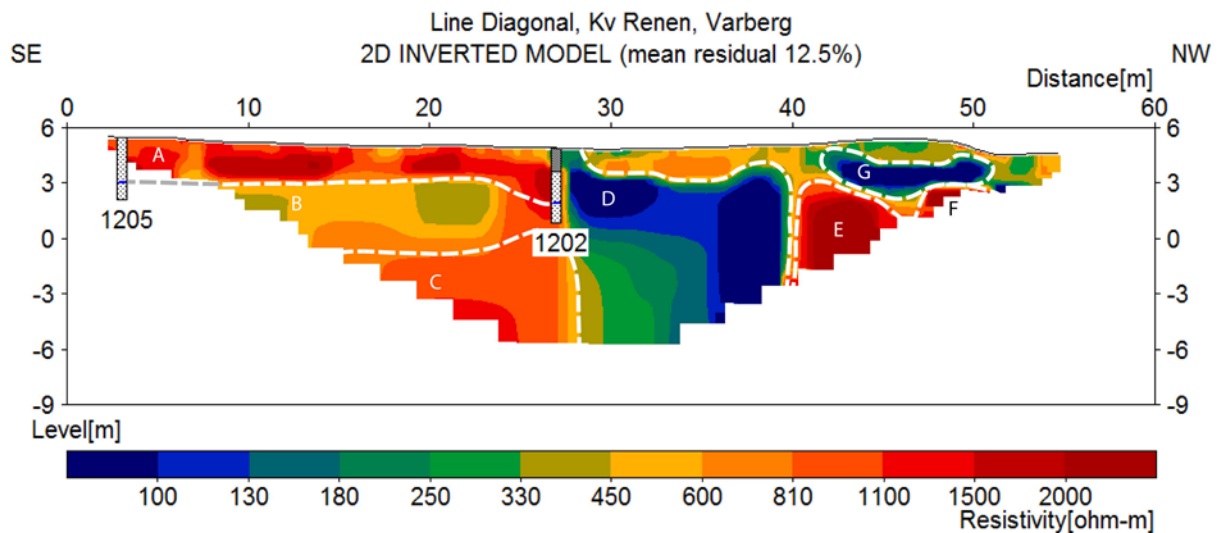


Fig. 34. The Diagonal DC-profile is shown in the figure. The patterns are similar to those in line 1a and line 2. However, there is an extra unit (F) identified. Note the orientation of the profile, from the left part of the figure showing the south-east and to the right, the north-west.

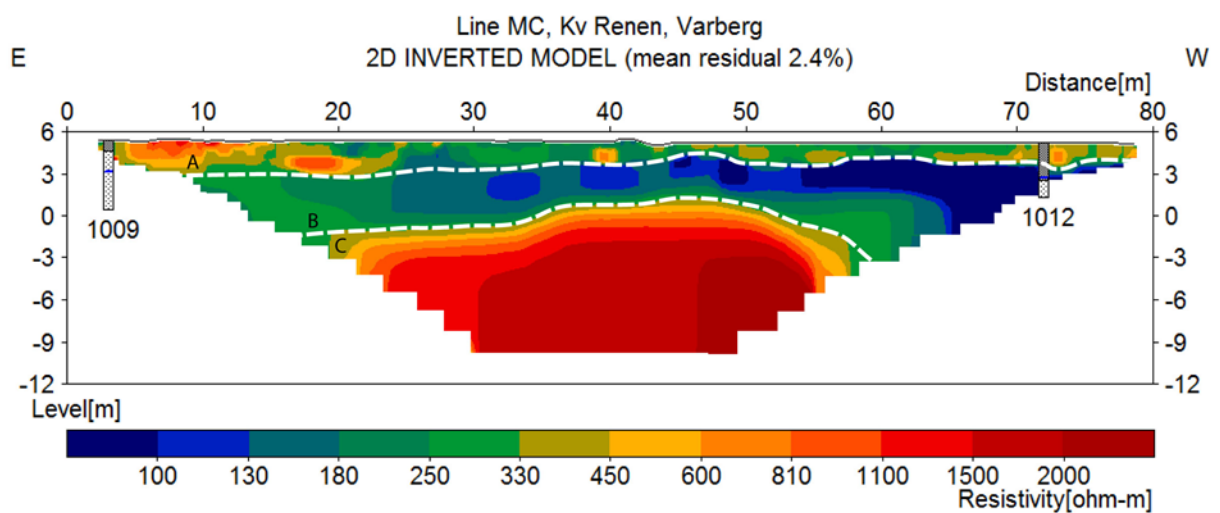


Fig. 35. This DC-profile for line MC located outside the estate, northwest of, Kv. Renen 13. The three main horizontal layers are distinct here, and unit B increases in thickness westwards. Note the orientation of the profile, from east to the left of the figure and towards the west in the right hand side.

## 5.2.2 Induced Polarization

The IP profiles measured in May are gathered in a fence diagram (Fig. 36). Two larger anomalies with high chargeability are identified, one in line 1a and one in line 2. Three smaller high chargeability anomalies are visualized in the line 3 IP profile. Important to notice is the lack of IP-response in line 4. Line 1a and a close view of line 2 are presented hereafter to have a closer look at the two interesting anomalies marked with black lines in Figs. 37-38.

### 5.2.2.1 IP-line 1a

In line 1a (Fig. 37), the large anomaly is identified between 45-65 m depth within the profile, and has a sharp contour. It has extremely high chargeability values above 60 mV/V (see also Appendix V.II). A smaller anomaly, B, in the southernmost part of the profile is identified at 10-20 m.

### 5.2.2.2 IP-line 2

The IP-profile from line 2 has a small anomaly, C, in the northern part of the profile. A closer view of the anomaly is presented in Fig. 38. The anomaly comprises almost the whole measured space from 65 m to 78 m, with some variations inside the anomaly and especially towards the ground surface.

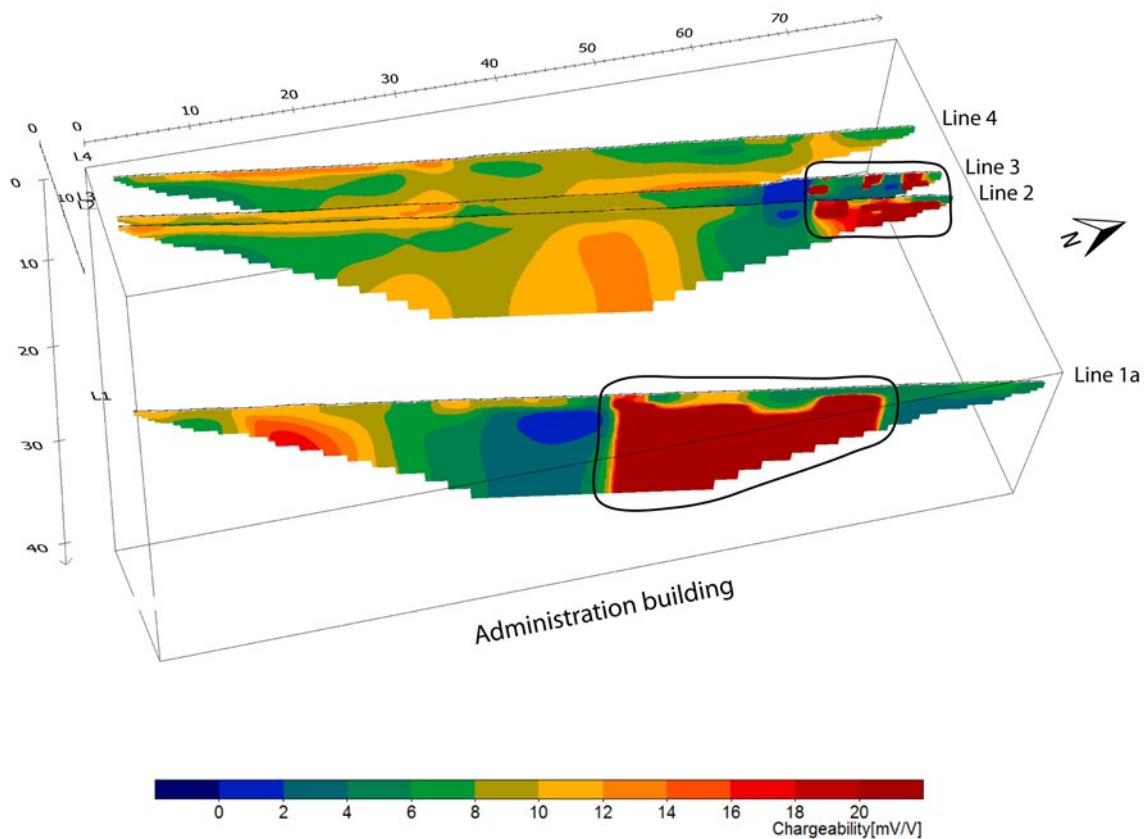


Fig. 36. IP profiles measured in May, line 1a, line 2, line 3 and line 4 (see Fig 23. for location within the map of the estate). One larger anomaly in line 1a is marked with a black rectangle, as well as the area of higher chargeability in IP-profiles 2 and 3. Note that north is towards the right hand side in the picture. It is presented this way to optimize the visualization of the most interesting features in the results. .

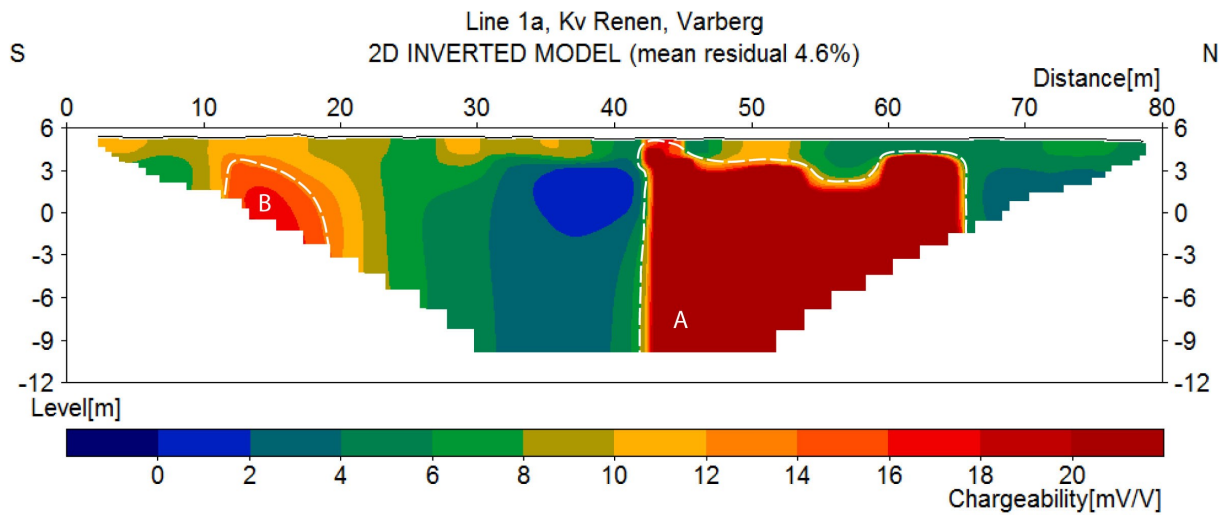


Fig. 37. IP-Profile for line 1a shows one large anomaly (A) between 45-65 m with extremely high chargeability. The smaller anomaly, B, is identified in the southern part of the profile, between 10-20 m.

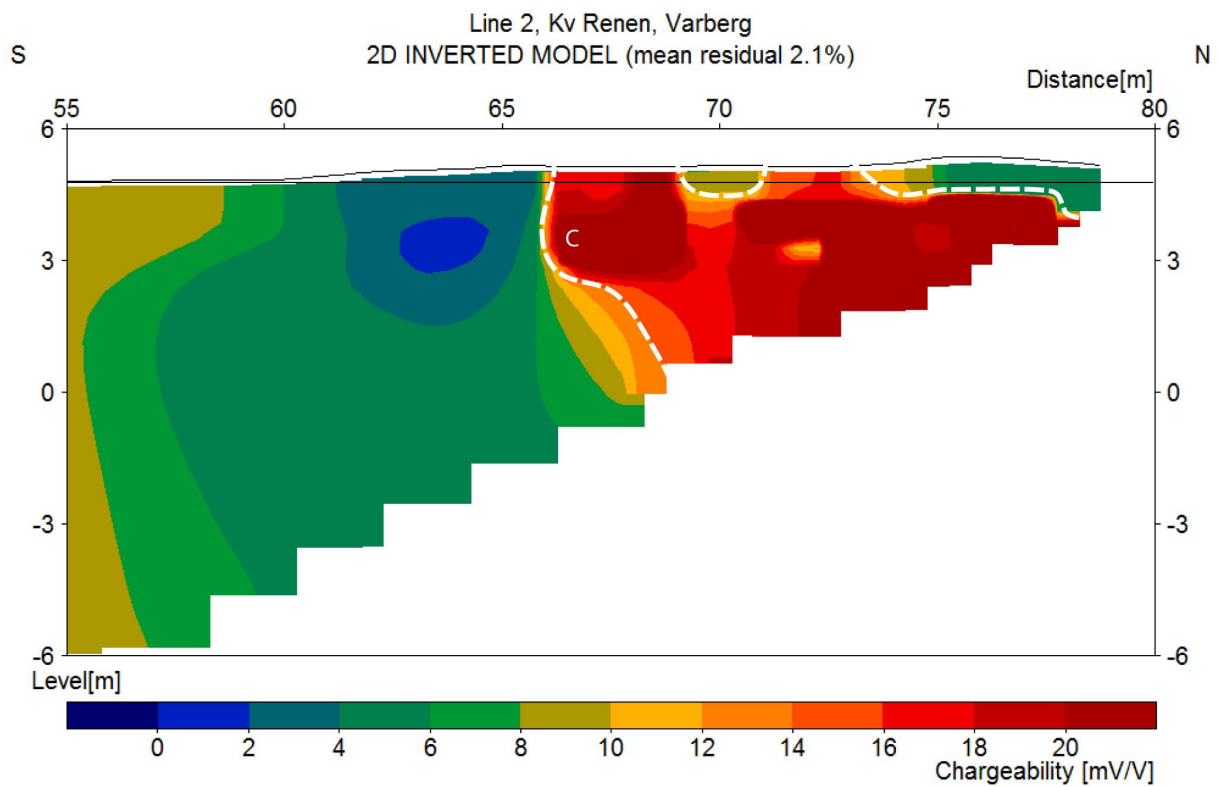


Fig. 38. A close-up of the interesting part in IP-profile of line 2; an anomaly (C) with high chargeability is identified, and appears at 65 m and covers the measured space towards the northern end of the profile.

### 5.2.2.3 Fence diagram—February

IP measurements were also performed in February for line 1c and line 6b. It is presented here in a joint fence diagram (Fig. 39). Both profiles have a high chargeability anomaly each. The profiles are presented individually as well in in Figs. 40 -41.

### 5.2.2.4 IP-line 1c

In the profile for IP-line 1c, three anomalies are identified (Fig. 40). One is in the southernmost of the profile, at 10-20 m, and is marked D. The largest anomaly with high chargeability marked E is identified in the middle of the profile. It is not completely continuous in the top of the southern part see Fig. 40. The profile has another isolated high chargeability anomaly, F, at 60 m into the profile.

### 5.2.2.5 IP-line 6b

In the IP-profile for line 6b, Fig. 41, is a large and clearly defined high chargeability zone identified. It slopes undulated from north to south.

### 5.2.3 Time-lapse

Line 1a and line 1c are measured at the same location, with the same measurement parameters, but at different times. They are thereby comparable and give the opportunity to make a comparison of changes in time, i.e. a time-lapse analysis. The resistivity measurements show no larger changes with time and it is therefore not considered and included in this sub-chapter. However, according to the IP measurements, the anomaly A in IP-line 1a has been reduced in extent during the time passed between the measurements, to anomalies E and F in IP-line 1c, see Fig. 42.

The time-lapse study of IP-profiles of line 1 shows both zones of lower and higher chargeability values, see Fig. 43. In the uppermost area and in the bottom of the profile, the chargeability is lower in February than in May. Between the zones of lowered chargeability, a zone with increasing chargeability is identified. The contour between anomaly  $\gamma$  and  $\delta$  are sharp (Fig. 43).

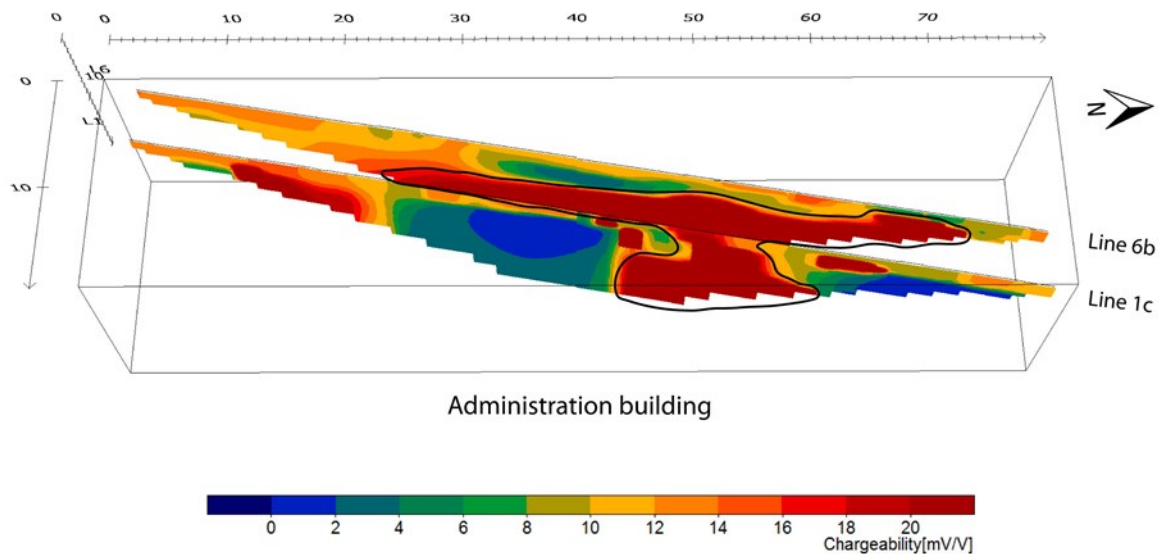


Fig. 39. The IP profiles measured in February, called line 1c and line 6b. Both profiles have an anomaly with high chargeability. Note that north is towards the right hand side in the picture. It is presented this way to optimize the visualization of the most interesting features in the results.

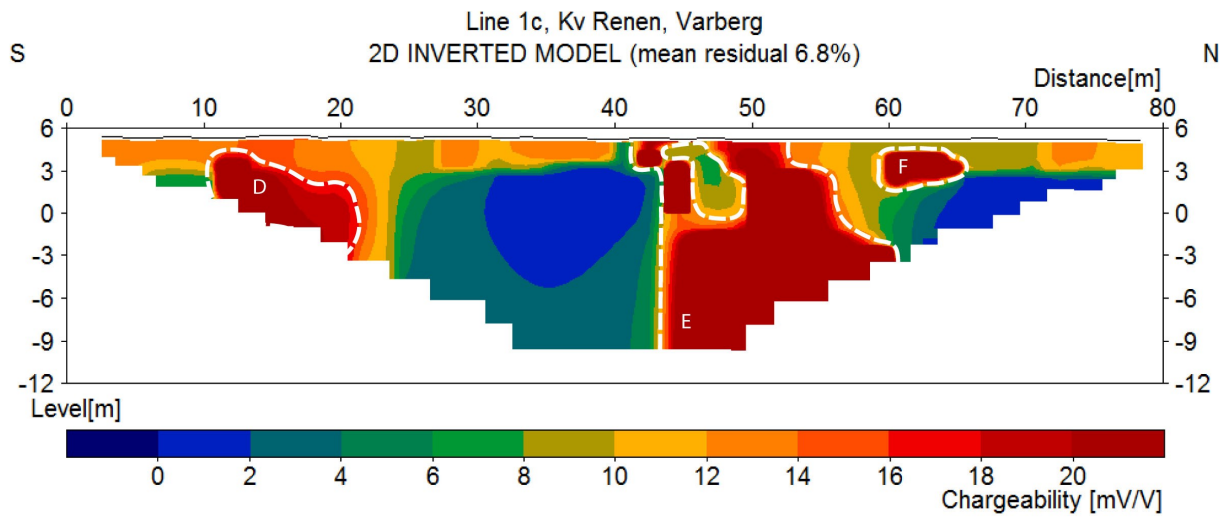


Fig. 40. The IP-profile from line 1c has three anomalies where high chargeability is identified, one in the southernmost of the profile (D), a large area (E) in the middle and one smaller isolated (F).

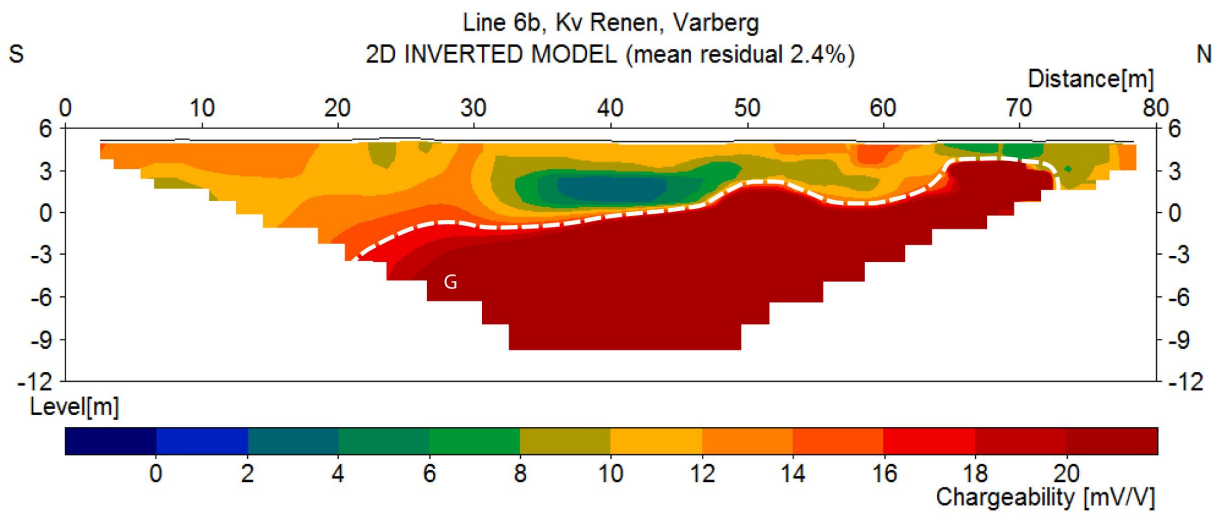


Fig. 41. IP-profile line 6b has one large anomaly identified at depths varying between +3 to -3 m a. s. l. smoothly sloping from the north towards the south.

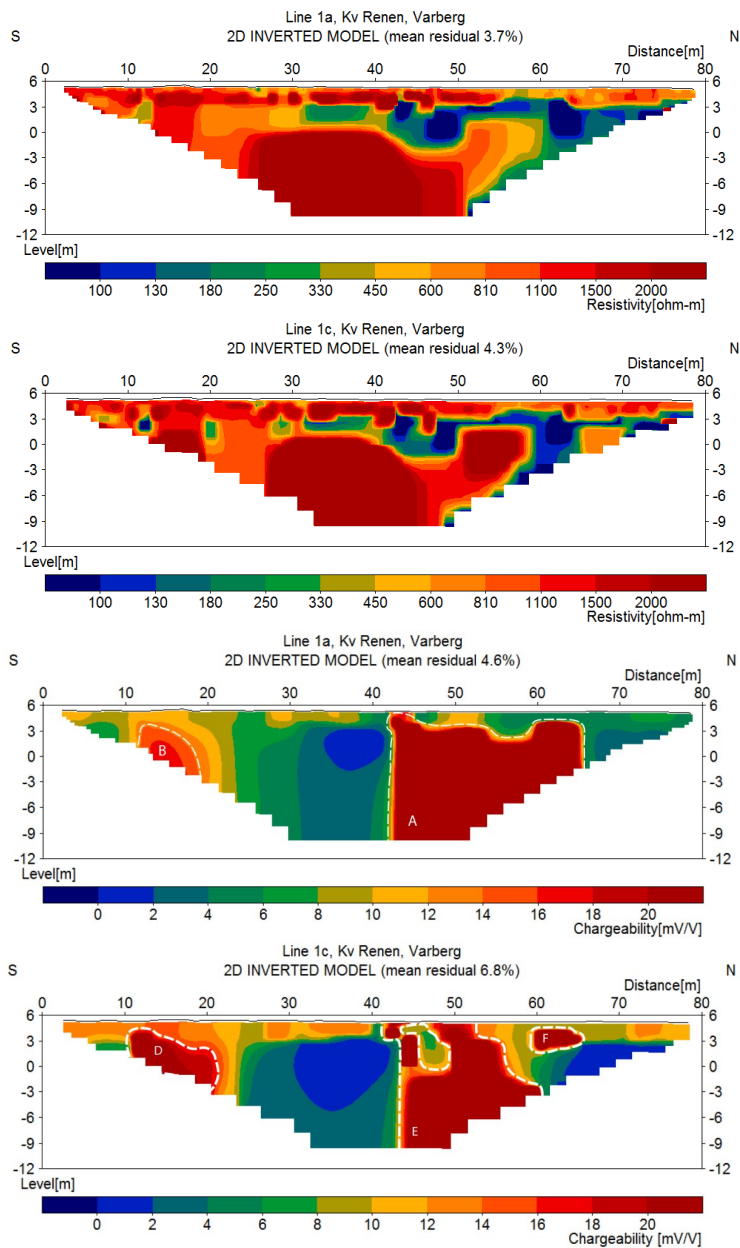


Fig. 42. (to the left) The resistivity of line 1a and line 1c, upper two profiles do not show any great differences and has not been considered further. Due to the change of size of anomaly A in the 1a IP profile, the change between the two measurements has been calculated and the result is shown in Fig. 43.

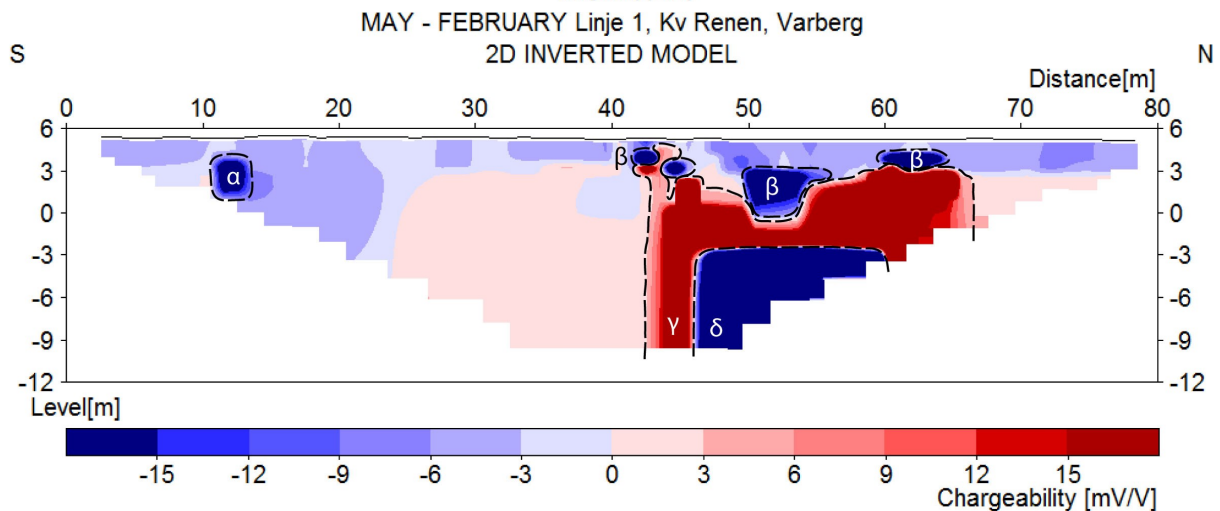


Fig. 43. Time-lapse data for the IP profiles measured along line 1 (see map in Fig. 23), where the IP-result acquired in May 2014 have been subtracted from the IP-result (inverted values) from February 2015. From the results, we can see that the anomaly has been reduced in extent from May (2014) to February (2015).



### 5.3 Groundwater chemistry

The results from the analysed groundwater samples and all parameters measured in the field are summarised in Table 7. The analysis protocols from the laboratory analyses are given in their complete extent in Appendix VI. Bolded values in Table 7 are higher than the national reference values (for that type of aquifer conditions), or guideline values (SGU 2013a). The electrical conductivity indicates contamination in all the wells (SGU 2013a). The levels of TCE, TCA, degradation products and OPR are visualized in Fig. 44.

GA2, the well closest to the sedimentation basin, has the highest levels of all the contaminant substances, except for vinyl chloride and zinc. It is also the only well where cyanide has been detected (0.42 mg/L). The levels of TCE, 1,1,1-TCA, cis-1,2-DCE and trans-1,2-DCE are very high and indicates that they exist in free-phase, at least TCE, where free-phase is assumed with concentrations higher 14,000 µg/l and most likely free-phase of cis-DCE (Swedish Geotechnical Society 2011a, Pankow & Cherry 1996).

The TCE level is measured to between 58-20,000 µg/l in five of the wells; 1201, 1204, 1205, GV105 and GA2, and levels are much higher than the national guideline value of 10 µg/L (SGU 2013a) for

TCE and PCE together in groundwater,. The most common DCE isomer detected is the cis-1,2-DCE, followed by trans-1,2-DCE (except in 1205), and the lowest detection is of 1,1-DCE. 1,1-DCA is found in higher levels than 1,1,1-TCA in all wells , except in 1201 and GA2. In addition to the results summarised in Table 7, PCE has been detected in two wells, 1205 (11 µg/L) and 1204 (0.12 µg/L).

The wells outside the estate have generally the lowest values of analysed substances and parameters; except for 1012 that has the highest level of zinc, which is the only Zn-value measured above the reference value (SGU 2013a). Well 1009 (outside the estate) is the only well with a positive OPR value, and thereby represent aerobic conditions. Regarding the induced reductive dechlorination, all the wells inside the estate shows anaerobic conditions (negative ORP values), with pH-value varying within the interval of 6.41-7.64, close to neutral.

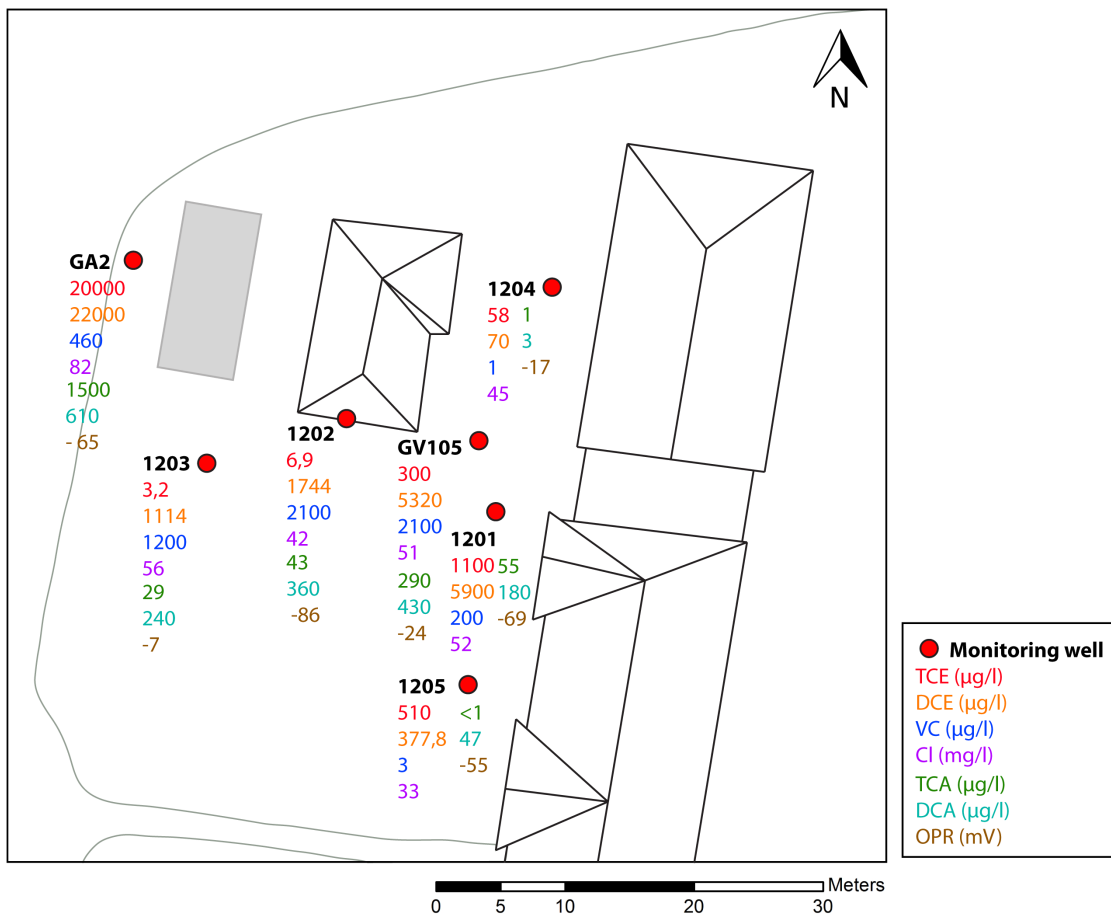


Fig. 44. Concentrations of TCE and TCA, metabolites, and OPR from November 2014. DCE is given as the sum of trans- and cis-DCE. All samples and measurements are from November 2014.

Table 7. Groundwater chemistry data where parts of the analysed parameters and all of the parameters measured within the field are given. Bold values are higher than the guideline values. The full data set of analysed substances and parameters is given in Appendix VI.

Well		1201	1202	1203	1204	1205	GV105	GA2	1012	1009	Guideline values
Analysed	Unit										
TCE	µg/L	<b>1100</b>	6.9	3.2	<b>58</b>	<b>510</b>	<b>300</b>	<b>20000</b>	0.64	0.57	10 <sup>a</sup>
1,1,1-TCA	µg/L	430	43	29	1.5	<1.0	290	1500	<0.1	<0.1	-
1,1-DCE	µg/L	55	16	10	0.86	9.6	50	120	<0.1	<0.1	-
cis-1,2-DCE	µg/L	5800	1700	1100	67	370	5100	21000	11	0.19	-
trans-1,2-DCE	µg/L	100	44	14	3	7.8	220	1000	3.5	<0,1	-
1,1-DCA	µg/L	180	360	240	3	47	430	610	0.72	<0,1	-
VC	µg/L	<b>200</b>	<b>2100</b>	<b>1200</b>	<b>1</b>	<b>3</b>	<b>2100</b>	<b>460</b>	<b>2</b>	<0,2	0.50 <sup>b</sup>
Cl	mg/L	52	42	56	45	33	51	82	39	28	100 <sup>b</sup>
DOC*	mg/L	12	16	16	6.7	5.1	18	9.5	4.5	13	See tab. 3
TOC**	mg/L	13	16	19	6.9	6.6	21	9.5	6.2	13	-
Cadmium	µg/L	0.035	0.016	0.011	0.021	0.015	0.010	0.016	<0.01	0.11	5 <sup>b</sup>
Chrome	µg/L	<b>1.9</b>	<b>3.1</b>	<b>3.1</b>	<b>1.0</b>	0.72	<b>2.1</b>	<b>6.1</b>	<0.05	0.34	1 <sup>a</sup>
Zinc	µg/L	9.9	2.4	2.0	4.7	1.3	1.2	65	<b>140</b>	45	100 <sup>a</sup>
Iron	mg/L	<b>0.53</b>	<b>5.7</b>	<b>3.1</b>	<b>0.18</b>	<b>0.1</b>	<b>1.7</b>	<b>1.2</b>	<b>0.22</b>	0.06	0.100 <sup>b</sup>
Manganese	mg/L	<b>0.07</b>	<b>0.26</b>	<b>0.13</b>	<0.03	0.03	<b>0.18</b>	<b>0.56</b>	<b>0.56</b>	<b>0.07</b>	0.050 <sup>b</sup>
Measured	Unit										
Temperature	°C	12.7	11.7	11.9	11.9	13.6	12.6	11.5	11.1	11.7	-
ORP***	mV	-69.1	-86	-6.6	-16.8	-54.5	-24.2	-33.4	-65.0	33.5	See tab. 3
pH		6.65	6.97	7.04	6.84	7.64	6.58	7.02	6.41	7.0	See tab. 3
Electrical conductivity	µS/cm	<b>459</b>	<b>372</b>	<b>395</b>	<b>450</b>	<b>413</b>	<b>414</b>	<b>466</b>	<b>361</b>	<b>186</b>	38 <sup>a</sup>
Total dissolved solids	mg/L	298	239	266	291	262	265	304	235	121	-
Salinity	ppt	0.23	0.18	0.19	0.22	0.19	0.20	0.23	0.17	0.09	-
Turbidity	NTU	<b>31.5</b>	<b>10.9</b>	<b>180</b>	<b>41</b>	<b>130</b>	<b>27.5</b>	<b>17.7</b>	<b>19.8</b>	<b>6.7</b>	0.5 <sup>b</sup>

\*Dissolved organic carbon, \*\* Total organic carbon, \*\*\*Oxidation-reduction potential  
a) SGU 2013a, (groundwater) b) SLV 2001, (drinking water)

## 6 Interpretation

### 6.1 Resistivity

The resistivity profiles shows a distinct three-layered profile, with a highly resistive layer at the base, overlain by a middle layer with low resistivity and an uppermost layer with a higher resistivity. This is consistent with the geological background information from the area. The high resistivity layer in the bottom of the profiles is interpreted as bedrock, as the bedrock consists of unweathered metamorphic rocks in Varberg (see Fig. 16 into chapter 3.1). The two upper layers are interpreted as sediment divided into two resistivity layers by the groundwater table, where the lower saturated zone has a lower resistivity than the unsaturated upper zone. This is supported by borehole logs

and well data, as the border between these two, unit A and B in Figs. 31-32 and 34-35, correlate well with the groundwater level.

Both the boundaries A-B and B-C in Figs. 31-32, 34-35, vary in depth across the studied area. This is a feature that can be expected for the bedrock boundary (B-C), as the geological profile suggests an undulating bedrock topography. However, a boundary representing the groundwater table (A-B), a more distinct transition within the DC results, can be expected corresponding to where the water pressure and the atmospheric pressure are equal. Variations in the sediment distribution could explain this more undulating surface between the saturated and unsaturated zone. The depth of the top filling varies across the area and it is also heterogeneous in content. Difficulties to insert the

measured groundwater table in the geological profiles confirm that there is a real variation, not only an artefact of the DCIP-results.

The northernmost continuous low resistivity unit crossing the area (see fence diagram in Fig. 30), is interpreted as a water-bearing fracture zone. The direction of the anomaly correlates well with one of the northeasterly trending lineaments (strike and dip of  $70^\circ/70^\circ$ ) recorded by the regional bedrock studies performed by SGU (2006), as well as Rahm *et al.* (2013), who studied the outcrop north of Kv. Renen 13. One out of five identified fracture-groups has, according to SGU (2006) and Rahm *et al.* (2013), the same direction. A water-bearing fracture zone has a lower resistivity compared to unweathered rock. This would explain the observed low resistivity anomaly. The unit that has been interpreted to extend northward is impossible to delineate with the data from this study. Anomaly F in Fig. 33 could be interpreted as part of the bedrock appearing, which is also indicated from geological profile 2. However, it is difficult from the resistivity data alone to confirm this as the anomaly is only detected along the edge of the measured profile.

The southern anomaly crossing the area (see Fig. 30), correlates to the walking path lined with lampposts and the anomaly likely represents lamppost wiring. The resulting response in the DCIP is greater than the cable dimension, but it could possibly be explained as an impact of 3D-effects.

For the anomaly with high resistivity, identified as F in the DC-profile from line 2 and E in the profile line Diagonal (Fig. 33 and 34), at least two interpretations are possible; either it represents fresh rock (thereby inferring the extent of the interpreted fracture zone), or a 3D effect of the neighbouring director residence's terrace. The shape of the unit appears to follow the contours of the terrace, thereby speaking for the latter. However, if the anomaly does represent the non-fractured/fractured bedrock limit, this would support the interpretation of anomaly F in Fig. 33 as bedrock. Both of these factors may interplay and be true at once, thereby reinforcing the anomaly.

When considering the isolated anomaly identified as E in line 2, and G in line Diagonal (Fig. 33-34), it can be noted that they are both located in the same area as the sedimentation basin. Based on their location and size, these anomalies are interpreted as reinforced concrete within the sedimentation construction, as shown by the additional geophysical measurements as well (chapter 2.5).

## 6.2 Induced polarization

The induced polarization shows three anomalies; one in the northwest, one larger in northeast and one smaller in the southeast of the studied area. An isolated anomaly in line 2-3 is found in the area of the sedimentation basin and likely represents the reinforced concrete of the basin. A prominent anomaly is found in line 1a. Additional geophysical measurements carried out by EM61 and Geonics G-858 MagMapper

revealed no subsurface object that could explain this high chargeability signal. Considering this and the fact that it correlates well with the location where the injection of a carbon source was performed during the pilot study of an *in situ* remediation test, the anomaly can be interpreted as the injected carbon source causing changed underground geochemical conditions. The anomaly is therefore interpreted as a plume including primary pollutants, degradation products and injected substances. Line 1c gives a similar response as line 1a, but a change in time is identified. The response is therefore interpreted to be caused by the microbiological changes taking place during the induced remediation. The isolated anomaly F in line 1c (Fig. 40) is inside the anomaly A in line 1a. The anomaly in line 6b (Fig. 41) is most likely correlated to the *in situ* remediation as well. The anomaly does not appear as high up in line 6b as in line 1, however, it is increasing in width, which could be considered as the contamination and injected substances being transported and dispersed in the main flow direction, westward and south-westward.

Another IP anomaly is possible to identify to the south in both line 1a (B) and 1c (D). This anomaly correlates to an anomaly identified with electromagnetic measurements, namely anomaly C in Fig. 14. The reasons for this anomaly are yet unclear, but there seems to be something leaking out.

## 6.3 Time-lapse

The large anomaly called A in both line 1a and 1c has changed through time. As shown in Fig. 43, there are areas of both increasing and decreasing chargeability. The  $\beta$  anomalies in the top have decreased in chargeability, and this can be explained as the injection/contaminant plume moving downwards with time, thereby decreasing in response level. Correspondingly, this may also explain why anomaly  $\gamma$  is increasing in value, as more organic source substances become available and used by the microbes with time.

Comparing the interpreted resistivity profile for line 1 (Fig. 31) with anomaly  $\delta$  (Fig 42), it is clear that the anomaly is located where the bedrock has been interpreted to protrude. This could maybe explain anomaly  $\delta$ , as these two coincide, but the reason for the decrease in chargeability cannot be deduced.

A change during time is measurable for anomaly  $\alpha$  in Fig. 43, confirming the interpretation in the additional geophysics of something leaking out, see C in Fig. 14 in chapter 2.5.

## 6.4 Groundwater chemistry

In the analyses of the groundwater chemistry, high concentrations of chlorinated solvents have been detected in two areas, one area located in the sedimentation basin, where the TCE levels indicate a free-phase and with high levels of DCE and very low redox values. The other area is in front of the administration building, mainly by wells 1201 and GV105, and westwards. The pollution spreading northwards appears

small according to the low levels of chlorinated solvents found in the well 1204 located to the north. Pollution levels are considerably higher southwards (well 1205; Fig. 44).

The redox potential inside the estate varies, according to SGU's groundwater quality criteria, between the lower part of class 2 and upper part of class 3 (redox values between -6.6 and -86 mV), which means anaerobic conditions. Such conditions increase iron and manganese concentrations within the groundwater (SGU 2013b). The pH-value, which ranges between 6.41-7.64, is optimal for microbial growth within the aquifer, a factor possibly contributing to the formation and supply of organic electron donors (Swedish Geotechnical Society 2011a).

Well 1009, outside the estate, is the only well with a positive redox value (33.5 mV), which also features aerobic conditions. It also has low levels of the analyzed substances. This could be interpreted as the shallow well has good potential to oxygenate the groundwater and the absence of the microbial activity taking place within the area of the other wells. The injected substances that stimulate the reductive dechlorination have not reached this well.

## 6.5 Conceptual model

From both existing data and new data, a conceptual model has been established of the subsurface conditions, see Fig. 45. DC-profile data have been used for the geological interpretation, for the orientation of the fracture zone and the boundary of layers. The contamination levels have primarily been interpreted from the results of the analyses of groundwater samples, and extensively by the IP-data.

Two areas with high contamination levels are known from previous studies. These findings have been confirmed, and further refined by this investigation, and are marked in Fig. 45 as contamination level 1. The eastern contamination is situated within the interpreted fracture zone and as DNAPLs sinks and move by gravity driven processes, regardless of the groundwater flow direction, it is highly probable that the fracture zone functions as a contaminant highway.

The highest levels of contaminants are found in the area of the sedimentation basin, in free-phase level. Due to lack of data outside the sedimentation basin the dispersal outside the estate can't be further constrained within this thesis. However, the plume has not reached the miniature golf-course in the northwest. Another fracture zone right underneath the sedimentation tank has previously been identified from a deeply drilled well (Rahm *et al.* 2013); this zone is included in the conceptual model in Fig 45. This fracture zone probably functions as a pathway for a northwestward dispersal of the contamination. In between the two primary contaminated areas, and beyond the fracture zones, chlorinated solvents have been detected and are likely a result of dispersal within the sediments and weathered top part of the bedrock. Figure 45 shows three generalized levels of contamination, which should be

understood as; level 1 with the highest contamination levels of around 1,000-20,000 µg/L of TCE and/or 6,000-22,000 µg/L for DCE, level 2 as a medium level contaminated zone with levels around 1,000-6,000 µg/L for DCE and level 3 as the lowest levels of contamination, between down to 1-60 µg/L for TCE.

## 7 Discussion

Resistivity gives the best resolution regarding the geological properties, whereas IP, with current subsurface conditions, appears better for investigating the contamination. From earlier investigations of Varberg, i.e. according to all the mentioned consultant reports in chapter 2.1.1, it is well-known that the contamination from Kv. Renen 13, both has reached the bedrock, and is being transported in a south-westwards and north-westwards direction. In other words, the contamination is transported out by the fractures. From this investigation, it is possible to interpret and pinpoint a fracture zone, especially with the resistivity measurement results. It should be possible to strengthen the interpretation by the IP-measurements, as a higher IP-effect in the fractures could be caused by the contamination. However, due to the lack of groundwater samples from each IP-measurement occasion, it is difficult to clearly draw this conclusion.

The anomaly in IP-profile line 6b (G in Fig. 41), is not shown on the IP profile line 2 to 4, which gives an impression that the interpreted fracture zone leads the pollution plume out from the estate in a *c.* 250° south-westerly direction. The escape sewer, used to lead production waste water into the sedimentation basin, is located in the area of the fracture zone, where it according to Tornberg *et al.* (2008), is a risk that the sewer has been leaking contaminated water. If this is the case, then the fracture zone could be functioning as an efficient pipeline for spreading the contamination down gradient and into the bedrock fracture system. As TCE is a dense and heavy substance, it could have led to storage of the solvent further down in the bedrock fracture system where the groundwater flow is slow.

The groundwater chemistry analyses show that this area has high levels of TCE and its degradation products. The three wells close to profile line 1a; 1201, 1205 and GV105, all have TCE levels higher than the guideline values (10µg/L, see Tab. 7). Wells 1201 and GV105 have concentrations higher than 5000 µg/L of *cis*-1,2-DCE. However, the concentrations have decreased during the period of *c.* 5 months after the injection for stimulated reductive dechlorination (for further details see chapter 2.6.1). A movement of the contaminant plume is likely to have been caused by an increase in the groundwater flow gradient when injecting large volumes of liquids into the subsurface. The contaminant is also likely to have been diluted due to the injection.

Profile line 4, which is located closest to the GA2 well, containing the highest levels of TCE, TCA, DCE and DCA, shows no significant response in the

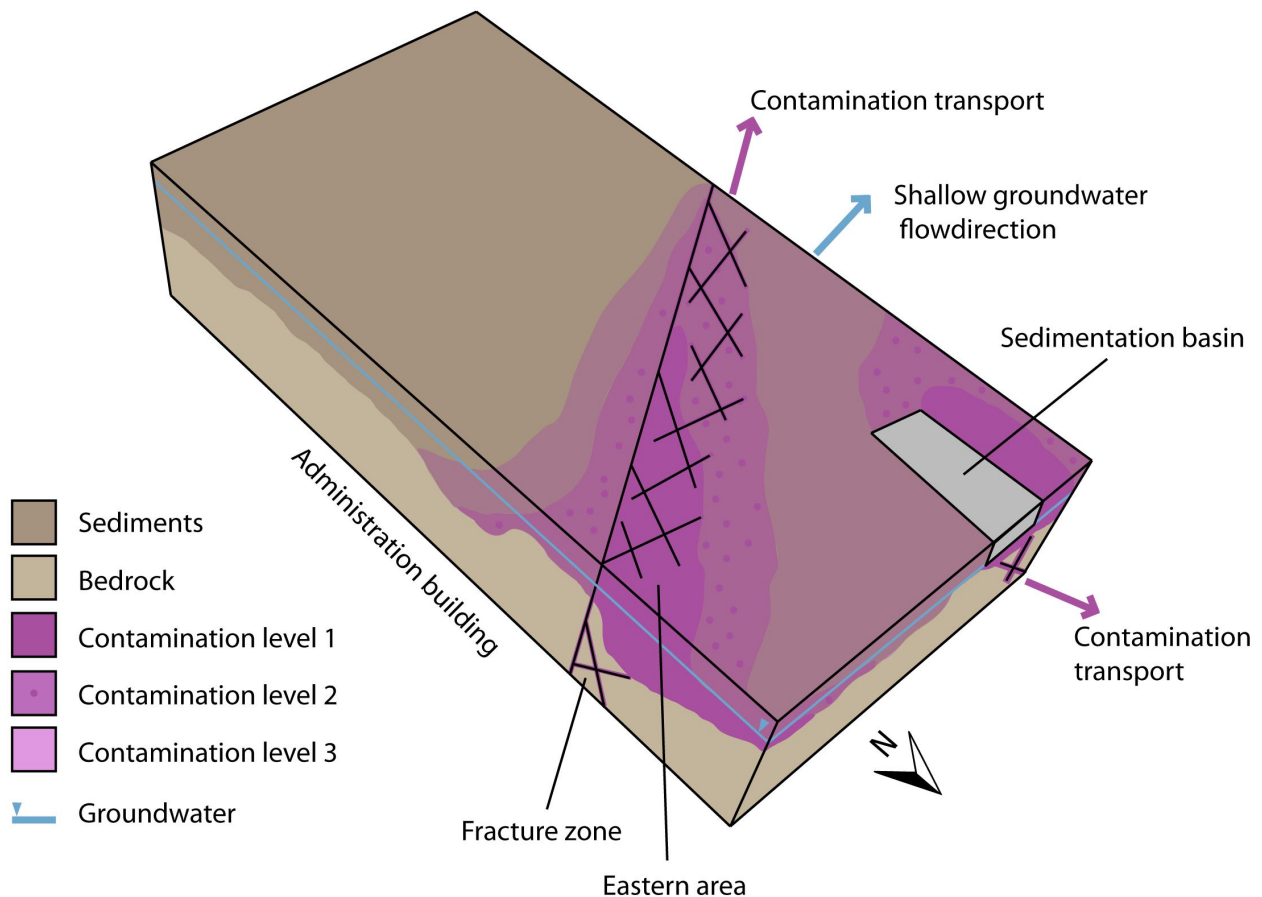


Fig. 45. A conceptual model of Kv. Renen 13, based on previous knowledge and new data collected within this work. Two primary zones with high contamination levels are detected, in the eastern source area and by the sedimentation basin, with lower levels in between and around the plumes. The interpreted fracture zone is in a southwest-northeast direction, and is marked and interpreted as a pathway of dispersal. Note the fracture zone beneath the sedimentation transporting pollutants in a NNW direction.

IP-measurement. This result is similar to that of former work presented by the TRUST 2.1 project. This could be explained by how the DNAPLs are located in the space of the sediment pores blocking the passage of charges. The DNAPL in free-phase can fill the pores fully and decrease the IP signal (Johansson *et al.* 2015), whereas the metabolites that are more charged and smaller in size will cause a charge around the free-phase plume. This could lead to the phenomenon with little IP response in the free-phase area, but larger IP effects in its vicinity.

Both temperature and amount of water in the soil affect the electrical conductivity. As the field work took place during different seasons and the weather differed, it is likely variations in the measurements vary due to this. This knowledge has been kept in mind when interpreting the data, and has not had a major influence on the interpreted models.

Settings of the instrument and the protocol used were designed to measure with separate cables to gather as high quality data as possible. The quality check of raw data before processing indicated that this was successful and that only a small number of “outliers”

had to be removed before processing and inverting. Standard settings were used for the inversion model parameters. Testing and identification of the impact of different parameter settings is beyond the scope of this thesis.

Time-lapse calculation is a featured function in the Res2Dinv (x64bit) and it is done by gathering the dat-files before starting the processing. However, when a comparison of manual excel calculations of the single profiles and the software made time-lapse ones were performed, the software result did not show a reasonable outcome, but had features that differed considerably from the manual controlled results. Therefore, the time-lapse results shown in this work, is calculated manually in excel, and for this reason it has not possible to exclude bad data points.

If we had the opportunity to redo the survey or make additional measurements, it should with our present knowledge, be performed further north in the garden and thereby reach deeper into the anomalies of interest. As it is now, parts of the most exciting new data are cut off both in depth and expanse. The reachable maximum depth with used field set up and spread

is approximately 14 meters, which with a more optimal location will give valuable data. An additional line south west of the estate would have been interesting, regarding the detected fracture zone and its further stretch downstream.

A weakness of DCIP is that it gives only a model of the subsurface conditions, however a reliable one, to use for the interpretation. Within this survey there was an abundance of data and knowledge available, but in the absence of this, it is difficult to interpret how the DCIP data relates to the actual geological conditions, but good for pinpointing where to drill. DCIP is a non-destructive investigation method and thereby favourable when working at contaminated sites. It is fast and more cost-effective than other traditional used methods, i.e. drilling, and the people carrying out the survey will not be exposed as heavily to the pollutants. However, here there is a need for “ground-truth data” to calibrate and understand what the DCIP-results can be interpreted as. In this study, we chose sampling of groundwater for a correlation of the acquired data as there are several observation wells installed within the area. Groundwater sampling within an area as heavily contaminated as this one is a large health risk, dealing with high concentrations of carcinogenic substances.

With this thesis’s results regarding the IP correlated to the *in situ* remediation study, it would be very interesting to follow an *in situ* remediation project for the dechlorination of an area. What to wish for is data collection before the injection and follow up in time steps during the whole cleansing period. In the current case, there has been a lack of DCIP information on the condition before the remediation started which left unanswered questions. DCIP-surveys can be constructed so that the subsurface conditions are received in a 3D-model. This type of survey together with collected data at different times, should give good monitoring of the impact of the remediation of a plume. Some qualified assumption on how the migration will proceed is required for an optimal location of the survey at the site, and this can be acquired by performing more detailed hydrogeological mapping before designing the DCIP monitoring. A resistivity survey from a landfill received successful results of water migrating in the ground due to infiltration of heavy rain (Loke *et al.* 2014). It would also be interesting to perform bacterial investigations to strengthen the interpretations of the *in situ* remediation.

DCIP has the potential to make surveys more effective both considering time and economy. If it is implemented as a first-step investigation method, or at least early in the process, it is possible to receive a reliable model of the subsurface including geology and contamination. The holistic overview is a great basis to make further planning for drilling and more intrusive methods. An example where DCIP would have been a good first-step survey tool is to study the location of the deep drilled wells at Kv. Renen 13, made by Rahm *et al.* (2013). They chose the location and direction from investigations of fractures at the outcrop north of

the estate, with the theory that smaller and larger structures correlate. They identified the direction of the fractures within the outcrop, but when performing the drilling, they missed the large fracture zone. If this survey would have been done before this, the location of the drill hole could have been different and the knowledge about the fracture zone would most likely have been greater today.

With more than 80,000 sites assessed as potentially contaminated in Sweden alone, is it important to perform smart investigations regarding both time and finances, to be able to solve and clean as many as possible, reaching our environmental goals of a non-toxic environment and good-quality groundwater.

## 8 Conclusion

The data from this investigation confirm, once again, that Kv. Renen 13 is heavily contaminated. The highest concentrations are detected west of the sedimentation basin. The DCIP-data gives a model of the subsurface conditions, where the plume of chlorinated solvents is limited southwards by the herein interpreted fracture zone, for which the extension has not been fully determined. Earlier investigations have indicated high levels of TCE-related substances northwest of the estate, but these results cannot be fully confirmed by the present study.

The geochemical parameters show anaerobic conditions, which are positive with regards to degradation of chlorinated solvents. The two sets of IP measurements in line 1 show a change in chargeability through time and indicate that the ongoing degradation is active, most likely stimulated by the injection related to the *in situ* pilot study. It is possibly with DCIP to study the changes due to degradation and the dilution, and therefore the variation in level of contamination through time. However, is it important to use the same instrumental set ups and protocols to be able to perform this time-lapse step and receive comparable results. To be meaningful, geophysical studies of contaminants need to be accompanied by chemical analyses of groundwater that has been sampled during the same time interval, as the geophysical measurements have been run. When performing time-lapse investigations, it is necessary to take water samples each time.

With this site in focus, and the current contaminant situation, it is possible to conclude that DCIP is a promising investigation tool at DNAPL contaminated sites regarding investigations of the subsurface conditions, both regarding the geological conditions and the contamination situation. The method should be considered in the beginning of the investigation process in order to detect areas and changes within the site for further detailed intrusive investigations. DCIP also shows possibilities as a monitoring tool for *in situ* remediation of chlorinated solvents.

## 9 Acknowledgments

To be able to make this thesis there are several persons along the journey that generously helped and supported me, I am very thankful for everything by everyone. However, some of you deserve to be mentioned specially; first and foremost I would like to thank the project group for the opportunity to work with an interesting topic. I would especially like to thank Sara Johansson for sharing your knowledge and for all help with data, processing and interpretation. I would also like to thank David Hagerberg for good cooperation during fieldwork in Varberg. I had some worthwhile trainee days with Carl-Henrik Månsson from Tyréns that was very appreciated and helpful. A great thank to the IT-administrator at the department of Geology, Gert Pettersson for all help. Furthermore I would like to thank my supervisor Torleif Dahlin for your technical support, both at home and by emergency call in field.

Finally the warmest thank to my supervisor Charlotte Sparrenbom for all your advice, suggestions, laughter and the TRUST you gave me.

## 10 References

- Ajo-Franklin, J.B., Geller, J.T. & Harris, J.M., 2006: A survey of geophysical properties of chlorinated DANPLs. *Journal of Applied Geophysics*, vol. 59, 177-189.
- Appelo, C.A.J. & Postman, D., 2009: *Chemistry, Groundwater & Pollution* (2<sup>nd</sup> Ed.). A.A. Balkema Publisher. Amsterdam, the Netherlands. 655 pp.
- Dahlin, T. & Leroux, V., 2012: Improvement in time-domain induced polarization data quality with multi-electrode systems by separating current and potential cables. *Near Surface Geophysics*, vol. 10, 545-565 pp.
- Davidsson, L., 2013: *Slutredovisning av utförda undersökningar och tester Renen 13 i Varberg*. [Unpublished consulting report.] WSP Environmental, Halmstad.
- ECHA, 2010: [http://echa.europa.eu/proposals-to-identify-substances-of-very-high-concern-preVIOUS-consultations/-/substance-rev/3498/search/+/del/50/col/staticField\\_-104/type/asc/pre/4/view](http://echa.europa.eu/proposals-to-identify-substances-of-very-high-concern-preVIOUS-consultations/-/substance-rev/3498/search/+/del/50/col/staticField_-104/type/asc/pre/4/view). Annex XV Report Proposal for identification of a substance as a CMR cat 1 or 2, PBT, vPvB or a substance of an equivalent level of concern Substance Name: TRICHLOROETHYLENE. Read 2015-01-18.
- Engelke, F., Hübinette, P. & Bank, A., 2013: *Kv Renen i centrala Varberg – Fördjupad analys av åtgärdsalternativ inför ansökan om statsbidrag för sanering av klorerade lösningsmedel i mark*. [Unpublished consulting report.] Structor Miljö Göteborg AB, Göteborg.
- Englöv, P., Cox, E.E., Duram, N.D., Dall-Jepsen, J., Højberg Jørgensen, T., Nilsen, J. & Törneman, N., 2007: Klorerade lösningsmedel – identifiering och val av efterbehandlingsmetod, *NV rapport 5663*. Naturvårdsverket. Stockholm, Sweden. 194 pp. (three parts) Electronic publication: reachable at: <http://www.naturvardsverket.se/Nerladdningssida/?fileType=pdf&pid=3273&downloadUrl=/Documents/publikationer/620-5663-8.pdf>. Read: 2014-12-15
- Geotomo Software, 2014: *Res2dinv\_Guide, RES2DINVx32 ver. 3.71 with multi-core support*. Penang, Malaysia. 124 pp. Electronic publication: reachable at: <http://www.geotomosoftware.com/downloads.php>
- Guha, N., Loomis, D., Grosse, Y., Lauby-Secretan, B., El Ghissassi, F., Bouvard, V., Benbrahim-Tallaa, L., Baan, R., Mattock, H. & Straif, K., 2012: Carcinogenicity of trichloroethylene, tetrachloroethylene, some other chlorinated solvents, and their metabolites. *Lancet Oncology*, vol. 13, issue 12, 1192-1193.
- Hinrichsen, H., Nord, H. & Davidsson, L., 2013: *Fördjupad åtgärdsutredning, förslag till fortsatta åtgärder*. [Unpublished consulting report.] RGS90, Norrköping. 140 pp.
- Hübinette, P. & Bank, A., 2011: *Kv Renen i centrala Varberg – Kompletterande miljöteknisk undersökning samt miljö- och hälsoriskbedömning och åtgärdsalternativ med avseende på klorerade lösningsmedel i mark*. [Unpublished consulting report.] Structor Miljö Göteborg AB, Göteborg.
- Johansson, S., Fiandaca, G. & Dahlin, T., 2015: Influence of non-aqueous phase liquid configuration on induced polarization parameters: Conceptual models applied to a time-domain field case study. *Journal of Applied Geophysics*, (Article in press).
- Jeppsson, H. & Dahlin, T., 2014: *Geoelektriska metoder inom tillämpad geofysik*. Compendium to Geophysical Investigation Methods, GEOC04. Department of Geology, Lund University. Unpublished.
- Karlqvist, L., De Geer, J., Fogdestam, B. & Engqvist, P., 1985: Description and appendices to the hydrogeological map of Halland county. *Serie Ah, Nr 8*. Geological Survey of Sweden (SGU), Uppsala.
- Lantmäteriet, Licens I2014/00579, map data.
- Larsson, J. & Hübinette, P., 2003: *Översiktlig miljöteknisk undersökning av föroreningsituationen i och kring slambassäng, Kv Renen*. [Unpublished consulting report.] Golder Associates AB, Göteborg.
- Loke, M-H., 2004: Tutorial : 2-D and 3-D electrical imaging surveys. (pdf)
- Loke, M-H., Dahlin, T. & Rucker, F., 2014: Smoothness-constrained time-lapse inversion of data from 3D resistivity surveys. *Near Surface Geo*

- physics*, 2014, 12 5-24.
- Little, J.C., Daisey, J.M. & Nazaroff, W.W., 1992: Transport of subsurface contaminants into buildings — an exposure pathway for volatile organics. *Environmental Science & Technology*, 26, 2058-2066.
- Lundqvist, I. & Kero, L., 2008: Beskrivning till berggrundskartan, 5B Varberg NO. *Serie K, Nr 105*, SGU, Uppsala.
- Magnusson, J. & Samuelsson, S., 2004a: *Kompletterande undersökning av förorening runt slam-bassäng, Kv Renen 13*. [Unpublished consulting report.] Tyréns, Göteborg.
- Menke, W., 1989: *Geophysical Data Analysis: Discrete Inverse Theory* (2<sup>nd</sup> Ed.). Academic Press. Inc.. San Diego, California, USA. 289 pp.
- Naturvårdsverket, 2002: Methods for Inventories of Contaminated Sites, Environmental Quality Criteria Guidance for data collection. In English. *Report: 5053*. Naturvårdsverket, Stockholm. 137 pp.
- Palacky, G.J., 1987: Resistivity characteristics of geologic target. *Geosciences Journal* 3, 138-144.
- Pankow, J.F. & Cherry, J.A., 1996: *Dense Chlorinated Solvents and other DNAPLs in Groundwater: History, Behavior, and Remediation*. Waterloo Press. Portland, Oregon, Canada. 538 pp.
- Påsse, T., 1990: Description to the quaternary map Varberg NO. *Serie Ae, Nr 102*. Geological Survey of Sweden (SGU), Uppsala.
- Rahm, N., Nordkvist, R., Hjerne, C. & Mell, S., 2013: *Fördjupade utredning om föroreningar i berg samt hydrogeologiska förhållanden vid Kv Renen*. [Unpublished consulting report.] Geosigma AB, Uppsala.
- Reynolds, J. M., 1997: *An Introduction to Applied and Environmental Geophysics*. John Wiley & Sons Ltd, Chichester, West Sussex, England. 796 pp.
- Sernrot, M., 2013: Ansvarsutredning beträffande föroreningar på grund av verksamhet vid Skandinaviska Textilfabriks AB:s m fl bolags fabriker på fastigheten Varberg Renen 13 I Varbergs kommun, Hallands län. Länsstyrelsen Hallands län. PM 2013-07-05 Dnr: 577-4436-13.
- SFS 1998:808: Svensk författningssamling, Miljöbalken, Miljödepartementet.
- SGU, 2006: Varberg, berggrund och grundvatten vid fastigheten Renen. DNR: 08-443/2006
- SGU, 2013a: Sveriges geologiska undersöknings föreskrifter om miljö kvalitetsnormer och statusklassificering för grundvatten, *SGU-FS 2013:2*. Sveriges geologiska undersökningar, Uppsala.
- SGU, 2013b: Bedömningsgrunder för grundvatten. *SGU-rapport 2013:01*, Sveriges geologiska undersökningar, Uppsala. 238 pp.
- Sharma, P.V., 1997: *Environmental and engineering geophysics*. Cambridge University Press, Cambridge. 475 pp.
- SMHI, 2013: Annual precipitation data, reachable at: <http://www.smhi.se/klimatdata/meteorologi/nederbord>, read 2014-09-14.
- SLV, 2001: Livsmedelsverkets föreskrifter om dricksvatten, *SLVFS 2001:30*. Svenska livsmedelsverket./National food agency, Sweden. 33pp.
- Swedish Geotechnical Society, 2011a: Klorerade lösningsmedel i mark och grundvatten. *Rapport 2:2011*. Göteborg, Sweden. 42 pp.
- Swedish Geotechnical Society, 2011b: Stimulerad reaktiv deklorering, en praktisk handledning, *Rapport 1:2011*. Göteborg, Sweden. 80 pp.
- Sällsten, G. & Barregård, L., 2004: *Miljömedicinsk riskbedömning avseende klorerade kolväten i inomhusmiljön i Bullerbyns förskola, Varberg*. [Unpublished consulting report.] Västra Göta landsregionens Miljömedicinska Centrum, Göteborg.
- Tornberg, K., Andersson, J. & Falkenberg, J. A., 2008: *Markundersökningar och fördjupad riskbedömning på Renen 13, Varberg*. [Unpublished consulting report.] Niras, Stockholm.
- Varbergs kommun, 2014: *Ansökan om bidrag till avhjälpandeåtgärd, Kv Renen, Varbergs kommun*. Version 2014-02-04



# 11 Appendix

## Appendix I – Geological profiles

Into Fig. 1 is a detailed view given of the geological profiles location and name of used wells.



### References list

GA2-GA3	Larsson & Hübinette (2003)
T0403-T0404,T0406	Magnusson & Samuelsson (2004)
0502-0503, 0508-0509	<i>unknown author, only there's measured latitude position have been used</i>
GV103-GV105	Tornberg <i>et al.</i> (2008)
GP86-GP89	Tornberg <i>et al.</i> (2008)
1007, 1009, 1012	Hübinette & Bank (2011)
1201-1205	Davidsson (2013)

## Appendix II – Differences in data acquisition setup

After processing the data from May and November, the changes between the measurements were higher than expected in line 1. Where the line crosses the location of the in situ remediation pilot test, there was an expectation of a change between the two periods. However, this change was larger than expected and mysteriously; the response in the southern part of the survey line from November was missing. We therefore took a closer look into the instrumental settings and protocols used. It turns out that they were not the same, which led to incomparable data regarding the IP-measurements. The main properties in the setting that gave rise to this were the differences in acquiring delay time, acquiring time and IP off time. All differences are summed up in table 1.

<b>Properties</b>	<b>RENEN01_Grad7sepcombi 82 Survey May/February</b>	<b>VarbergL2_GD7sepCP82fast Survey November</b>
Acq_DelaySec	1,4	0,4
Acq_TimeSec	0,6	0,6
CurrentLimitHighAmpere	0,2	0,5
CurrentLimitLowAmpere	0,02	0,01
IP_OffTimeSec	2	1
IP_windows	10	9
IP_WindowSecList	0,02 0,02 0,04 0,06 0,08 0,1 0,14 0,18 0,26 0,4 0,58	0,01 0,02 0,04 0,06 0,08 0,12 0,16 0,2 0,28
CurrentLimitHighAmpere	0,2	0,2
CurrentLimitLowAmpere	0,02	0,001
ElectrodeResistanceBadLimitHighOhm	500000	300000
ElectrodeResistanceBadLimitLowOhm	5000	20000
Fullwaveform	1	0

The decay-time from the first period was recalculated with help from ABEM AB (by Per Hedblom) to try to use the 1<sup>st</sup> second only of the decay, but even after, the results diverged and the dataset is incompatible. The main difference in data between May and November is the time the voltage was switched on, and this cannot be recalculated afterwards. Therefore, a third measurement was made in February 2015.

The Line 1 IP profiles are shown in Fig. 1. The upper left is line 1a and the upper right is line 1b, where in a comparison, the impact of the error is obvious. The lower left is the recalculated line 1a, where the high chargeability anomaly is smaller compared to the measurements in the upper left, this due to the cutting of the last acquiring time. It is similar but not comparable with the results in line 1b (upper right). The lower right show the IP profile of line 1c. This profile strongly diverge from the IP profile 1b.

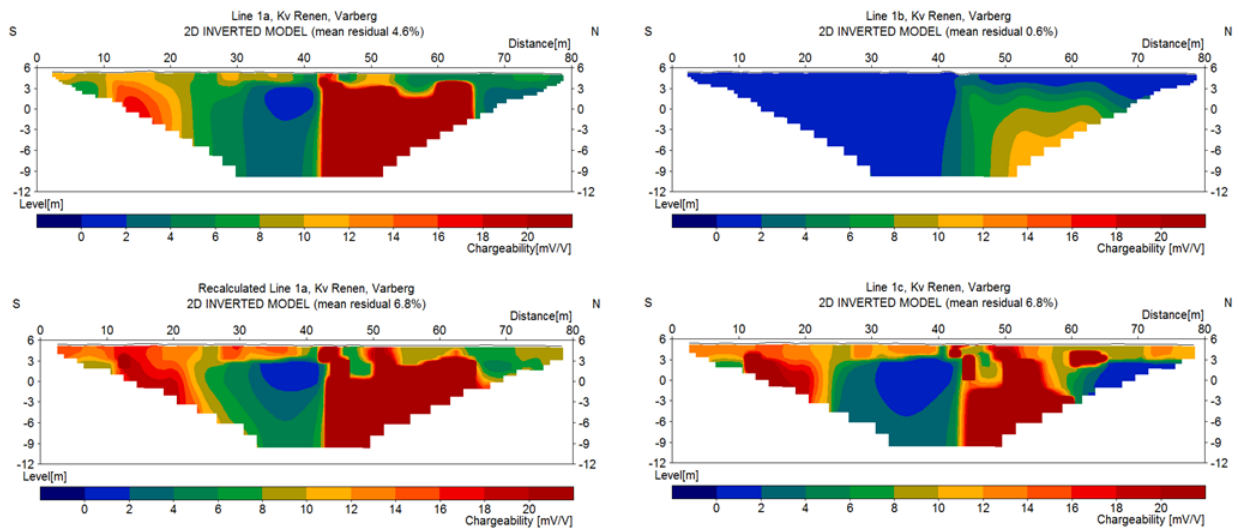


*Fig. 1.* A summary of the IP results from survey line 1. a) Survey line 1a, measured in May 2014, b) Survey line 1b, measured in November 2014, c) recalculated line 1a. d) Survey line 1c, measured in February 2015.

The lesson learnt from this, is to be aware of how the measurements are programmed, especially when the aim is to compare data with time. In this investigation the shortened time gave less information and as realised back in the office, not enough information about the subsurface. This shorter measurement time of course saved time during the fieldwork, but created much more work and spent more time in the long run.

## Appendix III – dat-file with topography

An example of a dat-file containing apparent data and added topography.

```

Grad7sepcombi82_2
1
11
15
Type of measurement (0=app.resistivity,1=resistance)
1
1603
2
1
Chargeability
mV/V
0.02 1.86
4 33 0 42 0 40 0 41 0 90.2334806554785 13.6805408912406
4 33 0 42 0 35 0 36 0 34.8922796063469 10.5757264438771
4 28 0 37 0 35 0 36 0 83.4822704883041 10.5426887324563
4 2 0 36 0 5 0 9 0 47.0258485901506 7.8955149691698
4 16 0 50 0 39 0 43 0 2.33840097521565 83.5056734620307
4 39 0 48 0 41 0 42 0 39.7561414404817 7.17794142608438
4 32 0 41 0 35 0 36 0 16.9876477733663 8.3746355655447
4 77 0 7 0 22 0 14 0 17.0257634821454 14.4873737864013
4 32 0 48 0 33 0 35 0 87.3300125987741 7.23708703514558
4 20 0 36 0 27 0 29 0 10.1130108191045 9.60839939341594
4 36 0 45 0 39 0 40 0 20.5242504459726 11.8533549825815
4 67 0 15 0 26 0 20 0 18.3308707640311 10.0200187508863
4 31 0 40 0 35 0 36 0 14.4322608232361 8.34144852958856
4 35 0 44 0 39 0 40 0 14.7307331497043 15.068005920594
4 30 0 46 0 33 0 35 0 19.8684087635805 7.47983566028803
4 34 0 43 0 39 0 40 0 15.5731670187046 14.8493700872962
4 10 0 80 0 49 0 57 0 0.448903706446267 87.8446190284379
4 75 0 41 0 52 0 48 0 2.76259829437293 27.5470916781314
4 33 0 ...
...
...
4 29 0 38 0 35 0 36 0 36.0269572946279 10.5045575395637
4 69 0 53 0 62 0 60 0 2.17753117050928 43.9474418002945
4 57 0 41 0 56 0 54 0 37.1987496877486 4.11321318570575
Topography in separate list
2
82
0 5.392
1 5.426
2 5.428
3 5.463
4 5.416
5 5.419
6 ...
...
...
79 5.157
80 5.163
81 5.159
1
0
0
0

```

## Appendix IV – 2D Inversion Settings

### Inversion settings

Initial damping factor (0.01 to 1.00)  
0.1500  
Minimum damping factor (0.001 to 0.75)  
0.0200  
Local optimization option (0=No, 1=Yes)  
1  
Convergence limit for relative change in RMS error in percent (0.1 to 20)  
1.0000  
Minimum change in RMS error for line search in percent (0.5 to 100)  
0.5000  
Number of iterations (1 to 30)  
20  
Vertical to horizontal flatness filter ratio (0.25 to 4.0)  
1.0000  
Model for increase in thickness of layers(0=default 10%, 1=default 25%, 2=user defined)  
2  
Number of nodes between adjacent electrodes (2 or 4)  
4  
Flatness filter type, Include smoothing of model resistivity (0=model changes on-ly,1=directly on model)  
1  
Reduce number of topographical data points? (0=No,1=Yes. Recommend leave at 0)  
0  
Carry out topography modeling? (0=No,1=Yes)  
1  
Type of topography trend removal (0=Average,1=Least-squares,2=End to end)  
2  
Type of Jacobian matrix calculation (0=Quasi-Newton, 1=Gauss-Newton, 2=Mixed)  
1  
Increase of damping factor with depth (1.0 to 2.0)  
1.0500  
Type of topographical modeling (0=None, 1=No longer supported so do not use, 2=uniform distorted FEM, 3=underwater, 4=damped FEM, 5=FEM with inverse Swartz-Christoffel)  
4  
Robust data constrain? (0=No, 1=Yes)  
1  
Cutoff factor for data constrain (0.0001 to 0.1))  
0.0500  
Robust model constrain? (0=No, 1=Yes)  
1  
Cutoff factor for model constrain (0.0001 to 1.0)  
0.0050  
Allow number of model parameters to exceed data points? (0=No, 1=Yes)  
1  
Use extended model? (0=No, 1=Yes)  
0  
Reduce effect of side blocks? (0=No, 1=Slight, 2=Severe, 3=Very Severe)  
1  
Type of mesh (0=Normal,1=Fine,2=Finest)  
0  
Optimise damping factor? (0=No, 1=Yes)  
1  
Time-lapse inversion constrain (0=None,1&2=Smooth,3=Robust)  
3  
Type of time-lapse inversion method (0=Simultaneous,1=Sequential)  
0  
Thickness of first layer (0.25 to 1.0)  
0.5000  
Factor to increase thickness layer with depth (1.0 to 1.25)  
1.1000  
USE FINITE ELEMENT METHOD (YES=1,NO=0)

```

0
WIDTH OF BLOCKS (1=NORMAL WIDTH, 2=DOUBLE, 3=TRIPLE, 4=QUADRAPLE, 5=QUINTIPLE)
1
MAKE SURE BLOCKS HAVE THE SAME WIDTH (YES=1,NO=0)
1
RMS CONVERGENCE LIMIT (IN PERCENT)
0.100
USE LOGARITHM OF APPARENT RESISTIVITY (0=USE LOG OF APPARENT RESISTIVITY, 1=USE RESISTANCE
VALUES, 2=USE APPARENT RESISTIVITY)
0
TYPE OF IP INVERSION METHOD (0=CONCURRENT,1=SEQUENTIAL)
0
PROCEED AUTOMATICALLY FOR SEQUENTIAL METHOD (1=YES,0=NO)
0
IP DAMPING FACTOR (0.01 to 1.0)
1.000
USE AUTOMATIC IP DAMPING FACTOR (YES=1,NO=0)
0
CUTOFF FACTOR FOR BOREHOLE DATA (0.0005 to 0.02)
0.00010

TYPE OF CROSS-BOREHOLE MODEL (0=normal,1=halfsize)
0
LIMIT RESISTIVITY VALUES(0=No,1=Yes)
1
Upper limit factor (10-50)
50.000
Lower limit factor (0.02 to 0.1)
0.020
Type of reference resistivity (0=average,1=first iteration)
0
Model refinement (1.0=Normal,0.5=Half-width cells)
1.00
Combined Combined Marquardt and Occam inversion (0=Not used,1=used)
0
Type of optimisation method (0=Gauss-Newton,2=Incomplete GN)
2
Convergence limit for Incomplete Gauss-Newton method (0.005 to 0.05)
0.005
Use data compression with Incomplete Gauss-Newton (0=No,1=Yes)
0
Use reference model in inversion (0=No,1=Yes)
1
Damping factor for reference model (0.0 to 0.3)
0.01000
Use fast method to calculate Jacobian matrix. (0=No,1=Yes)
0
Use higher damping for first layer? (0=No,1=Yes)
1
Extra damping factor for first layer (1.0 to 100.0)
5.00000
Type of finite-element method (0=Triangular,1=Trapezoidal elements)
1
Factor to increase model depth range (1.0 to 5.0)
1.050
Reduce model variations near borehole (0=No, 1=Yes)
0
Factor to control the degree variations near the boreholes are reduced (2 to 100)
5.0
Factor to control variation of borehole damping factor with distance (0.5 to 5.0)
1.0
Floating electrodes survey inversion method (0=use fixed water layer, 1=Incorporate water
layer into the model)
1
Resistivity variation within water layer (0=allow resistivity to vary freely,1=minimise
variation)
1
Use sparse inversion method for very long survey lines (0=No, 1=Yes)
0
Optimize Jacobian matrix calculation (0=No, 1=Yes)
0

```

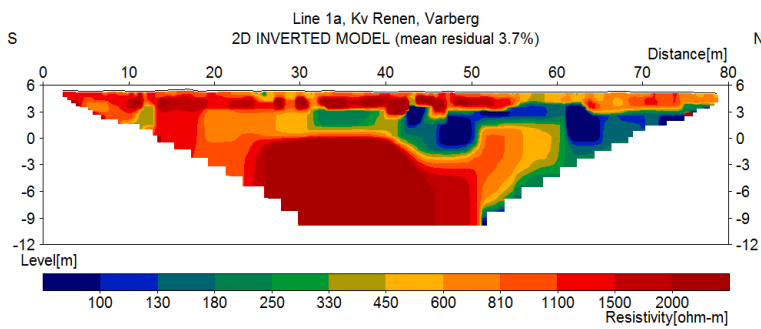
Automatically switch electrodes for negative geometric factor (0=No, 1=Yes)  
1  
Force resistance value to be consistent with the geometric factor (0=No, 1=Yes)  
0  
Shift the electrodes to round up positions of electrodes (0=No, 1=Yes)  
0  
Use difference of measurements in time-lapse inversion (0=No,1=Yes)  
0  
Use active constraint balancing (0=No,1=Yes)  
0  
Type of active constraints (0=Normal,1=Reverse)  
0  
Lower damping factor limit for active constraints  
0.4000  
Upper damping factor limit for active constraints  
2.5000  
Water resistivity variation damping factor  
8.0000  
Use automatic calculation for change of damping factor with depth (0=No,1=Yes)  
0

**Contents of Appendix V**

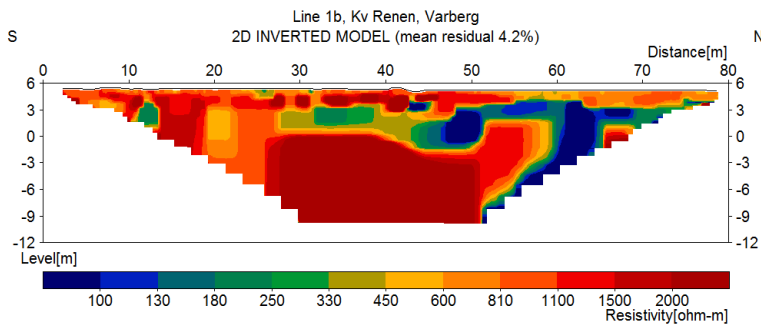
- V.I Resistivity
- V.II Induced Polarization
- V.III Recalculated IP (ABEM, P. Hedblom)
- V.IV Data not used

For map of profiles location, see Fig. 22-23

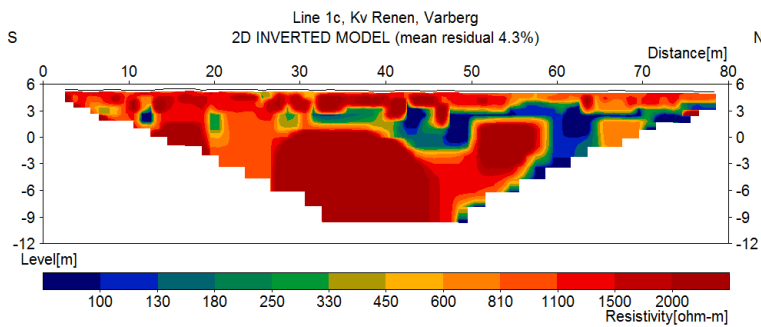
**V.I Resistivity**



Line 1a resistivity measured in May 2014

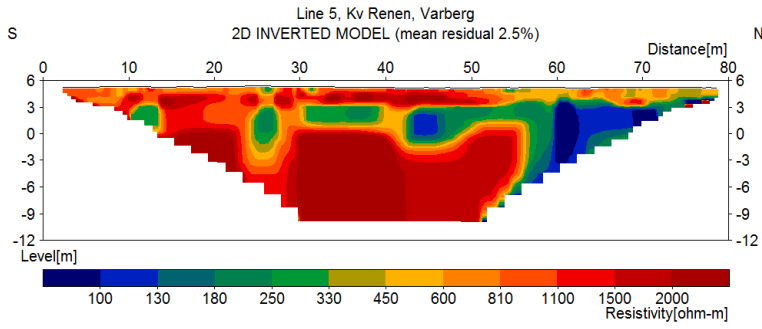


Line 1b resistivity measured in Nov. 2014

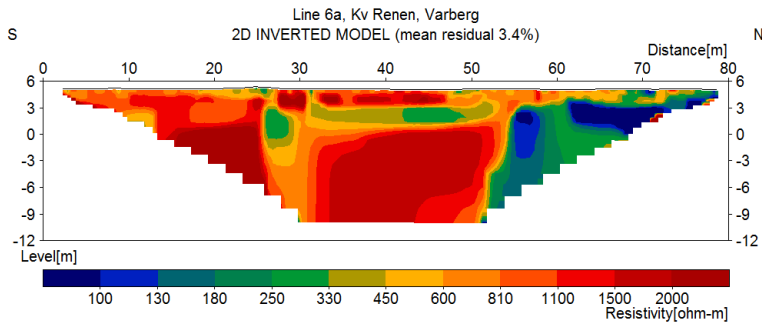


Line 1c resistivity measured in Feb. 2015

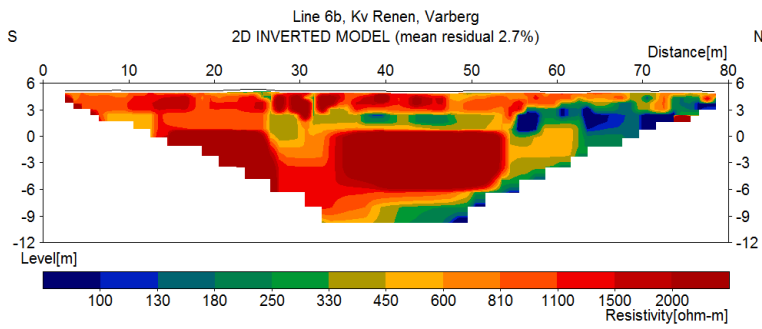




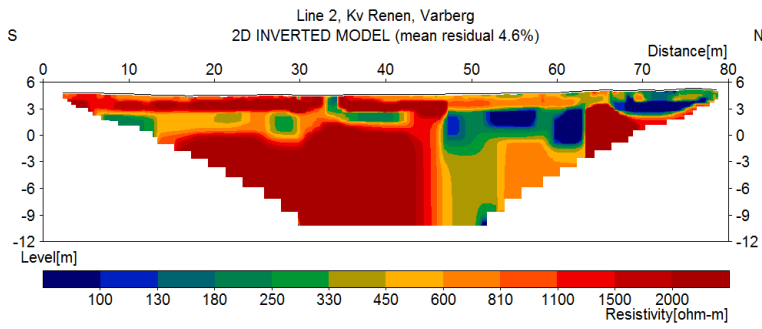
Line 5 resistivity measured in Nov. 2014



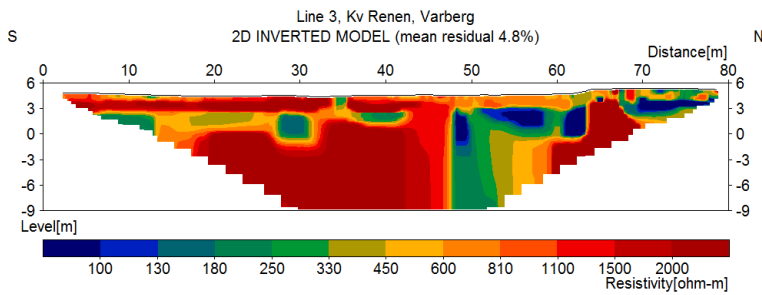
Line 6a resistivity measured in Nov. 2014



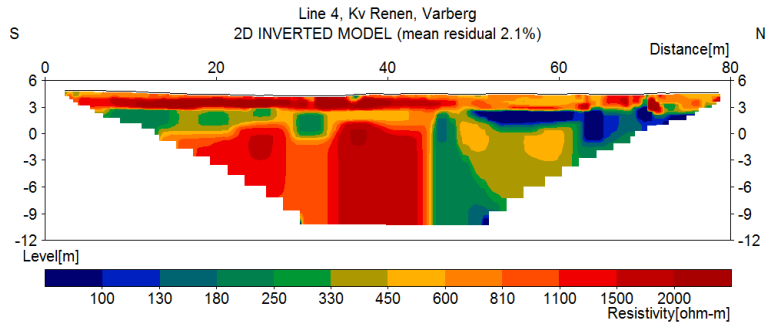
Line 6a resistivity measured in Feb. 2015



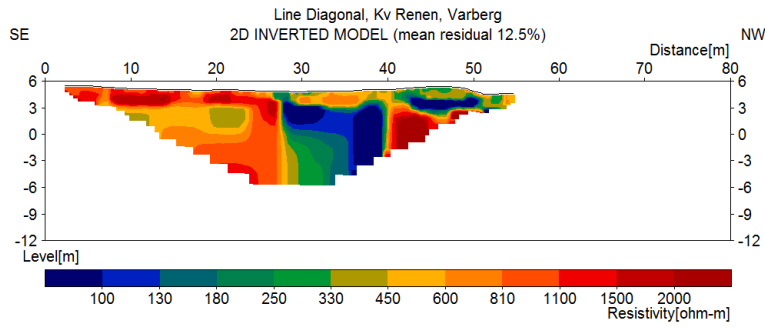
Line 2 resistivity measured in May 2014



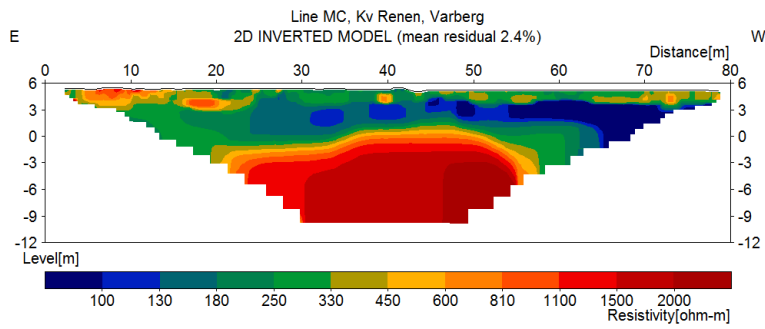
Line 3 resistivity measured in May 2014



Line 4 resistivity measured in May 2014

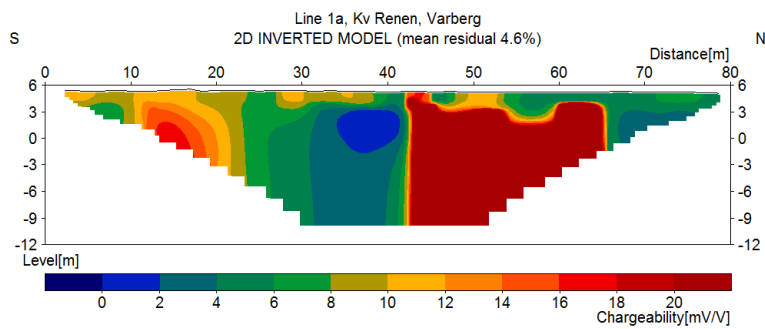


Line Diagonal resistivity measured in November 2014

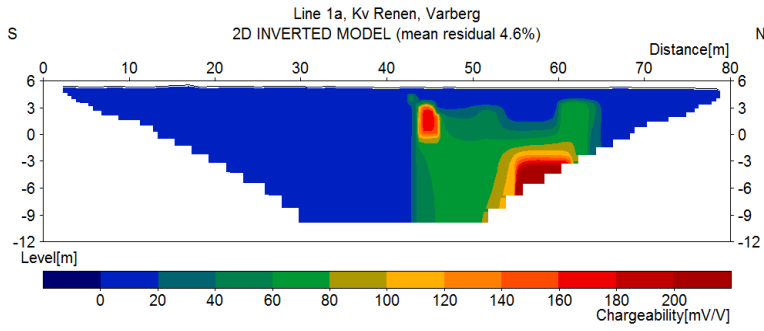


Line MC resistivity measured in November 2014

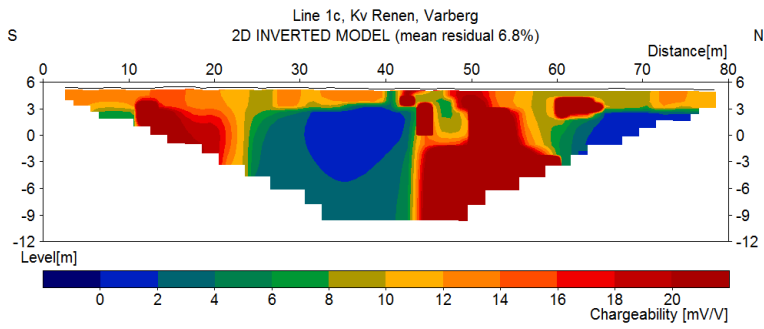
#### IV.II Induced polarization



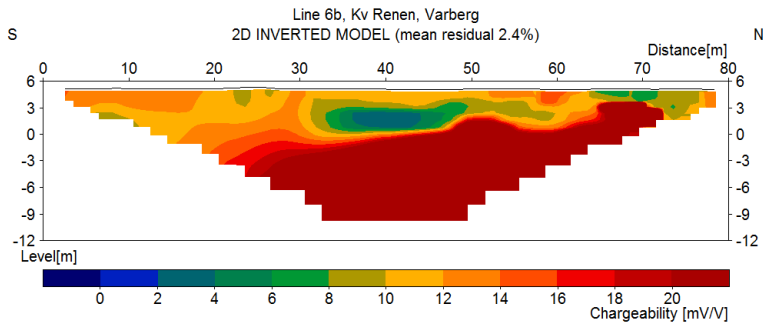
Line 1a IP measured in May 2014



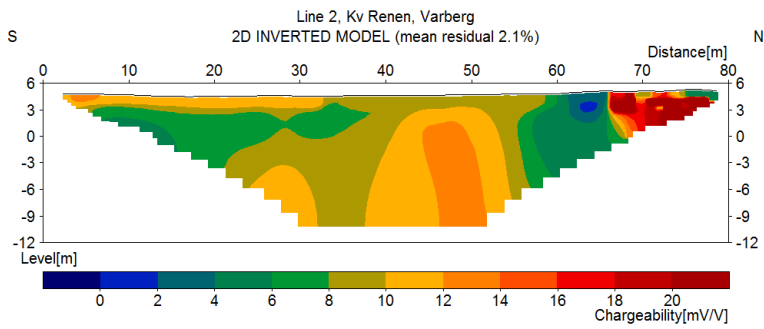
Line 1a IP measured in May 2014  
NB different scale!



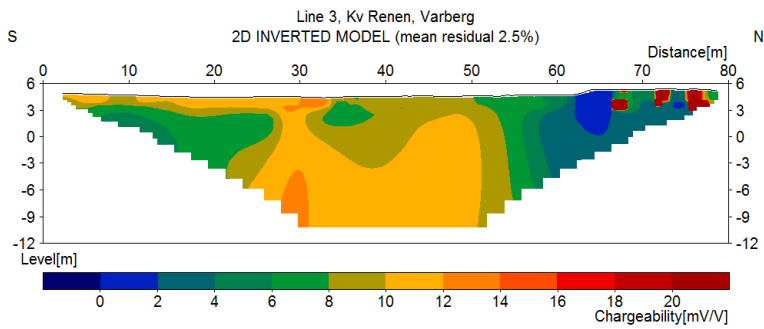
Line 1c IP measured in February 2015



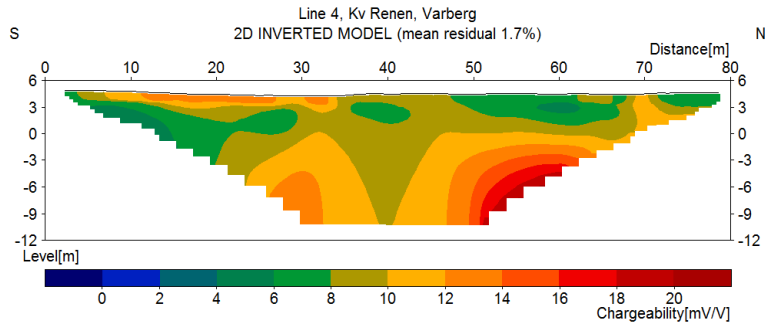
Line 6b IP measured in February 2015



Line 2 IP measured in May 2014

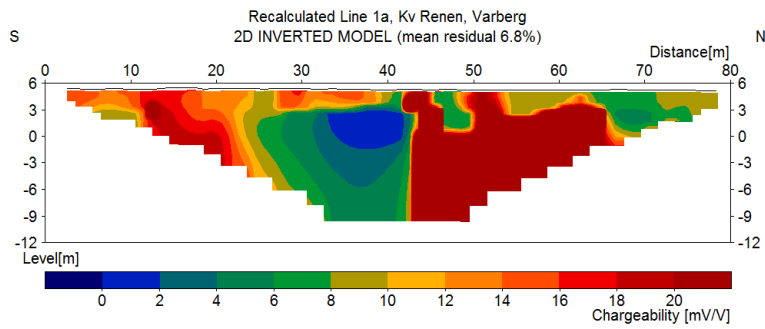


Line 3 IP measured in May 2014



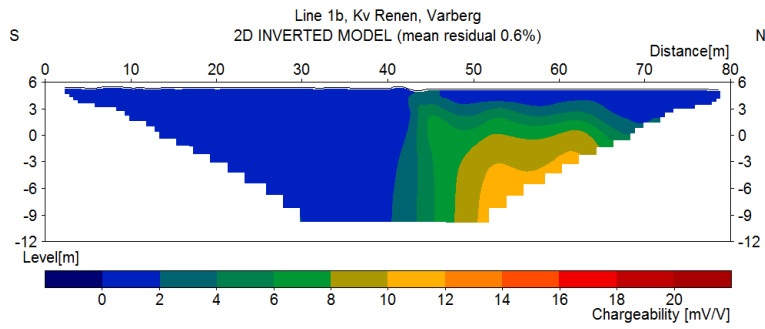
Line 4 IP measured in May 2014

V.III Recalculated (ABEM, P. Hedblom)

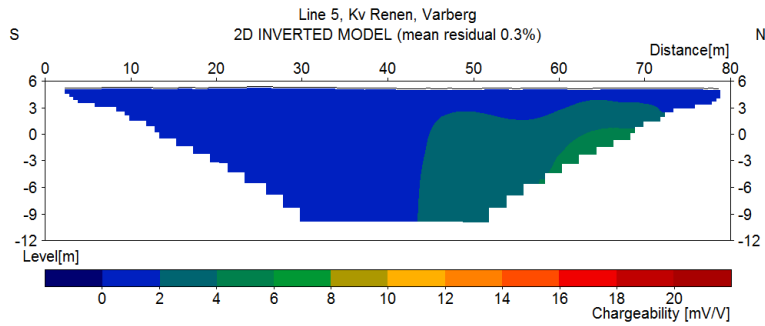


Line 1a IP recalculated, measured in May 2014

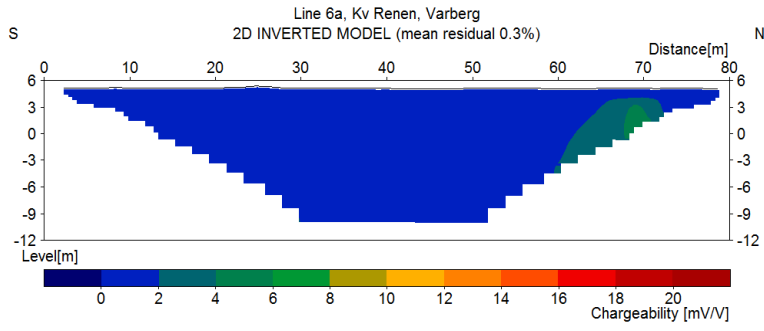
V.IV Data not used



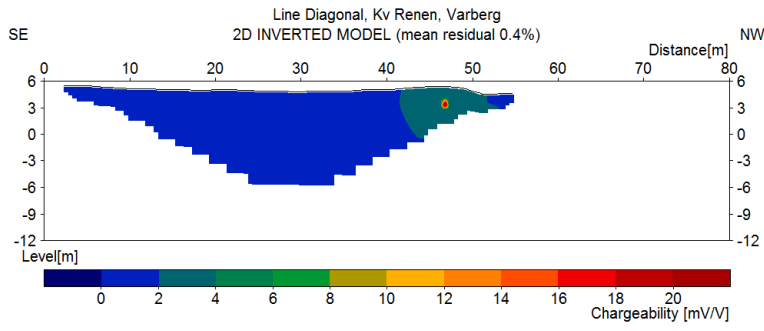
Line 1b IP measured in November 2014



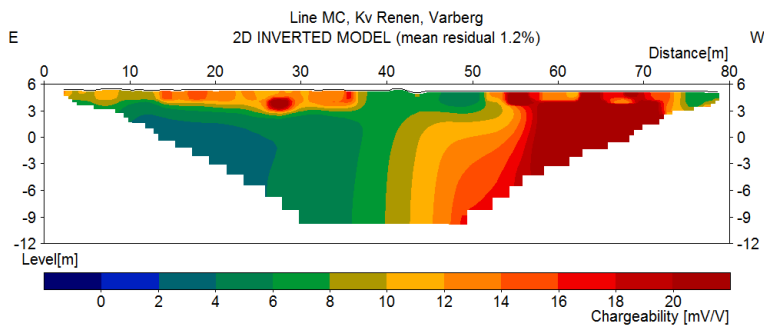
Line 5 IP measured in November 2014



Line 6a IP measured in November 2014



Line Diagonal IP measured in November 2014



Line MC IP measured in November 2014

## Appendix VI – Protocol water sample (AIControl AB)

Results from analyses at page 42, table 7.

Sampled observation wells (se maps in Fig. 22-23 for location);

1. 1201
2. 1202
3. 1203
4. 1204
5. 1205
6. GV105-1\*
7. GA2
8. 1012
9. 1009

\* GV105 has two filters and we have sampled the deeper within this study. (GV105-1). In the analyses protocol it is incorrectly called GV105-2, which is the shallower one, not sampled during this study.

**Avser**

<b>Projekt</b>	<b>Grundvatten</b>
Projekt	: 921456
Konsult/ProjNr	: David Hagerberg
Provtyp	: Grundvatten

**Information om provet och provtagningen**

Fakturareferens	: 921456	Ankomstdatum	: 2014-11-27
Provtagningsdatum	: 2014-11-26	Ankomsttidpunkt	: 2350
Provtagningsstidpunkt	: 1345	Temperatur vid ankomst	: 11 °C
Temperatur vid provtagning	: 7 °C		
Provets märkning	: 1201		
Provtagare	: David Hagerberg		

**Analysresultat**

<b>Metodbeteckning</b>	<b>Analys/Undersökning av</b>	<b>Resultat</b>	<b>Matosakerhet</b>	<b>Enhet</b>
SS-EN ISO 17294-2:2005	Arsenik, As, flit	10	± 2.0	µg/l
SS-EN ISO 17294-2:2005	Bly, Pb, flit	0.24	± 0.048	µg/l
SS-EN ISO 17294-2:2005	Kadmium, Cd, flit	0.035	± 0.007	µg/l
SS-EN ISO 17294-2:2005	Kobolt, Co, flit	1.5	± 0.30	µg/l
SS-EN ISO 17294-2:2005	Koppar, Cu, flit	33	± 6.6	µg/l
SS-EN ISO 17294-2:2005	Krom, Cr, flit	1.9	± 0.38	µg/l
SS-EN ISO 17294-2:2005	Nickel, Ni, flit	11	± 2.2	µg/l
SS-EN ISO 17294-2:2005	Vanadln, V, flit	26	± 5.2	µg/l
SS-EN ISO 17294-2:2005	Zink, Zn, flit	9.9	± 2.0	µg/l
SS-EN ISO 11885-2:2009	Järn, Fe, flit	0.53	± 0.11	mg/l
SS-EN ISO 11885-2:2009	Mangan, Mn, flit	0.07	± 0.01	mg/l
SS-EN 1484 utg 1	DOC	12	± 1.8	mg/l
SS-EN 1484 utg 1	TOC	13	± 2.0	mg/l
GC/MS	1,1-Dikloreten (1)	180	± 41	µg/l
GC/MS	1,2-Dikloreten (1)	< 4.0	± 0.60	µg/l
GC/MS	Diklormetan (1)	< 20	± 6.8	µg/l
GC/MS	Trans-1,2-Dikloreten (1)	100	± 30	µg/l
GC/MS	Cis-1,2-Dikloreten (1)	5800	± 1400	µg/l
GC/MS	1,1,1-Trikloreten (1)	430	± 180	µg/l
GC/MS	1,1,2-Trikloreten (1)	< 4.0	± 1.1	µg/l
GC/MS	Tetrakloreten(perkloretylen) (1)	11	± 2.5	µg/l
GC/MS	Tetraklormetan (koltetrakl.) (1)	< 4.0	± 1.1	µg/l
GC/MS	Triklloreten (1)	1100	± 310	µg/l
GC/MS	Triklormetan (Kloroform) (1)	< 4.0	± 1.5	µg/l
GC/MS	Monoklorbensen (1)	< 4.0	± 0.96	µg/l
GC/MS	Diklorbensener (1)	< 0.6		µg/l
GC/MS	1,2-Diklorpropan (1)	< 4.0	± 1.0	µg/l

(1) Resultat levererat av ALcontrol B.V.NL. RvA acknr L028

 Angiven måttosakerhet är beräknad med täckningsfaktor  $k = 2$ . Måttosakerheten för ackrediterade mikrobiologiska analyser kan variera från laboratoriet efter begäran.

(forts.)



ALcontrol Laboratories

ALcontrol AB

Box 1083, 581 10 Linköping · Tel: 013-25 49 00 · Fax: 013-12 17 28  
ORG.NR 556152-0016 STYRELSENS SÄTE: LINKÖPING



1005  
ISO/IEC 17025



## RAPPORT

Sida 2 (2)

utfärdad av ackrediterat laboratorium

REPORT Issued by an Accredited Laboratory

**Rapport Nr 14403277**

Uppdragsgivare

Tyréns AB

Sccheelevägen 17

223 70 LUND

### Avser

#### Projekt

#### Grundvatten

Projekt : 921456  
Konsult/ProjNr : David Hagerberg  
Provtyp : Grundvatten

### Information om provet och provtagningen

Fakturareferens	: 921456	Ankomstdatum	: 2014-11-27
Provtagningsdatum	: 2014-11-26	Ankomsttidpunkt	: 2350
Provtagningsstidpunkt	: 1345	Temperatur vid ankomst	: 11 °C
Temperatur vid provtagning	: 7 °C		
Provets märkning	: 1201		
Provtagare	: David Hagerberg		

### Analysresultat

Metodbeteckning	Analys/Undersökning av	Resultat	Matosakerhet	Enhet
GC/MS	1,1-Dikloreten (1)	55	±18	µg/l
GC/MS	Vinylklorid (1)	200		µg/l
SS-EN ISO 14403:2002	Cyanid tot, CN	<0.01	±0.002	mg/l
SS-EN ISO 10304-1:2009	Klorid, Cl	52	±7.8	mg/l

(1) Resultat levererat av ALcontrol B.V.NL. RvA acknr L028

Angiven måttåthet är beräknad med täthetsfaktor  $k = 2$ . Måttåtheten för ackrediterade mikrobiologiska analyser kan erhållas från laboratoriet efter begäran.

Linköping 2014-12-09

Rapporten har granskats och godkänns av

Mats Lindgren  
Laboratoriechef

Kontrollnr 2281 6050 5707 6778

Den här rapporten får endast återges i sin helhet, om inte utfärdande laboratorium i förväg skriftligen godkännt annat.



**Avser**
**Projekt**
**Grundvatten**

 Projekt : 921456  
 Konsult/ProjNr : David Hagerberg  
 Provtyp : Grundvatten

**Information om provet och provtagningen**

Fakturareferens	: 921456	Ankomstdatum	: 2014-11-27
Provtagningsdatum	: 2014-11-26	Ankomsttidpunkt	: 2350
Provtagningsstidpunkt	: 1440	Temperatur vid ankomst	: 11 °C
Temperatur vid provtagning	: 7 °C		
Provets märkning	: 1202		
Provtagare	: David Hagerberg		

**Analysresultat**

Metodbeteckning	Analys/Undersökning av	Resultat	Matosakerhet	Enhet
SS-EN ISO 17294-2:2005	Arsenik, As, flit	6.6	±1.3	µg/l
SS-EN ISO 17294-2:2005	Bly, Pb, flit	0.24	±0.048	µg/l
SS-EN ISO 17294-2:2005	Kadmium, Cd, flit	0.016	±0.003	µg/l
SS-EN ISO 17294-2:2005	Kobolt, Co, flit	0.26	±0.052	µg/l
SS-EN ISO 17294-2:2005	Koppar, Cu, flit	1.8	±0.36	µg/l
SS-EN ISO 17294-2:2005	Krom, Cr, flit	3.1	±0.62	µg/l
SS-EN ISO 17294-2:2005	Nickel, Ni, flit	1.8	±0.36	µg/l
SS-EN ISO 17294-2:2005	Vanadln, V, flit	21	±4.2	µg/l
SS-EN ISO 17294-2:2005	Zink, Zn, flit	2.4	±0.48	µg/l
SS-EN ISO 11885-2:2009	Järn, Fe, flit	5.7	±1.1	mg/l
SS-EN ISO 11885-2:2009	Mangan, Mn, flit	0.26	±0.05	mg/l
SS-EN 1484 utg 1	DOC	16	±2.4	mg/l
SS-EN 1484 utg 1	TOC	16	±2.4	mg/l
GC/MS	1,1-Dikloreten (1)	360	±83	µg/l
GC/MS	1,2-Dikloreten (1)	< 4.0	±0.60	µg/l
GC/MS	Diklormetan (1)	< 20	±6.8	µg/l
GC/MS	Trans-1,2-Dikloreten (1)	44	±13	µg/l
GC/MS	Cis-1,2-Dikloreten (1)	1700	±410	µg/l
GC/MS	1,1,1-Trikloreten (1)	43	±18	µg/l
GC/MS	1,1,2-Trikloreten (1)	< 4.0	±1.1	µg/l
GC/MS	Tetrakloreten(perkloretylen) (1)	< 4.0	±0.92	µg/l
GC/MS	Tetraklormetan (koltetrakl.) (1)	< 4.0	±1.1	µg/l
GC/MS	Triklloreten (1)	6.9	±1.9	µg/l
GC/MS	Triklormetan (Kloroform) (1)	< 4.0	±1.5	µg/l
GC/MS	Monoklorbensen (1)	< 4.0	±0.96	µg/l
GC/MS	Diklorbensener (1)	< 0.6		µg/l
GC/MS	1,2-Diklorpropan (1)	< 4.0	±1.0	µg/l

(1) Resultat levererat av ALcontrol B.V.NL. RvA acknr L028

Angiven måttosakerhet är beräknad med täckningsfaktor k = 2. Måttosakerheten för ackrediterade mikrobiologiska analyser kan skilja från laboratoriet efter begäran.

(forts.)



ALcontrol Laboratories

ALcontrol AB

Box 1083, 581 10 Linköping · Tel: 013-25 49 00 · Fax: 013-12 17 28  
ORG.NR 556152-0016 STYRELSENS SÄTE: LINKÖPING



1005  
ISO/IEC 17025



## RAPPORT

Sida 2 (2)

utförd av ackrediterat laboratorium

REPORT Issued by an Accredited Laboratory

**Rapport Nr 14403284**

Uppdragsgivare

Tyréns AB

Sccheelevägen 17

223 70 LUND

### Avser

#### Projekt

#### Grundvatten

Projekt : 921456  
Konsult/ProjNr : David Hagerberg  
Provtyp : Grundvatten

### Information om provet och provtagningen

Fakturareferens	: 921456	Ankomstdatum	: 2014-11-27
Provtagningsdatum	: 2014-11-26	Ankomsttidpunkt	: 2350
Provtagningsstidpunkt	: 1440	Temperatur vid ankomst	: 11 °C
Temperatur vid provtagning	: 7 °C		
Provets märkning	: 1202		
Provtagare	: David Hagerberg		

### Analysresultat

Metodbeteckning	Analys/Undersökning av	Resultat	Matosakerhet	Enhet
GC/MS	1,1-Dikloreten (1)	16	± 5.3	µg/l
GC/MS	Vinylklorid (1)	2100		µg/l
SS-EN ISO 14403:2002	Cyanid tot, CN	<0.01	±0.002	mg/l
SS-EN ISO 10304-1:2009	Klorid, Cl	42	± 6.3	mg/l

(1) Resultat levererat av ALcontrol B.V.NL. RvA acknr L028

Angivna måttosakerhet är beräknad med täckningsfaktor k = 2. Måttosakerheten för ackrediterade mikrobiologiska analyser kan erhållas från laboratoriet efter begäran.

Linköping 2014-12-05

Rapporten har granskats och godkänns av

Mats Lindgren  
Laboratoriechef

Kontrollnr 1516 8150 5903 6170

Den här rapporten får endast återges i sin helhet, om inte utfärdande laboratorium i förväg skriftligen godkännt annat.

**Avser**

<b>Projekt</b>	<b>Grundvatten</b>
Projekt	: 921456
Konsult/ProjNr	: David Hagerberg
Provtyp	: Grundvatten

**Information om provet och provtagningen**

Fakturareferens	: 921456	Ankomstdatum	: 2014-11-27
Provtagningsdatum	: 2014-11-26	Ankomsttidpunkt	: 2350
Provtagningsstidpunkt	: 1500	Temperatur vid ankomst	: 11 °C
Temperatur vid provtagning	: 7 °C		
Provets märkning	: 1203		
Provtagare	: David Hagerberg		

**Analysresultat**

<b>Metodbeteckning</b>	<b>Analys/Undersökning av</b>	<b>Resultat</b>	<b>Matosakerhet</b>	<b>Enhet</b>
SS-EN ISO 17294-2:2005	Arsenik, As, flit	3.8	±0.76	µg/l
SS-EN ISO 17294-2:2005	Bly, Pb, flit	0.52	±0.10	µg/l
SS-EN ISO 17294-2:2005	Kadmium, Cd, flit	0.011	±0.003	µg/l
SS-EN ISO 17294-2:2005	Kobolt, Co, flit	0.23	±0.046	µg/l
SS-EN ISO 17294-2:2005	Koppar, Cu, flit	1.9	±0.38	µg/l
SS-EN ISO 17294-2:2005	Krom, Cr, flit	3.1	±0.62	µg/l
SS-EN ISO 17294-2:2005	Nickel, Ni, flit	4.5	±0.90	µg/l
SS-EN ISO 17294-2:2005	Vanadin, V, flit	19	±3.8	µg/l
SS-EN ISO 17294-2:2005	Zink, Zn, flit	2.0	±0.40	µg/l
SS-EN ISO 11885-2:2009	Järn, Fe, flit	3.1	±0.62	mg/l
SS-EN ISO 11885-2:2009	Mangan, Mn, flit	0.13	±0.03	mg/l
SS-EN 1484 utg 1	DOC	16	±2.4	mg/l
SS-EN 1484 utg 1	TOC	19	±2.9	mg/l
GC/MS	1,1-Dikloreten (1)	240	±55	µg/l
GC/MS	1,2-Dikloreten (1)	<0.1	±0.02	µg/l
GC/MS	Diklormetan (1)	<0.5	±0.17	µg/l
GC/MS	Trans-1,2-Dikloreten (1)	14	±4.2	µg/l
GC/MS	Cis-1,2-Dikloreten (1)	1100	±260	µg/l
GC/MS	1,1,1-Trikloreten (1)	29	±12	µg/l
GC/MS	1,1,2-Trikloreten (1)	0.91	±0.25	µg/l
GC/MS	Tetrakloreten(perkloretylen) (1)	<0.1	±0.02	µg/l
GC/MS	Tetraklormetan (koltetrakt.) (1)	<0.1	±0.03	µg/l
GC/MS	Triklloreten (1)	3.2	±0.90	µg/l
GC/MS	Triklormetan (Kloroform) (1)	<0.1	±0.04	µg/l
GC/MS	Monoklorbensen (1)	<0.2	±0.05	µg/l
GC/MS	Diklorbensener (1)	<0.6		µg/l
GC/MS	1,2-Diklorpropan (1)	<0.2	±0.05	µg/l

(1) Resultat levererat av ALcontrol B.V.NL. RvA acknr L028

 Angiven målnärlighet är beräknad med täckningsfaktor  $k = 2$ . Målnärligheten för ackrediterade mikrobiologiska analyser kan erhållas från laboratoriet efter begäran.

(forts.)

**Avser****Projekt****Grundvatten**Projekt : 921456  
Konsult/ProjNr : David Hagerberg  
Provtyp : Grundvatten**Information om provet och provtagningen**Fakturareferens : 921456 Ankomstdatum : 2014-11-27  
Provtagningsdatum : 2014-11-26 Ankomsttidpunkt : 2350  
Provtagningstidpunkt : 1500 Temperatur vid ankomst : 11 °C  
Temperatur vid provtagning : 7 °C  
Provets märkning : 1203  
Provtagare : David Hagerberg**Analysresultat**

Metodbeteckning	Analys/Undersökning av	Resultat	Matosakerhet	Enhet
GC/MS	1,1-Dikloreten (1)	10	± 3.3	µg/l
GC/MS	Vinylklorid (1)	1200		µg/l
SS-EN ISO 14403:2002	Cyanid tot, CN	<0.01	±0.002	mg/l
SS-EN ISO 10304-1:2009	Klorid, Cl	56	± 8.4	mg/l

(1) Resultat levererat av ALcontrol B.V.NL. RvA acknr L028

Angiven måttosakerhet är beräknad med täckningsfaktor  $k = 2$ . Måttosakerheten för ackrediterade mikrobiologiska analyser kan erhållas från laboratoriet efter begäran.**Kommentar**

Rapporteringsgränser? ml 2014-12-08

Linköping 2014-12-11

Rapporten har granskats och godkänns av

Mats Lindgren  
Laboratoriechef

Kontrollnr 1116 8152 5503 6376

---

Denna rapport får endast återges i sin helhet, om inte utfärdande laboratorium i förväg skriftligen godkännt annat.

**Avser**
**Projekt**
**Grundvatten**

 Projekt : 921456  
 Konsult/ProjNr : David Hagerberg  
 Provtyp : Grundvatten

**Information om provet och provtagningen**

Fakturareferens	: 921456	Ankomstdatum	: 2014-11-27
Provtagningsdatum	: 2014-11-26	Ankomsttidpunkt	: 2350
Provtagningsstidpunkt	: 1420	Temperatur vid ankomst	: 11 °C
Temperatur vid provtagning	: 7 °C		
Provets märkning	: 1204		
Provtagare	: David Hagerberg		

**Analysresultat**

Metodbeteckning	Analys/Undersökning av	Resultat	Matosakerhet	Enhet
SS-EN ISO 17294-2:2005	Arsenik, As, flit	7.6	±1.5	µg/l
SS-EN ISO 17294-2:2005	Bly, Pb, flit	0.27	±0.054	µg/l
SS-EN ISO 17294-2:2005	Kadmium, Cd, flit	0.021	±0.004	µg/l
SS-EN ISO 17294-2:2005	Kobolt, Co, flit	0.34	±0.068	µg/l
SS-EN ISO 17294-2:2005	Koppar, Cu, flit	10	±2.0	µg/l
SS-EN ISO 17294-2:2005	Krom, Cr, flit	1.0	±0.20	µg/l
SS-EN ISO 17294-2:2005	Nickel, Ni, flit	3.2	±0.64	µg/l
SS-EN ISO 17294-2:2005	Vanadln, V, flit	17	±3.4	µg/l
SS-EN ISO 17294-2:2005	Zink, Zn, flit	4.7	±0.94	µg/l
SS-EN ISO 11885-2:2009	Järn, Fe, flit	0.18	±0.04	mg/l
SS-EN ISO 11885-2:2009	Mangan, Mn, flit	<0.03	±0.008	mg/l
SS-EN 1484 utg 1	DOC	6.7	±1.0	mg/l
SS-EN 1484 utg 1	TOC	6.9	±1.0	mg/l
GC/MS	1,1-Dikloreten (1)	3.0	±0.69	µg/l
GC/MS	1,2-Dikloreten (1)	<0.1	±0.02	µg/l
GC/MS	Diklormetan (1)	<0.5	±0.17	µg/l
GC/MS	Trans-1,2-Dikloreten (1)	3.0	±0.90	µg/l
GC/MS	Cis-1,2-Dikloreten (1)	67	±16	µg/l
GC/MS	1,1,1-Trikloreten (1)	1.5	±0.62	µg/l
GC/MS	1,1,2-Trikloreten (1)	<0.1	±0.03	µg/l
GC/MS	Tetrakloreten(perkloretylen) (1)	0.12	±0.03	µg/l
GC/MS	Tetraklormetan (koltetrakl.) (1)	<0.1	±0.03	µg/l
GC/MS	Triklloreten (1)	58	±16	µg/l
GC/MS	Triklormetan (Kloroform) (1)	<0.1	±0.04	µg/l
GC/MS	Monoklorbensen (1)	<0.2	±0.05	µg/l
GC/MS	Diklorbensener (1)	<0.6		µg/l
GC/MS	1,2-Diklorpropan (1)	<0.2	±0.05	µg/l

(1) Resultat levererat av ALcontrol B.V.NL. RvA acknr L028

Angiven måttosakerhet är beräknad med täckningsfaktor k = 2. Måttosakerheten för ackrediterade mikrobiologiska analyser kan erhållas från laboratoriet efter begäran.

(forts.)

**Avser**

<b>Projekt</b>		<b>Grundvatten</b>	
Projekt	: 921456		
Konsult/ProjNr	: David Hagerberg		
Provtyp	: Grundvatten		

**Information om provet och provtagningen**

Fakturareferens	: 921456	Ankomstdatum	: 2014-11-27
Provtagningsdatum	: 2014-11-26	Ankomsttidpunkt	: 2350
Provtagningsstidpunkt	: 1420	Temperatur vid ankomst	: 11 °C
Temperatur vid provtagning	: 7 °C		
Provets märkning	: 1204		
Provtagare	: David Hagerberg		

**Analysresultat**

Metodbeteckning	Analys/Undersökning av	Resultat	Matosakerhet	Enhet
GC/MS	1,1-Dikloreten (1)	0.86	±0.28	µg/l
GC/MS	Vinylklorid (1)	1		µg/l
SS-EN ISO 14403:2002	Cyanid tot, CN	<0.01	±0.002	mg/l
SS-EN ISO 10304-1:2009	Klorid, Cl	45	±6.8	mg/l

(1) Resultat levererat av ALcontrol B.V.NL. RvA acknr L028

Angivna måttosakerhet är beräknad med täckningsfaktor  $k = 2$ . Måttosakerheten för ackrediterade mikrobiologiska analyser kan erhållas från laboratoriet efter begäran.

Linköping 2014-12-11

Rapporten har granskats och godkänns av

Mats Lindgren  
Laboratoriechef

Kontrollnr 0164 8954 5206 6577

---

Denna rapport får endast återges i sin helhet, om inte utfärdande laboratorium i förväg skriftligen godkännt annat.

**Avser**

<b>Projekt</b>	<b>Grundvatten</b>
Projekt	: 921456
Konsult/ProjNr	: David Hagerberg
Provtyp	: Grundvatten

**Information om provet och provtagningen**

Fakturareferens	: 921456	Ankomstdatum	: 2014-11-27
Provtagningsdatum	: 2014-11-26	Ankomsttidpunkt	: 2350
Provtagningsstidpunkt	: 1200	Temperatur vid ankomst	: 11 °C
Temperatur vid provtagning	: 7 °C		
Provets märkning	: 1205		
Provtagare	: David Hagerberg		

**Analysresultat**

Metodbeteckning	Analys/Undersökning av	Resultat	Måttosakerhet	Enhet
SS-EN ISO 17294-2:2005	Arsenik, As, flit	0.84	±0.17	µg/l
SS-EN ISO 17294-2:2005	Bly, Pb, flit	0.033	±0.007	µg/l
SS-EN ISO 17294-2:2005	Kadmium, Cd, flit	0.015	±0.003	µg/l
SS-EN ISO 17294-2:2005	Kobolt, Co, flit	0.14	±0.028	µg/l
SS-EN ISO 17294-2:2005	Koppar, Cu, flit	1.1	±0.22	µg/l
SS-EN ISO 17294-2:2005	Krom, Cr, flit	0.72	±0.14	µg/l
SS-EN ISO 17294-2:2005	Nickel, Ni, flit	0.77	±0.15	µg/l
SS-EN ISO 17294-2:2005	Vanadin, V, flit	4.4	±0.88	µg/l
SS-EN ISO 17294-2:2005	Zink, Zn, flit	1.3	±0.26	µg/l
SS-EN ISO 11885-2:2009	Järn, Fe, flit	0.10	±0.02	mg/l
SS-EN ISO 11885-2:2009	Mangan, Mn, flit	0.03	±0.008	mg/l
SS-EN 1484 utg 1	DOC	5.1	±0.76	mg/l
SS-EN 1484 utg 1	TOC	6.6	±0.99	mg/l
GC/MS	1,1-Dikloreten (1)	47	±11	µg/l
GC/MS	1,2-Dikloreten (1)	<1.0	±0.15	µg/l
GC/MS	Diklormetan (1)	<5.0	±1.7	µg/l
GC/MS	Trans-1,2-Dikloreten (1)	7.8	±2.3	µg/l
GC/MS	Cis-1,2-Dikloreten (1)	370	±89	µg/l
GC/MS	1,1,1-Trikloreten (1)	<1.0	±0.41	µg/l
GC/MS	1,1,2-Trikloreten (1)	<1.0	±0.27	µg/l
GC/MS	Tetrakloreten(perkloretylen) (1)	<1.0	±0.23	µg/l
GC/MS	Tetraklormetan (koltetrakt.) (1)	<1.0	±0.27	µg/l
GC/MS	Triklöreten (1)	510	±140	µg/l
GC/MS	Triklormetan (Kloroform) (1)	<1.0	±0.37	µg/l
GC/MS	Monoklorbensen (1)	<1.0	±0.24	µg/l
GC/MS	Diklorbensener (1)	<0.6		µg/l
GC/MS	1,2-Diklorpropan (1)	<1.0	±0.26	µg/l

(1) Resultat levererat av ALcontrol B.V.NL. RvA acknr L028

 Angiven måttosakerhet är beräknad med täckningsfaktor  $k = 2$ . Måttosakerheten för ackrediterade mikrobiologiska analyser kan erhållas från laboratoriet efter begäran.

(forts.)



ALcontrol Laboratories

ALcontrol AB

Box 1083, 581 10 Linköping · Tel: 013-25 40 00 · Fax: 013-12 17 28  
ORG.NR 556152-0016 STYRELSENS SÄTE: LINKÖPING



1005  
ISO/IEC 17025



## RAPPORT

Sida 2 (2)

utfärdad av ackrediterat laboratorium  
REPORT Issued by an Accredited Laboratory

**Rapport Nr 14403298**

Uppdragsgivare

Tyréns AB

Sccheelevägen 17  
223 70 LUND

### Avser

Projekt	Grundvatten
Projekt	: 921456
Konsult/ProjNr	: David Hagerberg
Provtyp	: Grundvatten

### Information om provet och provtagningen

Fakturareferens	: 921456	Ankomstdatum	: 2014-11-27
Provtagningsdatum	: 2014-11-26	Ankomsttidpunkt	: 2350
Provtagningsstidpunkt	: 1200	Temperatur vid ankomst	: 11 °C
Temperatur vid provtagning	: 7 °C		
Provets märkning	: 1205		
Provtagare	: David Hagerberg		

### Analysresultat

Metodbeteckning	Analys/Undersökning av	Resultat	Mätosäkerhet	Enhet
GC/MS	1,1-Dikloreten (1)	9.6	± 3.2	µg/l
GC/MS	Vinylklorid (1)	3		µg/l
SS-EN ISO 14403:2002	Cyanid tot, CN	<0.01	±0.002	mg/l
SS-EN ISO 10304-1:2009	Klorid, Cl	33	± 5.0	mg/l

(1) Resultat levererat av ALcontrol B.V.NL. RvA acknr L028

Angiven mätosäkerhet är beräknad med täckningsfaktor  $k = 2$ . Mätosäkerheten för ackrediterade mikrobiologiska analyser kan erhållas från laboratoriet efter begäran.

### Kommentar

Förhöjd rapporteringsgräns för några av de klorerade lösningsmedlen på grund av störningar från andra ämnen i provet och nödvändig spädning.

Detta medför också att mätosäkerheten är högre än vad som angivits ovan.

Linköping 2014-12-05

Rapporten har granskats och godkänns av

Mats Lindgren  
Laboratoriechef

Kontrollnr 0161 8351 5701 6078

Den här rapporten får endast återges i sin helhet, om inte utfärdande laboratorium i förväg skriftligen godkännt annat.



**Avser**
**Projekt**
**Grundvatten**

 Projekt : 921456  
 Konsult/ProjNr : David Hagerberg  
 Provtyp : Grundvatten

**Information om provet och provtagningen**

Fakturareferens	: 921456	Ankomstdatum	: 2014-11-27
Provtagningsdatum	: 2014-11-26	Ankomsttidpunkt	: 2350
Provtagningsstidpunkt	: 1400	Temperatur vid ankomst	: 11 °C
Temperatur vid provtagning	: 7 °C		
Provets märkning	: GV105-2		
Provtagare	: David Hagerberg		

**Analysresultat**

Metodbeteckning	Analys/Undersökning av	Resultat	Matosakerhet	Enhet
SS-EN ISO 17294-2:2005	Arsenik, As, flit	9.1	±1.8	µg/l
SS-EN ISO 17294-2:2005	Bly, Pb, flit	0.061	±0.012	µg/l
SS-EN ISO 17294-2:2005	Kadmium, Cd, flit	0.010	±0.003	µg/l
SS-EN ISO 17294-2:2005	Kobolt, Co, flit	0.79	±0.16	µg/l
SS-EN ISO 17294-2:2005	Koppar, Cu, flit	1.3	±0.26	µg/l
SS-EN ISO 17294-2:2005	Krom, Cr, flit	2.1	±0.42	µg/l
SS-EN ISO 17294-2:2005	Nickel, Ni, flit	5.8	±1.2	µg/l
SS-EN ISO 17294-2:2005	Vanadln, V, flit	7.5	±1.5	µg/l
SS-EN ISO 17294-2:2005	Zink, Zn, flit	1.2	±0.25	µg/l
SS-EN ISO 11885-2:2009	Järn, Fe, flit	1.7	±0.34	mg/l
SS-EN ISO 11885-2:2009	Mangan, Mn, flit	0.18	±0.04	mg/l
SS-EN 1484 utg 1	DOC	18	±2.7	mg/l
SS-EN 1484 utg 1	TOC	21	±3.2	mg/l
GC/MS	1,1-Dikloreten (1)	430	±99	µg/l
GC/MS	1,2-Dikloreten (1)	<10	±1.5	µg/l
GC/MS	Diklormetan (1)	<50	±17	µg/l
GC/MS	Trans-1,2-Dikloreten (1)	220	±66	µg/l
GC/MS	Cis-1,2-Dikloreten (1)	5100	±1200	µg/l
GC/MS	1,1,1-Trikloreten (1)	290	±120	µg/l
GC/MS	1,1,2-Trikloreten (1)	<10	±2.7	µg/l
GC/MS	Tetrakloreten(perkloretylen) (1)	<10	±2.3	µg/l
GC/MS	Tetraklormetan (koltetrakl.) (1)	<10	±2.7	µg/l
GC/MS	Triklloreten (1)	300	±84	µg/l
GC/MS	Triklormetan (Kloroform) (1)	<10	±3.7	µg/l
GC/MS	Monoklorbensen (1)	<10	±2.4	µg/l
GC/MS	Diklorbensener (1)	<0.6		µg/l
GC/MS	1,2-Diklorpropan (1)	<10	±2.6	µg/l

(1) Resultat levererat av ALcontrol B.V.NL. RvA acknr L028

Angiven måttosakerhet är beräknad med täckningsfaktor k = 2. Måttosakerheten för ackrediterade mikrobiologiska analyser kan avvika från laboratoriet efter begäran.

(forts.)



ALcontrol Laboratories

ALcontrol AB

Box 1083, 581 10 Linköping · Tel: 013-25 40 00 · Fax: 013-12 17 28  
ORG.NR 556152-0016 STYRELSENS SÄTE: LINKÖPING



1005  
ISO/IEC 17025



## RAPPORT

Sida 2 (2)

utfärdad av ackrediterat laboratorium  
REPORT Issued by an Accredited Laboratory

**Rapport Nr 14403299**

Uppdragsgivare

Tyréns AB

Sccheelevägen 17

223 70 LUND

### Avser

Projekt	Grundvatten
Projekt	: 921456
Konsult/ProjNr	: David Hagerberg
Provtyp	: Grundvatten

### Information om provet och provtagningen

Fakturareferens	: 921456	Ankomstdatum	: 2014-11-27
Provtagningsdatum	: 2014-11-26	Ankomsttidpunkt	: 2350
Provtagningsstidpunkt	: 1400	Temperatur vid ankomst	: 11 °C
Temperatur vid provtagning	: 7 °C		
Provets märkning	: GV105-2		
Provtagare	: David Hagerberg		

### Analysresultat

Metodbeteckning	Analys/Undersökning av	Resultat	Mätosäkerhet	Enhet
GC/MS	1,1-Dikloreten (1)	50	± 17	µg/l
GC/MS	Vinylklorid (1)	2100		µg/l
SS-EN ISO 14403:2002	Cyanid tot, CN	<0.01	±0.002	mg/l
SS-EN ISO 10304-1:2009	Klorid, Cl	51	± 7.6	mg/l

(1) Resultat levererat av ALcontrol B.V.NL. RvA acknr L028

Angiven mätosäkerhet är beräknad med täckningsfaktor  $k = 2$ . Mätosäkerheten för ackrediterade mikrobiologiska analyser kan erhållas från laboratoriet efter begäran.

### Kommentar

Förhöjd rapporteringsgräns för några av de klorerade lösningsmedlen på grund av störningar från andra ämnen i provet och nödvändig spädning.

Detta medför också att mätosäkerheten är högre än vad som angivits ovan.

Linköping 2014-12-05

Rapporten har granskats och godkänns av

Mats Lindgren  
Laboratoriechef

Kontrollnr 0160 8758 5408 6872

Den här rapporten får endast återges i sin helhet, om inte utfärdande laboratorium i förväg skriftligen godkännt annat.

**Avser**

<b>Projekt</b>	<b>Grundvatten</b>
Projekt : 921456	
Konsult/ProjNr : David Hagerberg	
Provtyp : Grundvatten	

**Information om provet och provtagningen**

Fakturareferens : 921456	Ankomstdatum : 2014-11-27
Provtagningsdatum : 2014-11-26	Ankomsttidpunkt : 2350
Provtagningsstidpunkt : 1520	Temperatur vid ankomst : 11 °C
Temperatur vid provtagning : 7 °C	
Provets märkning : GA2	
Provtagare : David Hagerberg	

**Analysresultat**

<b>Metodbeteckning</b>	<b>Analys/Undersökning av</b>	<b>Resultat</b>	<b>Matosakerhet</b>	<b>Enhet</b>
SS-EN ISO 17294-2:2005	Arsenik, As, flit	0.95	±0.19	µg/l
SS-EN ISO 17294-2:2005	Bly, Pb, flit	0.082	±0.016	µg/l
SS-EN ISO 17294-2:2005	Kadmium, Cd, flit	0.016	±0.003	µg/l
SS-EN ISO 17294-2:2005	Kobolt, Co, flit	0.64	±0.13	µg/l
SS-EN ISO 17294-2:2005	Koppar, Cu, flit	0.33	±0.066	µg/l
SS-EN ISO 17294-2:2005	Krom, Cr, flit	6.1	±1.2	µg/l
SS-EN ISO 17294-2:2005	Nickel, Ni, flit	3.2	±0.64	µg/l
SS-EN ISO 17294-2:2005	Vanadin, V, flit	3.0	±0.60	µg/l
SS-EN ISO 17294-2:2005	Zink, Zn, flit	65	±13	µg/l
SS-EN ISO 11885-2:2009	Järn, Fe, flit	1.2	±0.24	mg/l
SS-EN ISO 11885-2:2009	Mangan, Mn, flit	0.56	±0.11	mg/l
SS-EN 1484 utg 1	DOC	9.5	±1.4	mg/l
SS-EN 1484 utg 1	TOC	9.9	±1.5	mg/l
GC/MS	1,1-Dikloreten (1)	610	±140	µg/l
GC/MS	1,2-Dikloreten (1)	<20	±3.0	µg/l
GC/MS	Diklormetan (1)	<100	±34	µg/l
GC/MS	Trans-1,2-Dikloreten (1)	1000	±300	µg/l
GC/MS	Cis-1,2-Dikloreten (1)	21000	±5000	µg/l
GC/MS	1,1,1-Trikloreten (1)	1500	±620	µg/l
GC/MS	1,1,2-Trikloreten (1)	<20	±5.4	µg/l
GC/MS	Tetrakloreten(perkloretylen) (1)	<20	±4.6	µg/l
GC/MS	Tetraklormetan (koltetrakt.) (1)	<20	±5.4	µg/l
GC/MS	Trikloreten (1)	20000	±5600	µg/l
GC/MS	Triklormetan (Kloroform) (1)	<20	±7.4	µg/l
GC/MS	Monoklorbensen (1)	<20	±4.8	µg/l
GC/MS	Diklorbensener (1)	<0.6		µg/l
GC/MS	1,2-Diklorpropan (1)	<20	±5.2	µg/l

(1) Resultat levererat av ALcontrol B.V.NL. RvA acknr L028

 Angivna målnöjshet & beräknad med täckningsfaktor  $k = 2$ . Målnöjsheten för ackrediterade mikrobiologiska analyser kan erhållas från laboratoriet efter begäran.

(forts.)

**Rapport Nr 14403300**

Uppdragsgivare

Tyréns AB

Sccheelevägen 17

223 70 LUND

**Avser**

<b>Projekt</b>		<b>Grundvatten</b>	
Projekt	: 921456		
Konsult/ProjNr	: David Hagerberg		
Provtyp	: Grundvatten		

**Information om provet och provtagningen**

Fakturareferens	: 921456	Ankomstdatum	: 2014-11-27
Provtagningsdatum	: 2014-11-26	Ankomsttidpunkt	: 2350
Provtagningsstidpunkt	: 1520	Temperatur vid ankomst	: 11 °C
Temperatur vid provtagning	: 7 °C		
Provets märkning	: GA2		
Provtagare	: David Hagerberg		

**Analysresultat**

Metodbeteckning	Analys/Undersökning av	Resultat	Mätosäkerhet	Enhet
GC/MS	1,1-Dikloreten (1)	120	±40	µg/l
GC/MS	Vinylklorid (1)	460		µg/l
SS-EN ISO 14403:2002	Cyanid tot, CN	0.47	±0.071	mg/l
SS-EN ISO 10304-1:2009	Klorid, Cl	82	±12	mg/l

(1) Resultat levererat av ALcontrol B.V.NL. RvA acknr L028

Angiven mätosäkerhet är beräknad med täckningsfaktor  $k = 2$ . Mätosäkerheten för ackrediterade mikrobiologiska analyser kan erhållas från laboratoriet efter begäran.

**Kommentar**

Förhöjd rapporteringsgräns för några av de klorerade lösningsmedlen på grund av störningar från andra ämnen i provet och nödvändig spädning.

Detta medför också att mätosäkerheten är högre än vad som angivits ovan.

Linköping 2014-12-05

Rapporten har granskats och godkänns av

Mats Lindgren  
Laboratoriechef

Kontrollnr 9085 5350 0316 6064

Den här rapporten får endast åberogas i sin helhet, om inte utfärdande laboratorium i förväg skriftligen godkännt annat.

**Avser**

Projekt	Grundvatten
Projekt	: 921456
Konsult/ProjNr	: David Hagerberg
Provtyp	: Grundvatten

**Information om provet och provtagningen**

Fakturareferens	: 921456	Ankomstdatum	: 2014-11-27
Provtagningsdatum	: 2014-11-26	Ankomsttidpunkt	: 2350
Provtagningsstidpunkt	: 1610	Temperatur vid ankomst	: 11 °C
Temperatur vid provtagning	: 7 °C		
Provet märkning	: 1012		
Provtagare	: David Hagerberg		

**Analysresultat**

Metodbeteckning	Analys/Undersökning av	Resultat	Matosakerhet	Enhet
SS-EN ISO 17294-2:2005	Arsenik, As, flit	0.13	±0.026	µg/l
SS-EN ISO 17294-2:2005	Bly, Pb, flit	<0.02	±0.005	µg/l
SS-EN ISO 17294-2:2005	Kadmium, Cd, flit	<0.01	±0.003	µg/l
SS-EN ISO 17294-2:2005	Kobolt, Co, flit	0.59	±0.12	µg/l
SS-EN ISO 17294-2:2005	Koppar, Cu, flit	<0.05	±0.013	µg/l
SS-EN ISO 17294-2:2005	Krom, Cr, flit	<0.05	±0.015	µg/l
SS-EN ISO 17294-2:2005	Nickel, Ni, flit	2.9	±0.58	µg/l
SS-EN ISO 17294-2:2005	Vanadln, V, flit	<0.05	±0.018	µg/l
SS-EN ISO 17294-2:2005	Zink, Zn, flit	140	±28	µg/l
SS-EN ISO 11885-2:2009	Järn, Fe, flit	0.22	±0.04	mg/l
SS-EN ISO 11885-2:2009	Mangan, Mn, flit	0.56	±0.11	mg/l
SS-EN 1484 utg 1	DOC	4.5	±0.87	mg/l
SS-EN 1484 utg 1	TOC	6.2	±0.93	mg/l
GC/MS	1,1-Dikloreten (1)	0.72	±0.17	µg/l
GC/MS	1,2-Dikloreten (1)	<0.1	±0.02	µg/l
GC/MS	Diklormetan (1)	<0.5	±0.17	µg/l
GC/MS	Trans-1,2-Dikloreten (1)	3.5	±1.1	µg/l
GC/MS	Cis-1,2-Dikloreten (1)	11	±2.6	µg/l
GC/MS	1,1,1-Trikloreten (1)	<0.1	±0.04	µg/l
GC/MS	1,1,2-Trikloreten (1)	<0.1	±0.03	µg/l
GC/MS	Tetrakloreten(perklöretylen) (1)	<0.1	±0.02	µg/l
GC/MS	Tetraklormetan (kolitetra.) (1)	<0.1	±0.03	µg/l
GC/MS	Triklöreten (1)	0.64	±0.18	µg/l
GC/MS	Triklormetan (Kloroform) (1)	<0.1	±0.04	µg/l
GC/MS	Monoklorbensen (1)	<0.2	±0.05	µg/l
GC/MS	Diklorbensener (1)	<0.6		µg/l
GC/MS	1,2-Diklorpropan (1)	<0.2	±0.05	µg/l

(1) Resultat levererat av ALcontrol B.V.NL. RvA acknr L028

 Angiven måttosakerhet är beräknad med täckningsfaktor  $k = 2$ . Måttosakerheten för ackrediterade mikrobiologiska analyser kan erhållas från laboratoriet efter begäran.

(forts.)



ALcontrol Laboratories

ALcontrol AB

Box 1083, 581 10 Linköping · Tel: 013-25 40 00 · Fax: 013-12 17 28  
ORG.NR 556152-0016 STYRELSENS SÄTE: LINKÖPING



1005  
ISO/IEC 17025



## RAPPORT

Sida 2 (2)

utfärdad av ackrediterat laboratorium  
REPORT Issued by an Accredited Laboratory

**Rapport Nr 14403303**

Uppdragsgivare

Tyréns AB

Sccheelevägen 17  
223 70 LUND

### Avser

#### Projekt

#### Grundvatten

Projekt : 921456  
Konsult/ProjNr : David Hagerberg  
Provtyp : Grundvatten

### Information om provet och provtagningen

Fakturareferens	: 921456	Ankomstdatum	: 2014-11-27
Provtagningsdatum	: 2014-11-26	Ankomsttidpunkt	: 2350
Provtagningsstidpunkt	: 1610	Temperatur vid ankomst	: 11 °C
Temperatur vid provtagning	: 7 °C		
Provets märkning	: 1012		
Provtagare	: David Hagerberg		

### Analysresultat

Metodbeteckning	Analys/Undersökning av	Resultat	Matosakerhet	Enhet
GC/MS	1,1-Dikloreten (1)	<0.1	±0.03	µg/l
GC/MS	Vinylklorid (1)	2		µg/l
SS-EN ISO 14403:2002	Cyanid tot, CN	<0.01	±0.002	mg/l
SS-EN ISO 10304-1:2009	Klorid, Cl	39	± 5.9	mg/l

(1) Resultat levererat av ALcontrol B.V.NL. RvA acknr L028

Angiven måttosakerhet är beräknad med täckningsfaktor  $k = 2$ . Måttosakerheten för ackrediterade mikrobiologiska analyser kan erhållas från laboratoriet efter begäran.

Linköping 2014-12-11

Rapporten har granskats och godkänns av

Mats Lindgren  
Laboratoriechef

Kontrollnr 9689 5351 0416 6868

Den här rapporten får endast återges i sin helhet, om inte utfärdande laboratorium i förväg skriftligen godkännt annat.

**Avser**

<b>Projekt</b>	<b>Grundvatten</b>
Projekt	: 921456
Konsult/ProjNr	: David Hagerberg
Provtyp	: Grundvatten

**Information om provet och provtagningen**

Fakturareferens	: 921456	Ankomstdatum	: 2014-11-27
Provtagningsdatum	: 2014-11-26	Ankomsttidpunkt	: 2350
Provtagningsstidpunkt	: 1550	Temperatur vid ankomst	: 11 °C
Temperatur vid provtagning	: 7 °C		
Provets märkning	: 1009		
Provtagare	: David Hagerberg		

**Analysresultat**

Metodbeteckning	Analys/Undersökning av	Resultat	Matosakerhet	Enhet
SS-EN ISO 17294-2:2005	Arsenik, As, flit	11	± 2.2	µg/l
SS-EN ISO 17294-2:2005	Bly, Pb, flit	0.023	± 0.005	µg/l
SS-EN ISO 17294-2:2005	Kadmium, Cd, flit	0.11	± 0.022	µg/l
SS-EN ISO 17294-2:2005	Kobolt, Co, flit	4.7	± 0.94	µg/l
SS-EN ISO 17294-2:2005	Koppar, Cu, flit	34	± 6.8	µg/l
SS-EN ISO 17294-2:2005	Krom, Cr, flit	0.34	± 0.068	µg/l
SS-EN ISO 17294-2:2005	Nickel, Ni, flit	7.0	± 1.4	µg/l
SS-EN ISO 17294-2:2005	Vanadln, V, flit	5.5	± 1.1	µg/l
SS-EN ISO 17294-2:2005	Zink, Zn, flit	45	± 9.0	µg/l
SS-EN ISO 11885-2:2009	Järn, Fe, flit	0.06	± 0.02	mg/l
SS-EN ISO 11885-2:2009	Mangan, Mn, flit	0.07	± 0.01	mg/l
SS-EN 1484 utg 1	DOC	13	± 2.0	mg/l
SS-EN 1484 utg 1	TOC	13	± 2.0	mg/l
GC/MS	1,1-Dikloreten (1)	< 0.1	± 0.02	µg/l
GC/MS	1,2-Dikloreten (1)	< 0.1	± 0.02	µg/l
GC/MS	Diklormetan (1)	< 0.5	± 0.17	µg/l
GC/MS	Trans-1,2-Dikloreten (1)	< 0.1	± 0.03	µg/l
GC/MS	Cis-1,2-Dikloreten (1)	0.19	± 0.05	µg/l
GC/MS	1,1,1-Trikloreten (1)	< 0.1	± 0.04	µg/l
GC/MS	1,1,2-Trikloreten (1)	< 0.1	± 0.03	µg/l
GC/MS	Tetrakloreten(perkloretylen) (1)	< 0.1	± 0.02	µg/l
GC/MS	Tetraklormetan (koltetrakl.) (1)	< 0.1	± 0.03	µg/l
GC/MS	Triklloreten (1)	0.57	± 0.16	µg/l
GC/MS	Triklormetan (Kloroform) (1)	< 0.1	± 0.04	µg/l
GC/MS	Monoklorbensen (1)	< 0.2	± 0.05	µg/l
GC/MS	Diklorbensener (1)	< 0.6		µg/l
GC/MS	1,2-Diklorpropan (1)	< 0.2	± 0.05	µg/l

(1) Resultat levererat av ALcontrol B.V.NL. RvA acknr L028

Angiven måttosakerhet är beräknad med täckningsfaktor k = 2. Måttosakerheten för ackrediterade mikrobiologiska analyser kan avvika från laboratoriet efter begäran.

(forts.)



ALcontrol Laboratories

ALcontrol AB

Box 1083, 581 10 Linköping · Tel: 013-25 40 00 · Fax: 013-12 17 28  
ORG.NR 556152-0016 STYRELSENS SÄTE: LINKÖPING



1005  
ISO/IEC 17025



## RAPPORT

Sida 2 (2)

utfärdad av ackrediterat laboratorium  
REPORT Issued by an Accredited Laboratory

**Rapport Nr 14403310**

Uppdragsgivare

Tyréns AB

Scchelevägen 17  
223 70 LUND

### Avser

#### Projekt

#### Grundvatten

Projekt : 921456  
Konsult/ProjNr : David Hagerberg  
Provtyp : Grundvatten

### Information om provet och provtagningen

Fakturareferens	: 921456	Ankomstdatum	: 2014-11-27
Provtagningsdatum	: 2014-11-26	Ankomsttidpunkt	: 2350
Provtagningsstidpunkt	: 1550	Temperatur vid ankomst	: 11 °C
Temperatur vid provtagning	: 7 °C		
Provets märkning	: 1009		
Provtagare	: David Hagerberg		

### Analysresultat

Metodbeteckning	Analys/Undersökning av	Resultat	Matosakerhet	Enhet
GC/MS	1,1-Dikloreten (1)	<0.1	±0.03	µg/l
GC/MS	Vinylklorid (1)	<0.2		µg/l
SS-EN ISO 14403:2002	Cyanid tot, CN	<0.01	±0.002	mg/l
SS-EN ISO 10304-1:2009	Klorid, Cl	28	±4.2	mg/l

(1) Resultat levererat av ALcontrol B.V.NL. RvA acknr L028

Angiven måttosakerhet är beräknad med täckningsfaktor  $k = 2$ . Måttosakerheten för ackrediterade mikrobiologiska analyser kan erhållas från laboratoriet efter begäran.

Linköping 2014-12-11

Rapporten har granskats och godkänns av

Mats Lindgren  
Laboratoriechef

Kontrollnr 8080 5750 0165 6269

Den här rapporten får endast återges i sin helhet, om inte utfärdande laboratorium i förväg skriftligen godkännt annat.



## Tidigare skrifter i serien

### ”Examensarbeten i Geologi vid Lunds universitet”:

394. Westlund, Kristian, 2014: Geomorphological evidence for an ongoing transgression on northwestern Svalbard. (15 hp)
395. Rooth, Richard, 2014: Uppföljning av utlastningsgrad vid Dannemora gruva; april 2012 - april 2014. (15 hp)
396. Persson, Daniel, 2014: Miljögeologisk undersökning av deponin vid Getabjär, Sölvesborg. (15 hp)
397. Jennerheim, Jessica, 2014: Undersökning av långsiktiga effekter på mark och grundvatten vid infiltration av lakvatten – fältundersökning och utvärdering av förhållanden vid Kejsarkullens avfallsanläggning, Hultsfred. (15 hp)
398. Särman, Kim, 2014: Utvärdering av befintliga vattenskyddsområden i Sverige. (15 hp)
399. Tuveesson, Henrik, 2014: Från hav till land – en beskrivning av geologin i Skrylle. (15 hp)
400. Nilsson Brunlid, Anette, 2014: Paleogeologisk och kemisk-fysikalisk undersökning av ett avvikande sedimentlager i Barsebäcks mosse, sydvästra Skåne, bil dat för ca 13 000 år sedan. (15 hp)
401. Falkenhaus, Jorunn, 2014: Vattnets kretslopp i området vid Lilla Klåveröd: ett kunskapsprojekt med vatten i fokus. (15 hp)
402. Heingård, Miriam, 2014: Long bone and vertebral microanatomy and osteohistology of 'Platecarpus' ptychodon (Reptilia, Mosasauridae) – implications for marine adaptations. (15 hp)
403. Kall, Christoffer, 2014: Microscopic echinoderm remains from the Darriwilian (Middle Ordovician) of Västergötland, Sweden – faunal composition and applicability as environmental proxies. (15 hp)
404. Preis Bergdahl, Daniel, 2014: Geoenergi för växthusjordbruk – Möjlig anläggning av värme och kyla i Västsåne. (15 hp)
405. Jakobsson, Mikael, 2014: Geophysical characterization and petrographic analysis of cap and reservoir rocks within the Lund Sandstone in Kyrkheddinge. (15 hp)
406. Björnfors, Oliver, 2014: A comparison of size fractions in faunal assemblages of deep-water benthic foraminifera—A case study from the coast of SW-Africa.. (15 hp)
407. Rådman, Johan, 2014: U-Pb baddeleyite geochronology and geochemistry of the White Mfolozi Dyke Swarm: unravelling the complexities of 2.70-2.66 Ga dyke swarms on the eastern Kaapvaal Craton, South Africa. (45 hp)
408. Andersson, Monica, 2014: Drumliner vid moderna glaciärer — hur vanliga är de? (15 hp)
409. Olsenius, Björn, 2014: Vinderosion, sanddrift och markanvändning på Kristianstadsslätten. (15 hp)
410. Bokhari Friberg, Yasmin, 2014: Oxygen isotopes in corals and their use as proxies for El Niño. (15 hp)
411. Fullerton, Wayne, 2014: REE mineralisation and metasomatic alteration in the Olserum metasediments. (45 hp)
412. Mekhaldi, Florian, 2014: The cosmic-ray events around AD 775 and AD 993 - Assessing their causes and possible effects on climate. (45 hp)
413. Timms Eliasson, Isabelle, 2014: Is it possible to reconstruct local presence of pine on bogs during the Holocene based on pollen data? A study based on surface and stratigraphical samples from three bogs in southern Sweden. (45 hp)
414. Hjulström, Joakim, 2014: Bortforsling av kaxblandat vatten från borrhinar via dagvattenledningar: Riskanalys, karaktärisering av kaxvatten och reningsmetoder. (45 hp)
415. Fredrich, Birgit, 2014: Metadolerites as quantitative P-T markers for Sveconorwegian metamorphism, SW Sweden. (45 hp)
416. Alebouyeh Semami, Farnaz, 2014: U-Pb geochronology of the Tsineng dyke swarm and paleomagnetism of the Hartley Basalt, South Africa – evidence for two separate magmatic events at 1.93-1.92 and 1.88-1.84 Ga in the Kalahari craton. (45 hp)
417. Reiche, Sophie, 2014: Ascertaining the lithological boundaries of the Yoldia Sea of the Baltic Sea – a geochemical approach. (45 hp)
418. Mroczek, Robert, 2014: Microscopic shock-metamorphic features in crystalline bedrock: A comparison between shocked and unshocked granite from the Siljan impact structure. (15 hp)
419. Balija, Fismik, 2014: Radon ett samhällsproblem - En litteraturstudie om geolo-

- giskt sammanhang, hälsoeffekter och möjliga lösningar. (15 hp)
420. Andersson, Sandra, 2014: Undersökning av kalciumkarbonatförekomsten i infiltrationsområdet i Sydsvattens vattenverk, Vombverket. (15 hp)
421. Martin, Ellinor, 2014: Chrome spinel grains from the Komstad Limestone Formation, Killeröd, southern Sweden: A high-resolution study of an increased meteorite flux in the Middle Ordovician. (45 hp)
422. Gabrielsson, Johan, 2014: A study over Mg/Ca in benthic foraminifera sampled across a large salinity gradient. (45 hp)
423. Ingvaldson, Ola, 2015: Ansvarsutredningar av tre potentiellt förorenade fastigheter i Helsingborgs stad. (15 hp)
424. Robygd, Joakim, 2015: Geochemical and palaeomagnetic characteristics of a Swedish Holocene sediment sequence from Lake Storsjön, Jämtland. (45 hp)
425. Larsson, Måns, 2015: Geofysiska undersökningsmetoder för geoenergisystem. (15 hp)
426. Hertzman, Hanna, 2015: Pharmaceuticals in groundwater - a literature review. (15 hp)
427. Thulin Olander, Henric, 2015: A contribution to the knowledge of Fårö's hydrogeology. (45 hp)
428. Peterffy, Olof, 2015: Sedimentology and carbon isotope stratigraphy of Lower-Middle Ordovician successions of Slemestad (Oslo-Asker, Norway) and Brunflo (Jämtland, Sweden). (45 hp)
429. Sjunnesson, Alexandra, 2015: Spårämnesförsök med nitrat för bedömning av spridning och uppehållstid vid återinfiltration av grundvatten. (15 hp)
430. Henao, Victor, 2015: A palaeoenvironmental study of a peat sequence from Iles Kerguelen (49° S, Indian Ocean) for the Last Deglaciation based on pollen analysis. (45 hp)
431. Landgren, Susanne, 2015: Using calcein-filled osmotic pumps to study the calcification response of benthic foraminifera to induced hypoxia under *in situ* conditions: An experimental approach. (45 hp)
432. von Knorring, Robert, 2015: Undersökning av karstvittring inom Kristianstadsslättens NV randområde och bedömning av dess betydelse för grundvattnets sårbarhet. (30 hp)
433. Rezvani, Azadeh, 2015: Spectral Time Domain Induced Polarization - Factors Affecting Spectral Data Information Content and Applicability to Geological Characterization. (45 hp)
434. Vasilica, Alexander, 2015: Geofysisk karaktärisering av de ordoviciska kalkstensenheter på södra Gotland. (15 hp)
435. Olsson, Sofia, 2015: Naturlig nedbrytning av klorerade lösningsmedel: en modellering i Biochlor baserat på en fallstudie. (15 hp)
436. Huitema, Moa, 2015: Inventering av föroreningar vid en brandövningsplats i Linköpings kommun. (15 hp)
437. Nordlander, Lina, 2015: Borrningsteknikens påverkan vid provtagning inför dimensionering av formationsfilter. (15 hp)
438. Fennvik, Erik, 2015: Resistivitet och IP-mätningar vid Äspö Hard Rock Laboratory. (15 hp)
439. Pettersson, Johan, 2015: Paleoekologisk undersökning av Triberga mosse, sydöstra Öland. (15 hp)
440. Larsson, Alfred, 2015: Mantelpolymer - realitet eller *ad hoc*? (15 hp)
441. Holm, Julia, 2015: Markskador inom skogsbruket - jordartens betydelse (15 hp)
442. Åkesson, Sofia, 2015: The application of resistivity and IP-measurements as investigation tools at contaminated sites - A case study from Kv Renen 13, Varberg, SW Sweden. (45 hp)



**LUNDS UNIVERSITET**

Geologiska institutionen  
Lunds universitet  
Sölvegatan 12, 223 62 Lund